Interferon-γ Aptamers for the Diagnosis of Extra-Pulmonary Tuberculosis

BOITUMELO LOUISA FANAMPE

Thesis Presented for the Degree of

DOCTOR OF PHILOSOPHY

In the Department of Medicine

Faculty of Health Sciences

UNIVERSITY OF CAPE TOWN

June 2015

DECLARATION OF CANDIDATE

I, **Boitumelo Louisa Fanampe** hereby declare that the work on which this thesis is based on is my original work (except where acknowledgements indicate otherwise) and that neither the whole work nor any part of it has been, is being, or is to be submitted for another degree in this or any other university. I empower the university to reproduce for the purpose of research either the whole or any portion of the contents in any manner whatsoever.

Signature: Signed by candidate

Date: 29 June 2015

DEDICATION

To my late grandparents, Monnapula Sight Fanampe and Eshupang Vivian Fanampe, who taught me the value of good education and would have been proud of this achievement

To my mom, whose love, constant encouragement and support got me this far

"YOU are my rock"

ACKNOWLEDGEMENTS

Many people contributed to this achievement and I would like to take this opportunity to thank them.

Firstly, I would like to thank God Almighty for giving me the strength during this journey. For allowing me to draw strength and seek thee whenever times were tough. The serenity to be patient even when at times I felt like I was not cut out for this.

My sincere gratitude goes out to Professor Keertan Dheda, for affording me the opportunity to undertake this project under his supervision. I would like to thank him for his guidance, constant support and for the invaluable teachings he instilled in me. He taught me how to be a good scientist, write science and always deliver good presentations; for that I am grateful.

Thanks to my co-supervisor Dr Makobetsa Khati (Shooz). You allowed me to work in your lab whenever I needed to and for that I am grateful. Thanks for encouraging me to persevere even when the project got tough. You and your team truly made me feel like I belonged. You encouraged me to apply for fellowships like the FOGARTY and the DST women in science awards, and for that I am truly grateful.

To my other co-supervisor, Dr Grant Theron, you have been and continue to be a good mentor to me. You have taught me how to think critically, how to write science and how to ask specific questions, and for that I am immensely grateful. You taught me how to approach problems scientifically, and I will cherish the moments we spent on your drawing board whenever those hurdles were getting higher.

I am grateful to Professor Kevin Plaxco, from the University of California, Santa Barbara for agreeing to host me in his lab for 6 months during my FOGARTY fellowship. Thanks to my lab mates in the Plaxco Lab, especially Ms Hannah

Kallewaard for making me feel at home during my stay in Santa Barbara, and Dr Emir Yasun, for advice on my project and for continuing to be a good friend.

I would like to express my gratitude to all the members of the Lung Infection and Immunity Unit (LIIU) for their support during my doctoral studies. Special thanks to Dr Philippa Randall for assisting with final experiments and for reading my thesis drafts. Dr Malika Davids for assisting with statistical analyses. Mr Anil Pooran (fellow postgraduate student) for encouragements during the writing-up stage. Sr Marietjie Pretorius and Dr Liesel Smith for always being there to give words of encouragement.

Thanks to my CSIR lab mates "The APTAMER Team" for making me feel at home whenever I had to undertake experiments in their lab in Pretoria. Special thanks Dr Lia Rotherham for training me in the P3 Lab, advising on experimental work and for reading my thesis drafts, Dr Laura Millroy for training me on the BIAcore, Dr Hazel Mufhandu for reading my thesis drafts, and for invaluable advice and guidance. To Charlotte Maserumule for always sparking good conversations during our "camping sessions" in the lab.

Special thanks goes out to Professor Anwar Mall and his team at the Department of Surgery, University of Cape Town. I appreciate all the assistance with the protein experiments I had to carry out in your lab. Thanks for always making me feel like I was part of the team.

To my special friends: Dimakatso "Maks" Dinokana, Lesedi Kesiamang, Sandy Maponya, Refilwe Mofokeng, Dr Mashiko Setshedi, Babalwa Damane, Koketso Kujane, and Jacques Bigirimana, thank you all for your support during the past few years. You always knew how to cheer me up. Special thanks to Dr Mankgopo "Kgops" Kgatle for constant support and assisting with final formatting of this thesis.

Most importantly, I am indebted to my family; my two brothers Tuks and Petse have always been there to give me unconditional love and support. Thanks to all my uncles, especially Milyn for rubbing his love for Science off onto me while I was still very young, and for his constant support and unconditional love. To my nieces, Tlotli and Momo, for always being there to brighten up my days no matter how difficult the journey got. To my mother, thanks for making many sacrifices in order to ensure that we always have the best in life.

I would like to thank my funders for investing in this project: The South African Medical Research Council (SA-MRC), the European & Developing Countries Clinical Trials Partnership (EDCTP), and the Oppenheimer Memorial Trust (OMT), and the Health and Wellness Sector Education and Training Authority (HWSETA). Thanks to the PHRI-AURUM-Global Infectious Diseases Research Training Program (FOGARTY) fellowship, which allowed me to spend 6 months at the University of California, Santa Barbara, USA, under the supervision of Professor. Kevin Plaxco in the Department of Biochemistry and Chemical Engineering.

CONFERENCE PRESENTATIONS

1. **Fanampe B,** Theron G, Khati M, Plaxco K, Dheda K**.** An aptamer-based probe for development of an electrochemical biosensor for the diagnosis of extra-pulmonary tuberculosis. 41 st Annual Department of Medicine Research Day. 9 October 2014. **Cape Town, South Africa**. Oral **Won the Bernard Pimstone Prize for best oral presentation*

2. **Fanampe B**, Mzyece J, Theron G, Khati M, Plaxco K, Dheda K. Characterisation of aptamer-based probes and the development of an electrochemical biosensor: Potential TB diagnostic tools. 248th American Chemistry Society (ACS) National Meeting & Exposition, 10-14 August, 2014, **San Francisco, California, United States**. Oral **Awarded travel grant by UCT*

3. **Boitumelo Fanampe,** Lia Rotherham, Makobetsa Khati, Grant Theron, Keertan Dheda. Development of an aptamer to a Th1 cytokine. 8th European & Developing Countries Clinical Trials Partnership (EDCTP) Forum. 30 June-02 July 2014, **Berlin, Germany.** Oral * *Awarded travel scholarship by EDCTP*

4. J Mzyece, **B Fanampe**, K Dheda, G Theron, M Khati. Characterisation and Kinetics of Aptamer binding to Interferon gamma for the diagnosis of Human Extra-pulmonary Tuberculosis. 4th SA TB Conference. June 10-13 2014, International Convention Centre (ICC), **Durban, South Africa.** Poster

5. **B. Fanampe**, J. Mzyece, M. Khati, G. Theron, K. Dheda. The isolation and characterisation of novel probes for the development of TB diagnostic tools. 4th SA TB Conference. June 10-13 2014, International Convention Centre (ICC), **Durban, South Africa.** Poster

6. Mzyece J, **Fanampe B**, Theron G, Dheda K, Khati M, Characterisation and Kinetics of Aptamer binding to Interferon gamma for the diagnosis of Human Extra-pulmonary Tuberculosis. Keystone Symposia Conference. March 30 - 4 April 2014, **Denver, Colorado, USA.** Poster

7. **Fanampe B**, Rotherham L, Khati M, Theron G, Dheda K. Development of an aptamer based array for the diagnosis of tuberculosis**.** Medical Research Council (MRC) Early Career Scientist Annual Conference**.** 24-25 October 2012. **Cape Town, South Africa.** Poster

TABLE OF CONTENTS

CHAPTER 2: ISOLATION OF SINGLE-STRANDED DNA APTAMERS THAT BIND IFN-γ

CHAPTER3: CHARACTERISATION AND BINDING KINETICS OF APTAMERS TO IFN-γ

CHAPTER 4: DETERMINATION OF SPECIFICITY OF THE APTAMERS TO IFN-γ , TRUNCATION AND CHARACTERISATION OF DERIVATIVES APTAMER A1

CHAPTER 5: GENERAL DISCUSSION AND CONCLUSION

LIST OF FIGURES

List of figures

LIST OF TABLES

ABBREVIATIONS

K_a	: Association rate constant
°C	: Degrees Celsius
Δ	: Delta
K_d	: Dissociation rate constant
K_D	: Equilibrium dissociation constant
≥	: Greater than or equals to
µg	: Microgram
µl	: Microlitre
kDa	: Kilodalton
≤	: Less than or equals to
%	: Percentage
vs.	: Versus
AFB	: Acid-fast bacilli
AIDS	: Acquired immune deficiency syndrome
ATP	: Adenosine triphosphate
ADA	: Adenosine deaminase assay
AuNP	: Gold nanoparticles
BCG	: Bacillus Calmette-Guérin
BSA	: Bovine serum albumin
bp	: Base pair
CFP-10	: Culture filtrate protein-10
CFP-10/ESAT-6	: Culture filtrate protein-10 and early secreted antigenic target, 6 kDa heterodimer
DNA	: Deoxyribonucleic acid
dsDNA	: Double-stranded deoxyribonucleic acid
E. coli	: *Escherichia coli*
EDC	: N-ethyl-N-(3,-dimethylaminopropyl)-carbodiimide hydrochloride
ELISA	: Enzyme-linked immunosorbent assay
ELONA	: Enzyme-linked oligonucleotide assay
EMSA	: Electrophoretic mobility shift assay
EPTB	: Extra-pulmonary tuberculosis
ESAT-6	: Early secreted antigenic target, 6 kDa
Esx	: ESAT-6 system
gp120	: 120 kDa glycoprotein
HBS-N	: 4-(2-hydroxyethyl)-1-piperazineethanesulfonic acid, sodium chloride buffer
HEPES	: 4-(2-hydroxyethyl)-1-piperazineethanesulfonic acid
HRP	: Horse-radish peroxidase
HIV	: Human immunodeficiency virus
h	: Hour
ID	: Identity
IFN-γ	: Interferon gamma
IgG	: Immunoglobulin G
IGRA	: Interferon—release assay
IL-4	: Interleukin 4
KOH	: Potassium hydroxide
LAM	: Lipoarabinomannan
LB	: Luria-Bertani broth
M	: Molar
ml	: Millilitre

Min	: Minutes
M.tb	: *Mycobacterium tuberculosis*
MGIT	: Mycobacteria Growth Indicator Tube
MTD	: M. tuberculosis Direct test
MPT64	: Mycobacterial protein from species tuberculosis-64
NAATs	: Nucleic acid amplification tests
NM	: Nanometre
NaOAc	: Sodium acetate
NHS	: N-hydroxysuccinimide
nM	: Nanomolar
nt	: Nucleotides
p	: P-value
PBMC	: Peripheral blood mononuclear cells
PBS	: Phosphate-buffered saline
PBS-T	: Phosphate-buffered saline containing 0.005% Tween-20
PCR	: Polymerase chain reaction
PDGF	: Platelet-derived growth factor
pg	: Picograms
PhaB	: Phage-amplified biological assay
PE	: Proline-glutamic acid
PPD	: Purified protein derivative
PPE	: Proline-proline-glutamic acid
PPK2	: Polyphosphate kinase 2
RD	: Region of difference
RNA	: Ribonucleic acid
Sec	: Seconds
SPR	: Surface plasmon resonance

ABSTRACT

Background: Tuberculosis (TB) is a major global health problem. About 15-20% of the global population who are HIV negative have extra-pulmonary TB (EPTB) such as pleural TB. This increases to 50-70% in HIV positive people. The diagnosis of EPTB is challenging because of the low bacillary burden. Interferon gamma (IFN-γ) has been identified as a promising biomarker for the diagnosis of EPTB. The development of rapid and accurate point-of-care (POC) diagnostic technologies becomes crucial in controlling EPTB. Aptamers referred to as "synthetic antibodies" have been recently explored as a replacement for antibodies in diagnostic platforms. These single-stranded nucleic acid molecules have high affinity and specificity comparable, and in some instances even superior, to those of antibodies; in addition to their relatively low cost and simple method of production they have the potential to reduce assay turnaround time.

Aim: The aim of this thesis was to develop aptamers to IFN-γ, a biomarker specific for EPTB, thus facilitating the development of aptamer-based POC tests for the diagnosis of EPTB.

Methods: Single-stranded DNA aptamers were selected against IFN-γ using the Systematic Evolution of Ligands by Exponential Enrichment (SELEX) protocol. Eight rounds of selection were performed. Enrichment of the recovered RNA that bound IFN-γ reached 50% and plateaued at round 6. Therefore DNA pool recovered from round 6 was cloned and sequenced. Binding studies were performed using enzyme-linked oligonucleotide assay (ELONA), Biacore™ surface plasmon resonance (SPR) technology and bioinformatics, respectively.

Results: 41 of the 60 (68%) aptamers screened significantly bound IFN-γ ($p \leq 0.05$). Homology and phylogenetic analyses revealed 60% shared homology of the aptamers. Bioinformatic analysis for secondary structure predictions for the six selected aptamer displayed more than two possible structure predictions for each aptamer. Furthermore, aptamers A1 and B4 had the ability to form a G-quadruplex. A limit of detection of 10 µg/ml (IFN-γ) was determined. A time-course assay showed that aptamers A1, B2 and H12 had no difference in binding at 60 min vs.120 min. All six aptamers had an equilibrium dissociation constant (K_D) in the sub-nanomolar to picomlar range, with aptamers H12 and A9 having the lowest at 2.06E-10 (206 pM) and 3.90E-10 (390 pM), respectively. All the aptamers had high specificity for IFN-γ when tested against TB-related and unrelated molecules ($p \leq 0.001$). A competition assay with an anti-IFN-γ antibody, CD66, showed that aptamer H12 did not compete with CD66; this suggests that the two reagents could be used together in a sandwich

assay. Aptamer A1 was further truncated to yield derivatives, 49mer, 36mer and 29mer. When binding affinities of the full length (90mer) was compared to truncated derivatives 49mer, 36mer and 29mer at OD450, the binding of the 49mer was significantly reduced (OD of 49mer = 0.403 vs. 90mer = 0.651 ($p \leq 0.01$).

Conclusion: In this study, I selected at least six aptamers, which bound IFN-γ with high affinity and specificity, and have a potential for use in POC diagnostic platforms for EPTB.

CHAPTER 1
INTRODUCTION AND LITERATURE REVIEW

1.1 INTRODUCTION

In 1993, the World Health Organization (WHO) declared tuberculosis (TB) a global public health emergency. Although the TB epidemic has plateaued in several regions of the world, in Africa, fuelled by poverty and HIV co-infection, TB is out of control (WHO, 2010). South Africa is facing a TB problem of such magnitude that this disease has been declared a national health emergency. To minimize transmission, early case detection and subsequent treatment initiation are important. However, the development of new TB diagnostic technologies remains a challenge. Thus, a number of technologies have been endorsed by the WHO; however, most of these still have limitations according to the guidelines set by the organization (WHO, 2012). The major gap missing in diagnostics is the lack of suitable technologies to test existing biomarkers on. The ideal POC test should follow the ASSURED guidelines (Mabey et al., 2004) (**Table 1.1**).

Table 1.1: ASSURED criteria specifying ideal characteristics of a POC test

A	Affordable	Less than US $10 (equivalent to R100.00 per test)
S	Sensitive	Have high sensitivity
S	Specific	Have high specificity
U	User-friendly	Simple to perform with no training required
R	Robust and rapid	Availability of results in <30 minutes
E	Equipment-free	Should ideally be battery-operated
D	Deliverable to the end-user	Should be suitable for use in the field

Aptamers, a new promising technology, has been introduced in diagnostics and therapeutics (Ellington and Szostak, 1990a) and may have proven to satisfy the characteristics of a suitable POC test. These molecules have been successfully used in therapeutics as delivery vehicles (Nimjee et al., 2005a, Nimjee et al., 2005b,

Rusconi et al., 2002, Keefe et al., 2010) and in the development of diagnostics such as aptasensors, aptamer arrays and in sandwich ELISA formats (Drolet et al., 1996, Hong et al., 2012, Inoue et al., 2011, Pultar et al., 2009). Aptamers are known for their specificity and high binding affinity to their targets (Ellington and Szostak, 1990a, Eaton et al., 1995) and thus, these characteristics make them attractive as molecules of choice for the abovementioned applications. Aptamers for TB biomarkers such as ESAT6-CFP10, IFN-γ, MPT64 and EsxG proteins have been previously identified (Qin et al., 2009, Rotherham et al., 2012, Ngubane et al., 2014, Tang et al., 2014, Lee et al., 1996, Cao et al., 2014). This chapter summarises the current knowledge on TB and EPTB with a focus on diagnostics. The gaps and potential ways to fill them will be discussed including the use of the aptamer technology as an alternative to developing new TB diagnostic tools. This will be followed by stating the objectives and aims of this study together with an outline of the structure of the thesis.

1.2 TUBERCULOSIS

1.2.1 Pathogenesis of Mycobacterium Tuberculosis

Mycobacterium tuberculosis (M.tb) is a causative agent of TB. It is a slow growing, acid fast bacilli whose cell wall structure is very complex compared to its other counterparts within the Mycobacterium Tuberculous Complex (MTBC) genus (Lawn and Zumla, 2011). Due to its complex cell wall, which is lipid-rich and hence highly impermeable, infected patients are required to stay on treatment for periods of up to 6-9 months (Lawn and Zumla, 2011, Knechel, 2009, Todar, 2008). *M.tb* is an aerobic bacterium; hence it prefers organs or tissues in the body which are high in oxygen, such as lungs. It is transmitted through inhalation of small aerosol droplets usually through sneezing, talking or coughing from an infected person. Settling of these aerosols in the lungs cause pulmonary tuberculosis (PTB) (Knechel, 2009). Should the TB disseminate to other parts of the body, which is likely to occur in those with compromised immune systems, such as those with HIV (Sharma et al., 2005, Raviglione et al., 1992), diabetes (Singla et al., 2006, Martinez and Kornfeld,

2014, van Crevel and Dockrell, 2014), the elderly (Negin et al., 2015) and young children (Zar et al., 2010, Connell et al., 2011, Madhi et al., 2000, Maltezou et al., 2000, Marais and Schaaf, 2014), then the disease is termed EPTB (Golden and Vikram, 2005). A simple definition for EPTB would therefore be TB affecting any other organ within the body (**Figure 1.1**) excluding the lungs (WHO, 2014).

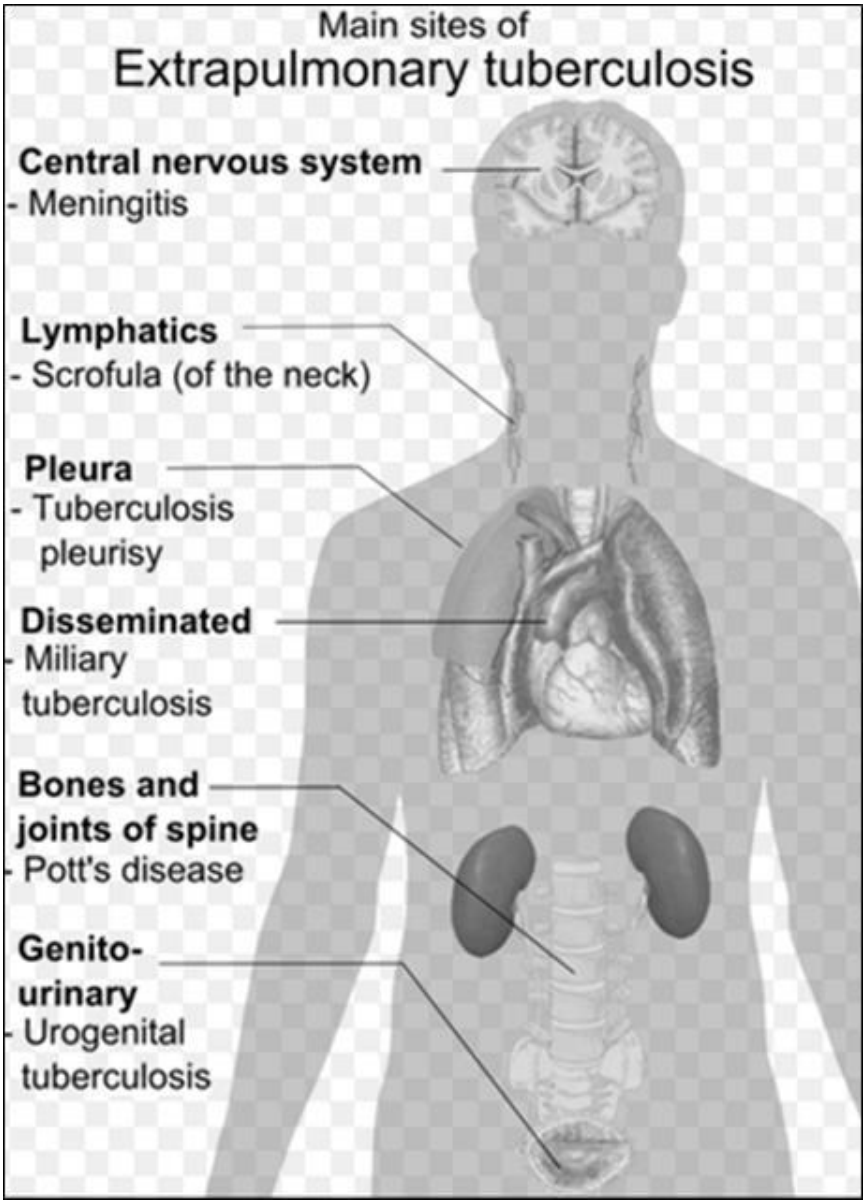

Figure 1.1: A schematic depicting the main organs of the body affected by extra-pulmonary tuberculosis (Häggström, 2009).

1.2.2 Tuberculosis Epidemiology

Tuberculosis accounts globally for 9 million new cases and 1.5 million deaths annually (WHO, 2014). This was an annual increase from 8.6 and 1.3 million for new cases and deaths, respectively. This mortality rate is unacceptably high given that TB is treatable if only people can access health care facilities and receive a timely diagnosis (WHO, 2014) resulting in preventable deaths. Children and women were the most affected accounting for 550 000 and 3.3 million of the 9 million incident cases, respectively. South Africa, India, Indonesia, China, Nigeria and Pakistan were countries with the highest incident cases. South Africa reported between 410 000 and 520 000 cases in 2013. Of the 1.5 million people who died of TB, 1.1 million were HIV-negative and about a quarter were HIV-positive with South Africa as one of the countries with the highest proportion of TB cases co-infected with HIV (**Figure 1.2**) (WHO, 2014).

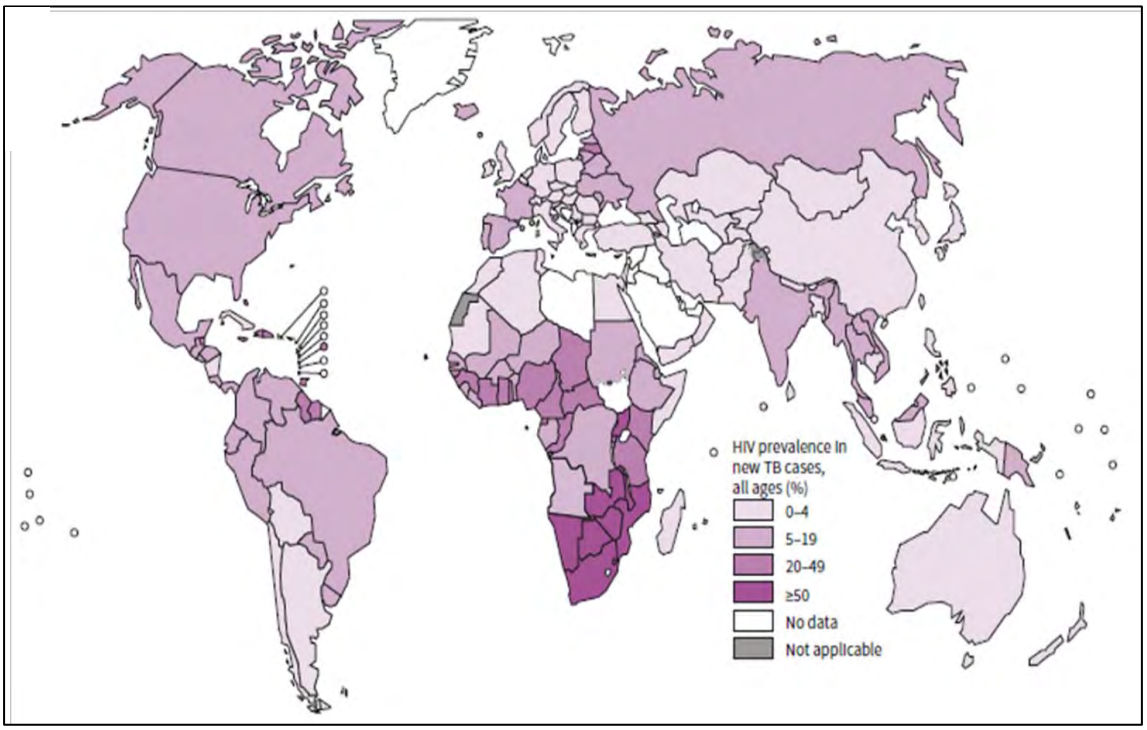

Figure 1.2: Estimated HIV prevalence in new and relapsed TB cases 2013 (WHO, Global Tuberculosis Report, 2014).

1.3 EXTRA-PULMONARY TUBERCULOSIS

1.3.1 Prevalence of EPTB

The African region reported the highest TB cases co-infected with HIV (WHO, 2014). Many organs can be involved in EPTB. Extra-pulmonary TB has increased over the last two decades; it accounted for between 15-20% of all reported TB cases (WHO, 2012) (**Figure 1.3: A**). In sub-Saharan Africa, however, this figure increased immensely since the advent of HIV with over 50% of these TB cases being persons with TB-HIV co-infection (WHO, 2014). In general, lymph node TB seems to be the most common of all EPTB cases accounting for about 35%, followed closely by pleural TB at 20% (**Figure 1.3: B**) (Sharma and Mohan, 2004, Peto et al., 2009). The disseminated form of the disease allows some patients to present with both PTB and EPTB, especially those co-infected with HIV (**Figure 1.3: B**). In the absence of HIV, lymph node TB is the most common in children under the age of 14 years (Norbis et al., 2014). Genitourinary and joint TB cases are mostly seen with increasing age, and the elderly are mostly infected with meningeal and miliary TB (**Figure 1.3: B**) (Fanning, 1999, Sharma and Mohan, 2004).

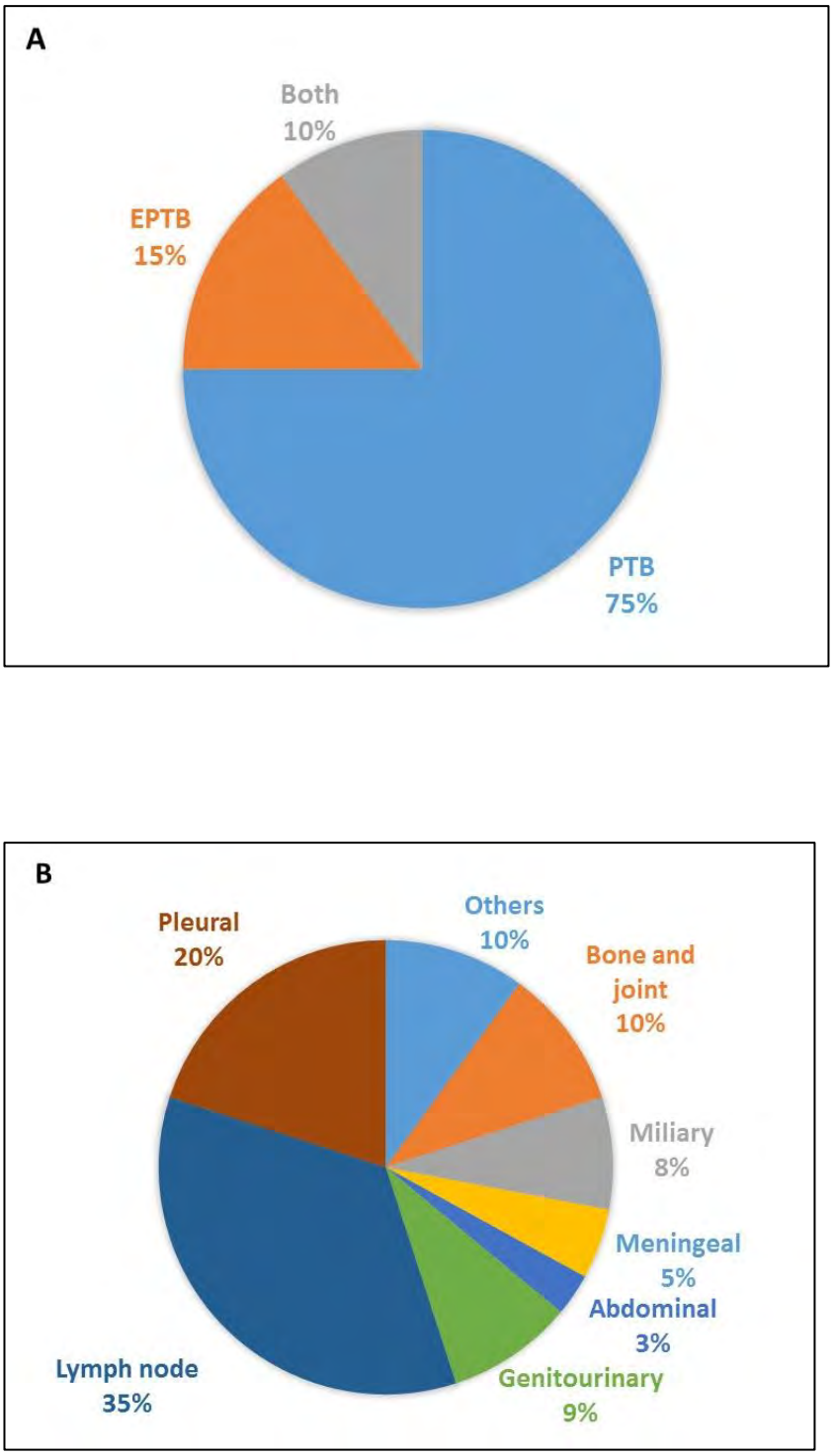

Figure 1.3: Prevalence of PTB vs. EPTB and distribution of EPTB by disease site in HIV-uninfected individuals.

(A) Prevalence of PTB and EPTB of all TB cases. PTB accounts for 75% and EPTB 15-20% of all TB cases. (B) Distribution of TB by anatomical site in HIV-uninfected patients of the constituted 15-20% of all TB cases. PTB-pulmonary TB, EPTB-extra-pulmonary TB (Adapted from Sharma and Mohan, 2004).

1.3.2 Current status of EPTB in sub-Saharan Africa

People living with HIV are 29 times more likely to contract TB compared to those who are HIV-negative, with the worst statistics reported in Southern and Eastern Africa (WHO, 2014). In South Africa, the epidemic of HIV/AIDS in the last two decades has changed the whole spectrum of TB. In HIV-positive patients, *M.tb* infection tends to be more aggressive, sometimes presenting with both manifestations of the disease i.e. PTB and EPTB (WHO, 2013). For this reason, it becomes clinically challenging to treat and diagnose (Lee, 2015, Al-Otaibi et al., 2012). In the 20% of patients estimated to have EPTB and are HIV-positive the majority of them are sputum scarce, as is the case in very young children and the elderly (Negin et al., 2015).

1.4 CURRENT DIAGNOSTIC TOOLS FOR EPTB – A CHALLENGE

Due to EPTB being able to affect almost any organ of the body, the clinical specimens for diagnosis are diverse. The type of EPTB a patient might get varies with gender, age, ethnicity, geographical area and predisposing risk factors such as previous history of TB, high prevalence of TB, HIV and diabetes (Norbis et al., 2014, Sharma et al., 2005, Martinez and Kornfeld, 2014). Samples from EPTB patients tend to be paucibacillary, thus decreasing the sensitivity of diagnostic tests (Al-Otaibi et al., 2012, Moure et al., 2012, Harries et al., 1998). Furthermore, some specimens (e.g. deep lymph nodes) are sometimes difficult to obtain depending on which organ is affected (Golden and Vikram, 2005). In addition, patients with EPTB have a wide spectrum of atypical clinical features and often present late in order to seek medical attention. This unfortunately leads to late diagnosis and thus delayed treatment initiation. This is a danger, especially in patients infected with meningeal TB who can die within a few days if not treated (Rock et al., 2008, Golden and Vikram, 2005). According to the WHO, the new regulation for EPTB diagnosis should be based on:

- One-culture positive specimen, or
- Positive histology, or
- Strong clinical evidence consistent with active EPTB (Norbis et al., 2014, WHO, 2014).

The clinical diversity of EPTB does not allow its diagnosis to be straightforward. None of the recommended diagnostic tests can be used in isolation mainly because most of them lack accuracy and have major drawbacks such as cross-contamination (Norbis et al., 2014). Culture is considered the gold standard for EPTB diagnosis in many countries (Davies and Pai, 2008). However, an approach where a combination of tests is used is still preferred (Tortoli et al., 2012, Kim et al., 2013, Valdés et al., 1998). Currently available diagnostic tests for EPTB are discussed below.

1.4.1 Smear microscopy

The principle of this test is based on the identification of the acid-fast bacilli (AFB) under the microscope following staining with Ziel-Neelsen (ZN). This test however lacks sensitivity even though it is used as a reference standard in low to middle income countries (WHO, 2014). In specimens with a high bacillary load (PTB patients) the sensitivity is low 50-60% (Perkins and Cunningham, 2007). In paucibacillary specimens, the sensitivity drops below 30% such as in paediatric TB (Chintu, 2007) or HIV-associated TB (Harries et al., 1998). In 2007, WHO rolled out and issued recommendations on the use of fluorescence microscopy (Marais et al., 2008, WHO, 2011). The principle of this technology is the identification of AFB after staining with auramine-rhodamine or auramine-O for visualization under the fluorescent microscope where the bacteria will fluoresce. The reason for the WHO endorsement was based on the improved sensitivity of 10% observed with this technology (Steingart et al., 2006). Furthermore, this technology had similar specificity and fast turnaround time when compared to conventional microscopy. However, it proved to be expensive (WHO, 2011, Steingart et al., 2006). Conventional microscopy is by far the simplest, most inexpensive test even though in

some cases more than one specimen per patient has to be processed (Craft et al., 2000), or an additional step of sample preparation has to be performed (Peterson et al., 1999, Uddin et al., 2013).

1.4.2 Culture

1.4.2.1. Solid Culture

Solid cultures are performed from clinical specimens on the Löwenstein-Jensen medium, which is egg-based, or the Middlebrook 7H9 or 7H10, which is agar-based. They have increased sensitivity compared to microscopy and are thus used as the "gold standard" in many countries (WHO, 2007). This test however requires about 3-8 weeks before a diagnosis can be made as it depends on bacterial growth (Davies and Pai, 2008). When drug-susceptibility testing is required an additional 3-4 week turnaround is expected. Further limitations include requirement for Biosafety level 3 (BSL-3) facilities and trained personnel; thereby precluding the use of solid culture in resource constrained settings.

1.4.2.2. Automated liquid culture

Compared to the solid culture, liquid culture offers increased sensitivity together with a speedy turnaround time of only 9-10 days. This test is based on the BACTEC Mycobacterial Growth Indicator Tube 960 (BACTEC MGIT 960, Becton-Dickson, USA), which is an improved version of the Middlebrook 7H9 broth with an oxygen-sensitive fluorescent detection technology (Tortoli et al., 1999). Additional advantages of this method include the possibility of performing drug-susceptibility testing as well as molecular epidemiology studies (Bergmann and Woods, 1997, Bemer et al., 2002). When these additional tests are required, however, the time to diagnosis increases to 1-3 weeks. The duration of the test to obtaining results depends on the requested test(s). The limitation of this test is the requirement of highly trained personnel and high costs. Although sensitive, such long waiting periods before obtaining results are not helpful in managing the TB epidemic,

especially EPTB (Thwaites et al., 2009). For example, because an EPTB specimen will likely have a low-bacillary load, chances are that the culture will be incubated for up to 6 weeks, which will then subsequently be discarded if negative. Moreover, despite the desired sensitivity of this test, it still does not meet requirements of a POC test (as outlined in **Table 1.1**).

1.4.3 Adenosine deaminase (ADA)

Adenosine deaminase (ADA) is an enzyme that catalyses the conversion of adenosine to inosine (Piras et al., 1978) and is implicated in mononuclear phagocyte maturation (Carson and Seegmiller, 1976, Fischer et al., 1976). Elevated levels of this ADA have been reported in cases of pleural TB (Valdes et al., 1996). ADA testing is in a colorimetric assay format, which is inexpensive, quick and fairly simple to perform in diagnosing pleural TB. This test has shown increased sensitivity when compared to culture (Banales et al., 1991, Diacon et al., 2003). Two meta-analyses by Greco et al and Liang et al reported sensitivity ranging between 47 and 100% and specificity ranging between 41 and 100% (Greco et al., 2003, Liang et al., 2008). However, when ADA levels were tested in immunocompromised patients such as HIV positive patients, the sensitivity was only 40-57% (Hsu et al., 1993, Corral et al., 2004). Therefore, testing ADA levels in pleural TB patients in an HIV-endemic setting might not be feasible.

1.4.4 Interferon-γ release assays (IGRAs)

Interferon-γ release assays (IGRAs) are *in vitro* immunodiagnostic tests, which use whole-blood to detect TB. The principle of IGRAs is based on the measurement of the IFN-γ released after the stimulation of T-cells following incubation with highly MTBC-specific antigens such as early secretory antigenic target (ESAT)-6 and culture filtrate protein (CFP)-10, which are encoded within the region of difference (RD)-1 not found in other species of the MTBC (Lein and Von Reyn, 1997, Pai et al., 2004). The test has high sensitivity; patients require a single visit and it takes

approximately 8-16 hours before results are available. There are currently two IGRA tests, which have been approved by the U.S. Food and Drug Administration (FDA) and commercially available. The first is the QuantiFERON®-TB Gold In-Tube test (QFT-GIT) (Cellestis Inc., Carnegie, Australia) and T-SPOT®.*TB* test (T-Spot) (Oxford Immunotec Ltd., Abingdon, UK). The key differences between the two tests are outlined in **Table 1.2**. These tests have sub-optimal accuracy and are unable to differentiate between active disease and latent infection (LTBI), especially in high TB or TB-HIV burden settings (Bendayan et al., 2012, Ling et al., 2011, Santin et al., 2012) and thus are not suitable to diagnose active TB. Furthermore, IGRAs have limited accuracy in diagnosing EPTB. Dheda and co-workers evaluate the performance of the two commercial tests, T-SPOT®.*TB* and QFT-GIT using pleural mononuclear cells to diagnose pleural TB. They reported sensitivities of 80% and 51%, and specificities of 65% and 94%, respectively. The T-SPOT®.*TB* was more sensitive, however its specificity was very poor (Dheda et al., 2009). In the same study, unstimulated IFN-γ in pleural fluid was measured using the QuantiFERON®-ELISA kit and yielded a sensitivity of 97% and specificity of 100%. The high level of accuracy using unstimulated IFN-γ suggested that it could be a good biomarker for the diagnosis of pleural TB (Dheda et al., 2009). A recent study investigating the utility of IGRAs in diagnosing EPTB reported the sensitivity and specificity of 81.8% and 80% for TB lymphadenitis. In addition, they also reported the sensitivity and specificity of 38.5% and 50.0% for pleural TB (Shin et al., 2015). Moreover, a meta-analysis by Fan et al reported pooled sensitivity of 72% and 90%, and specificity of 82% and 68% for GIT and T-SPOT®.*TB*, respectively (Fan et al., 2012).

Table 1.2: Differences in currently available IGRAs (Adapted from CDC, 2005)

	QuantiFERON®-TB Gold In-Tube test (QFT-GIT)	T-SPOT®.*TB* test (T-Spot)
Initial Process	Process whole blood within 16 hours	Process peripheral blood mononuclear cells (PBMCs) within 8 hours, or if T-Cell Xtend® is used, within 30 hours
***M. tuberculosis* Antigen**	Single mixture of synthetic peptides representing ESAT-6, CFP-10 & TB7.7.	Separate mixtures of synthetic peptides representing ESAT-6 & CFP-10
Measurement	IFN-γ concentration	Number of IFN-γ producing cells (spots)
Possible Results	Positive, negative, indeterminate	Positive, negative, indeterminate, borderline

1.4.5 Nucleic acid amplification tests (NAATs)

Molecular-based diagnostics are generally referred to as nucleic acid amplification tests (NAATs). These testes allow for detection of minimal amounts of DNA or RNA and the amplification thereof. In terms of TB, NAATs have (i) enabled identification of mycobacteria, (ii) detection of MTB directly from clinical samples, and in addition (iii) detection of drug-resistant TB (Cheng et al., 2005). They use different approaches, but mainly polymerase chain reaction (PCR), which can be conventional or real-time (Laraque et al., 2009, Reddington et al., 2011). These tests are based on the amplification of the DNA of either the host bacteria (*M.tb*) or the human DNA.

Many researchers have developed their own "in-house" PCR diagnostic assays. Flores and co-workers (2005) performed a meta-analysis of "in-house" diagnostic PCR assays of 84 studies reporting sensitivities and specificities ranging from 9.4-100% and 5.6-100%, respectively (Flores et al., 2005). Recently after this analysis, some studies reported sensitivity of 96 and 97%, and specificity of 81 and 95.3% in smear positive patients (Greco et al., 2009, Laraque et al., 2009). These results were

comparable to the commercially available NAATs developed specifically for the diagnosis of active TB. These include the Amplicor® mycobacterium tuberculosis (Amplicor MTB) assay (Roche® Diagnostic systems, Mannheim, Germany) and Amplified *Mycobacterium tuberculosis* Direct test (MTD test; Gen-Probe, San Diego, CA, USA), which performed with sensitivity below 95% and specificity of 100% in smear-positive TB (Cheng et al., 2005). Both these tests have also been evaluated on EPTB diagnosis. However, they yielded variable results. Using the MTD and the Cobas Amplicor test, the sensitivities were only 33% and 55.6%, respectively (Lang et al., 1998, Jönsson and Ridell, 2003). In-house PCR assays on pleural fluid had a sensitivity of below 70% and specificity of below 90% (Villegas et al., 2000, Nagesh et al., 2001, Davis et al., 2011).

A recent improvement of the NAAT is the Xpert® MTB/RIF assay commonly referred to as the GeneXpert® (Cepheid, Sunnyvale, CA, USA). The GeneXpert® is an automated test that uses heminested real-time PCR for the simultaneous detection of TB presence and drug resistance using RNA polymerase β-subunit (*rpo B)* gene as a target. The *rpo B* gene, a marker for rifampicin resistance, is encoded with a highly conserved 81-bp hot spot region (codon 507-533) comprised of more than 12 mutations (Miller et al., 1994). Rifampicin is an important first-line drug for MDR-TB treatment. This test is rapid with a turnaround time of 2 hours. The system is completely automated with the only manual step being the addition of buffer to the sample (Boehme et al., 2010, Helb et al., 2010). The test had a limit of detection of 131 CFU/ml (Blakemore et al., 2010). Many studies have been carried out using the GeneXpert® for the diagnosis of PTB reporting good sensitivities (95-100%) and specificities (94-100%) (Boehme et al., 2010, Helb et al., 2010, Theron et al., 2011), especially in smear positive samples.

With the global worry of the performance of this assay in HIV-endemic areas, where most TB cases are smear negative (as is also the case in EPTB), the performance was found to be different, with reported decreased sensitivities (49. 5% in cases of low

rates of HIV vs 40.6% in cases with high rate of HIV) for pleural TB diagnosis (Denkinger et al., 2014). In the case of TB meningitis however, the presence of HIV-co-infection did not affect sensitivity, but the addition of a concentration step in sample processing enhanced the sensitivity (84.2% vs. 51.3% for unconcentrated) (Denkinger et al., 2014). In addition, a South African study by Bates et al revealed a sensitivity of 68.8% using samples obtained from paediatrics and young children which included induced sputum and broncho-alveolar lavage, and were smear-negative (Bates et al., 2013). Moreover, Giang and co-workers (2015) reported a sensitivity of only 20.6% in paediatric TB, which was an increase of 11% of smear microscopy at a sensitivity of 9.2%, where they used clinical diagnosis as a gold standard (Giang et al., 2015).

More studies were performed using different EPTB samples. In a study by Patel and co-workers (2013) where CSF was used for the diagnosis of TB meningitis (TBM) on the GeneXpert®, they reported a sensitivity of 62% compared to smear microscopy at 12% and culture at 30% (Patel et al., 2013). Recent work in our laboratory showed that the accuracy of the GeneXpert® was limited when used to diagnose pleural TB, with the sensitivity and specificity of 22.5% and 98%, respectively (Meldau et al., 2014). Additionally, Tortoli et al reported the sensitivity and specificity of 33% and 100%, respectively (Tortoli et al., 2012). These data, therefore, suggest that the performance of the GeneXpert® for pleural TB detection is very poor. Other studies where lymph node aspirates and pericardial fluid were used reported suboptimal performance (Pandie et al., 2014, Scott et al., 2014). In contrast, improved sensitivity of 50-100% for lymph node TB and pooled specificity of 80% for TB meningitis were reported using GeneXpert® (Denkinger et al., 2014). Therefore, the data allowed the WHO to consider the use of GeneXpert® in EPTB diagnosis, except for pleural TB (where the performance was poor). Below is a table with all the studies that used the GeneXpert® to diagnose EPTB using different samples (**Table 1.3**).

Table 1.3: Meta-analysis of the sensitivity and specificity of Xpert MTB/RIF in the diagnosis of extra-pulmonary TB and rifampicin resistance in adults and children compared against culture as a reference standard (Adapted from WHO, Xpert MTB/RIF assay for diagnosis of PTB and EPTB Report, 2013).

Specimen type	Comparison to culture as reference standard	Median (%) pooled Sensitivity (pooled 95% Crl)	Median (%) pooled Specificity (pooled 95% Crl)
Lymph node and aspirate	14 studies, 849 samples	84.9 (72-92)	92.5 (80-97)
Cerebrospinal fluid	16 studies, 709 samples	79.5% (62-90)	98.6 (96-100)
Pleural fluid	17 studies, 1385 samples	43.7 (25-65)	98.1 (95-99)
Gastric lavage and aspirates	12 studies, 1258 samples	83.8 (66-93)	98.1 (92-100)
Other tissue samples	12 studies, 699 samples	81.2 (68-90)	98.1 (87-100)

Crl: credible interval (the Crl is the Bayesian equivalent of the confidence interval)

Diagnosing EPTB, especially pleural TB, is challenging. In light of the performance of the diagnostic tests discussed above, the need for developing a rapid diagnostic test has become urgent. None of these tests are POC. However, with the identification of good biomarkers and development of new technologies, a rapid, robust, inexpensive POC test can be developed.

1.5 IDENTIFICATION OF INTERFERON GAMMA (IFN-γ) AS A BIOMARKER FOR PLEURAL TB DIAGNOSIS

Current biomarker discovery studies focus more on PTB than on EPTB. To date there is a limited number of biomarkers identified for EPTB diagnosis. One of the biomarkers currently identified for use in EPTB diagnostics is IFN-γ, which plays a fundamental role in the immune response to tuberculosis infection. The first study undertaken to prove this showed that activated T-helper (Th) cells tend to localise themselves at the site of disease and are thus capable of producing huge amounts of cytokines including IFN-γ (Shimokata et al., 1982). After that, a few studies further proved the hypothesis that individuals infected with pleural TB had significantly higher IFN-γ levels compared to those without TB (Kim et al., 1997, Yamada et al., 2001, Sharma and Banga, 2004, Krenke et al., 2008, Wang et al., 2012, Keng et al., 2013, Meldau et al., 2014). The studies reported good diagnostic accuracy with sensitivities between 74 and 100% and specificities of 89-100% (Kim et al., 1997, Yamada et al., 2001, Sharma and Banga, 2004, Krenke et al., 2008, Wang et al., 2012, Keng et al., 2013, Meldau et al., 2014). Although these findings were promising, the assays used up until today are immuno-based. For examples, assays such as ELISA, make immunoassays still laborious, expensive, and with long turnaround times. One major drawback associated with this test is the batch-to-batch variability of the antibodies and a limited shelf life, which all leads to inconsistent results. To overcome this challenge, we thus explored the use of aptamers.

1.6 APTAMER TECHNOLOGY

1.6.1 What are aptamers?

Aptamers were first discovered in 1990 by two separate research groups (Ellington and Szostak, 1990a, Tuerk and Gold, 1990). Aptamers are synthetic single stranded nucleic acid molecules specifically generated against a variety of targets such as proteins, peptides and whole pathogenic micro-organisms (e.g. bacteria and viruses). They are known to bind their targets with high affinity and specificity through a

lock-and-key mechanism (**Figure 1.4**) (Tuerk and Gold, 1990). Aptamers can also fold into 3D-structures, and their length ranges between 30 and 90 nucleotides (Brody and Gold, 2000, Hermann and Patel, 2000).

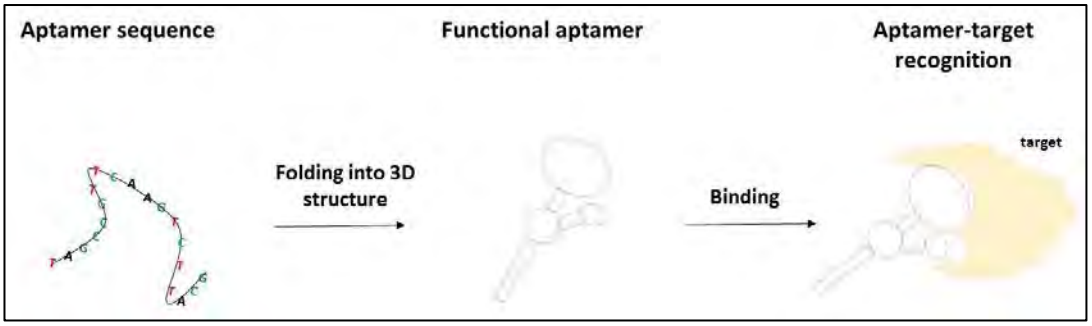

Figure 1.4: Schematic representation of aptamer-target binding.

Aptamers fold into 3-D nucleic acid structures that bind to target molecules via a high affinity lock-and-key mechanism.

1.6.2 How are aptamers made?

The method used to generate aptamers is known as SELEX, which stands for **S**ystematic **E**volution of **L**igands by **Ex**ponential enrichment (Ellington and Szostak, 1990a, Tuerk and Gold, 1990). SELEX is an iterative process performed in vitro using a combinatorial library. It involves three major steps: (i) incubation of target with library, (ii) separation of target-bound from unbound sequences and, (iii) the amplification of target-bound sequences (**Figure 1.5**). The library is comprised of about 10^{15} different random sequence nucleotides which have a fixed central region and two primers on either side. The library is incubated with the target of interest, and then the unbound oligonucleotide-target complexes are separated by using a suitable partitioning method such as nitrocellulose membrane (Gopinath, 2007, Kulbachinskiy, 2007). The bound oligonucleotide-target complexes are amplified using PCR and universal primers. The amplified pool is then used for the next round of selection. Once the saturation point is reached, the pool is cloned into a vector and subsequently sequenced (Stoltenburg et al., 2007). Since its inception, researches have optimised and modified the SELEX process. For example, Smith and

colleagues modified certain bases of the sequences contained in the starting library to ensure that the aptamers will be nuclease resistant (Smith et al., 1995). Over the years there have been many different SELEX protocols that have been developed and these are described briefly in **Table 1.4**.

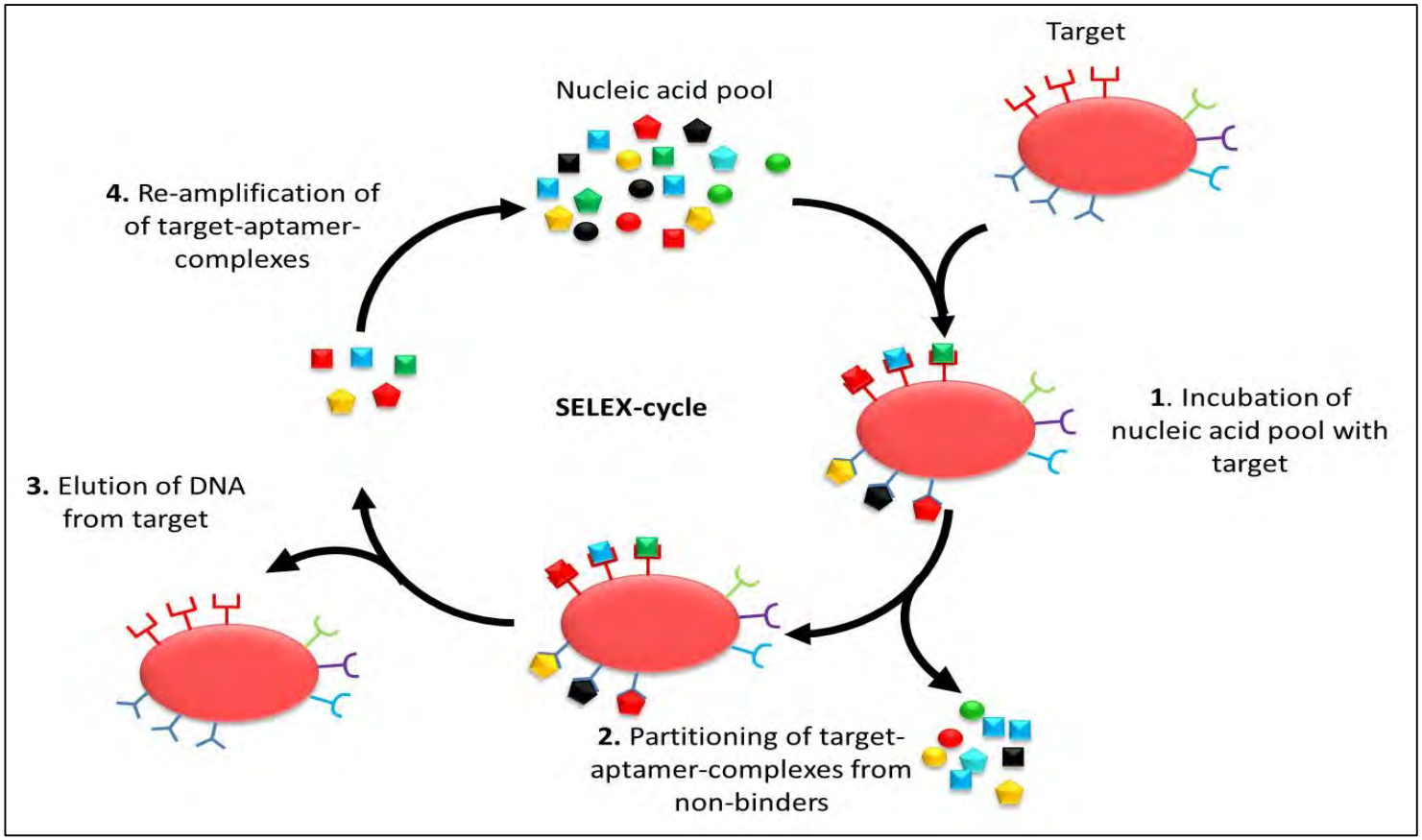

Figure 1.5: The Systematic Evolution of Ligand by EXponential enrichment (SELEX) process.

Briefly, typical SELEX procedures involve binding a random nucleic acid library to a target, separating the bound and unbound nucleic acids, and amplifying the bound nucleic acids by PCR for use in the next round of selection. After each round of selection, a smaller pool of nucleic acid sequences binding to the target is retained and the unbound nucleic acids are discarded. Typically, 8–15 rounds of SELEX are carried out in order to generate a pool of aptamers with sequences enabling the highest binding affinity for the target. These aptamers can then be cloned and sequenced.

Table 1.4: Timeline of SELEX procedure modifications (Adapted and modified from Millroy, 2013)

Year	SELEX Name	Brief description/ Improvement	Reference
1990	Classical Selection	Generation of aptamers selected using recombinant proteins.	(Teurk and Gold, 1990, Ellington and Szostak, 1990b)
1992	Negative selection	Process used to eliminate aptamers that bind to the partitioning matrix in use.	(Ellington and Szostak, 1992)
1994	Counter selection	Similar to negative selection, however uses analogues of the target to improve the selectivity.	(Jenison et al., 1994)
1995	Crosslinking/ Covalent SELEX	Selects aptamers that contains a reactive groups which covalently links to the target.	(Jensen et al., 1995a)
1995	Blended SELEX	Uses an RNA library which is annealed to a DNA that is attached to an enzyme inhibitor.	(Smith et al., 1995)
1995	Photo SELEX	Selection of aptamers that are high in specificity and have the ability to form photo induced bonds with the target.	(Jensen et al., 1995a, Jensen et al., 1995b, Brody et al., 1999)
1995	cDNA or Genomic SELEX	Uses the organism's genome to construct a SELEX library.	(Dobbelstein and Shenk, 1995)
1996	Spiegelmers or Mirror-image SELEX	Aptamers are chemically modified to include unnatural nucleotides making them nuclease resistant.	(Klussmann et al., 1996)
1997	Magnetic bead-based SELEX	Selection of aptamers by immobilising target protein on magnetic beads.	(Bruno, 1997)
1997	*In vivo* SELEX	Selected aptamers within cultured vertebrate cells.	(Coulter et al., 1997)
1998	Chimeric SELEX	Generates aptamers with more than one function through the use of different oligonucleotide libraries	(Burke and Willis, 1998)

Year	SELEX Name	Brief description/ Improvement	Reference
1998	Deconvolution SELEX	Selection is performed on mixtures to generate aptamers against complex targets.	(Morris et al., 1998)
1998	EMSA SELEX	Selection through the use of electrophoretic mobility shift assay (EMSA) as a partitioning method.	(Tsai and Reed, 1998)
1998	Automated SELEX	Uses an automated system to perform the SELEX for high throughput generation for aptamers.	(Cox et al., 1998)
1999	SELEX against live organism	Selection of aptamers through the use of surface proteins of live parasites.	(Homann and Goringer, 1999)
1999	Multi-stage SELEX	Modification of chimeric SELEX. The fused aptamer components undergo an additional selection step with all the targets.	(Wu and Curran, 1999)
2000	Indirect SELEX	Not the actual target is used during the selection, however the molecule used is target-dependent during binding with aptamer.	(Kawakami et al., 2000)
2000	Signalling Aptamer	Aptamers are labelled with fluorescent dyes and are able to detect molecules in solution.	(Jhaveri et al., 2000)
2001	Truncation SELEX	Selection of aptamers by complete elimination or reduction of fixed sequences of the oligonucleotide library.	(Pagratis et al., 2001)
2001	Crossover SELEX	Two targets are used in parallel during the selection.	(Hicke et al., 2001)
2001	Toggle SELEX	Aptamers able to cross-react with two homologous targets.	(White et al., 2001, Bianchini et al., 2001)
2002	Serial Analysis of gene expression (SAGE) SELEX	Links oligomers identified from SELEX with longer DNA molecules to enhance efficient sequencing	(Roulet et al., 2002)

Year	SELEX Name	Brief description/ Improvement	Reference
2003	SPR- SELEX	Isolation of aptamers using surface plasmon resonance (SPR) technology	(Khati, 2003)
2003	Subtractive SELEX	Isolation of aptamers which are able to distinguish between two closely related structures.	(Wang et al., 2003)
2003	Beacon Aptamer SELEX	Aptamer beacons are identified through the use of a fluorophore and a quencher.	(Rajendran and Ellington, 2003)
2003	On-chip selection	The technique selectively recognizes target using on-chip screening in combination with an *in silico* evolution method.	(Asai et al., 2003)
2003	Tailored SELEX	Generation of aptamers which are primer-free.	(Vater et al., 2003)
2004	Primer-free SELEX	The method involves the complete removal of primer-annealing sequences prior to the selection process.	(Wen and Gray, 2004)
2004	CE-SELEX	The selection of aptamers using capillary electrophoresis for separation of bound from unbound oligonucleotides.	(Mendonsa and Bowser, 2004)
2005	FluMag SELEX	The library is modified with fluorescein and the target is immobilised on magnetic beads during selection.	(Stoltenburg et al., 2005)
2005	Automated SELEX	The system used microfluidics and magnetic beads to generate aptamers.	(Eulberg, 2005)
2006	TECS-SELEX	Used to isolate aptamers for proteins expressed on the cell surface.	(Ohuchi et al., 2006)
2007	DeSELEX or Convergent SELEX	Selection strategy to isolate both proteins that are abundant and less abundant within the same proteome using two different modifications to the conventional SELEX.	(Layzer and Sullenger, 2007)

Year	SELEX Name	Brief description/ Improvement	Reference
2007	MonoLEX	Generation of aptamers in a single round of selection.	(Nitsche et al., 2007b, Peng et al., 2007, Nitsche et al., 2007a)
2008	Minimal primer-free SELEX	Procedure involves the partly removal of the primer annealing sequences prior to selection process (Adapted from Wen and Gray, 2004)	(Pan et al., 2008)
2008	Mod-SELEX	Generation of aptamers which are nuclease-resistant through the use of a chemically modified SELEX library.	(Keefe and Cload, 2008)
2008	Sol-gel SELEX	A SELEX-on-a-chip system, which utilized nanoporous sol-gel droplet microarrays to immobilize different target proteins in microfluidic chambers.	(Park et al., 2009)
2008	Cell Specific (CS) SELEX	Isolation of aptamers for specific cell receptors (adapted from Homann and Goringer, 1999).	(Shangguan et al., 2008, Homann and Goringer, 1999, Kim et al., 2009)
2009	Next generation SELEX	This approach entails specifically designed oligonucleotide libraries that tile through a pre-mRNA sequence. The pool is then partitioned into bound and unbound fractions, which are quantified by a two-colour microarray.	(Reid et al., 2009)
2009	*In silico* SELEX	The use of computational models in aptamer selection.	(Chushak and Stone, 2009)
2009	Microfluidic SELEX (M-SELEX)	Selection through the use of microfluidic channels creating a miniature SELEX platform.	(Lou et al., 2009)
2010	Multiplexed massively parallel SELEX	Selection allows for large numbers of transcription factors in parallel through the use of affinity-tagged proteins (adapted from Roulet et al., 2002).	(Jolma et al., 2010, Roulet et al., 2002)

Year	SELEX Name	Brief description/ Improvement	Reference
2010	Slow Off-rate Modified Aptamers (SOMAmer)	Selection of high-affinity aptamers for almost any protein target and the development of a novel highly-multiplexed assay for high-performance proteomics.	(Gold et al., 2010)
2010	Fluorescence-activated cell sorting (FACS) SELEX	Aptamers generated through the use of a fluorescence-activated cell sorter to differentiate and separate cell-bound aptamers from the non-bound.	(Mayer et al., 2010)
2012	Multivalent aptamer isolation (MAI) SELEX	Strategy for generating of aptamers pairs to bind distinct sites on a protein target.	(Gong et al., 2012)
2012	Internalising cell SELEX	The SELEX procedure is specifically for internalising aptamers.	(Thiel et al., 2012)
2012	GO-SELEX	The procedure is based on non-specific adsorption of ssDNA by graphene oxide (GO) and is an immobilization-free platform for screening of aptamers.	(Park et al., 2012)
2012	Capture-SELEX	Selection strategy is based on libraries with randomized region of only 30-50nt split in two by a non-variable region required for the capturing.	(Stoltenburg et al., 2012)
2013	RNA Aptamer Isolation via Dual-cycles (RAPID) SELEX	Selection process eliminates unnecessary amplification steps and performs amplifications only when higher numbers pool concentrations are required	(Szeto et al., 2013)
2014	Artificially expanded genetic information systems (AEGISs) AEGIS-SELEX	AEGISs are unnatural forms of DNA that increase the number of independently replicating nucleotide building blocks. AEGISs paired and joined by different arrangements of hydrogen bond donor and acceptor groups	(Sefah et al., 2014)

Year	SELEX Name	Brief description/ Improvement	Reference
2014	Multi-GO SELEX	A simple, high-throughput aptamer screening for a group of small molecules using graphene oxide without target immobilization (adapted from Park et al., 2012)	(Nguyen et al., 2014)
2014	Epitope-specific (ES)-SELEX	A selection of aptamers targeting a specific protein epitope with the aid of a known and specific ligand competitor and report	(Lao et al., 2014)
2014	Rapid Semi-automated SELEX	A semi-automated two-step method for *in vitro* selection of DNA aptamers using magnetic separation and solid-phase emulsion PCR	(Hünniger et al., 2014)
2015	Array-based discovery platform for multivalent aptamers (AD-MAP)	Selection process used to identify aptamer pairs through the use of M-SELEX and high-throughput sequencing (HTS)	(Cho et al., 2015)
2015	Capture-SELEX coupled with SPR evaluation and HTS analysis	Protocol developed for targeting small drug. Selection process features a long randomized sequence and the number of cycles required is reduced	(Spiga et al., 2015)

1.7 CLINICAL APPLICATIONS OF APTAMERS

Aptamers have widely been used in both therapeutics (Nimjee et al., 2005a, Nimjee et al., 2005b, Keefe et al., 2010) and diagnostics (Jayasena, 1999, Hesselberth et al., 2000, Santosh and Yadava, 2014). In therapeutics, aptamers need to have characteristics which include high specificity, stability and most importantly, be safe to be administered to humans. Studies have shown that aptamers do not illicit an immune response in therapeutic applications (White et al., 2001, Wlotzka et al., 2002). In diagnostics, aptamers have been used in many different assay formats. These include biosensors, sandwich assays similar to an enzyme-linked oligonucleotide assays (ELONAs), imaging, and recently microarrays, to mention a few (Drolet et al., 1996, Bang et al., 2005, Collett et al., 2005, Cho et al., 2006,

Citartan et al., 2012, McCauley et al., 2003, Pultar et al., 2009, Kara et al., 2010a, Kara et al., 2010b, Yao et al., 2009, Yao et al., 2010). Furthermore, companies have been setup to exploit the SELEX technology and aptamers. Two American companies, namely; SomaLogic, Inc. (Boulder, CO, USA) and Archemix Corporation. (Cambridge, MA, USA) hold licenses in diagnostic and therapeutic applications, respectively. The latter was the first to produce the aptamer-based drug, Pegaptanib, used to treat age-related macular degeneration (ARMD). This drug received FDA approval in 2004.

1.8 APTAMERS IN DIAGNOSTICS

The detection of molecules from pathogens (antigens and genetic material) and host molecules in response to infections (antibodies) is the basic principle of molecular diagnostics. Up until now, antibodies are the most widely used affinity tools in routine diagnostics. In spite of their relatively high production costs, reduced shelf life and variability in performance, antibodies are still the molecules of choice in diagnostic platforms (Ruigrok et al., 2011). To date, the most commonly used antibody-based used tests are the Western blot assay and ELISA. These tests however have limitations which aptamers have the potential to overcome. Thus, aptamers have been exploited as possible alternative tools in the development of different diagnostics platforms (Jayasena, 1999, Hesselberth et al., 2000, Ruigrok et al., 2011). **Table 1.5** outlines the different characteristics of aptamers compared to antibodies.

Table 1.5: Comparisons of properties of aptamers and antibodies

Property	Aptamers	Antibodies
Production	*In-vitro* through chemical synthesis	*In vivo* through the use of animal models
Size	5-20 kDa	15-25 kDa
Affinity	Low nanomolar to picomolar	Low nanomolar to picomolar
Stability	Not sensitive to temperature	Sensitive to temperature and undergo irreversible denaturation
Shelf life	Long-term storage at room temperature	Limited (require continuous cold chain storage)
Modification	Easy modification with no loss in affinity	Modification may cause possible loss in affinity
Kinetic parameters	On/off rates can be changed on demand	Cannot be changed on demand
Quality control	Little to no batch-to-batch variability	Batch-to-batch variability

In diagnostics, aptamers have mostly been used in detection systems and recognition elements (Proske et al., 2005). A few researchers have proved the utility of aptamers in different diagnostic platforms (**Figure 1.6**) to be feasible. This was achieved by incorporating aptamers in lateral flow systems (Chen et al., 2012, Xu et al., 2009), ELONA (Ferreira et al., 2008, Guo and Kim, 2012, Pultar et al., 2009, Barthelmebs et al., 2011), arrays (Cho et al., 2006, McCauley et al., 2003, Platt et al., 2009, Syrett et al., 2009) and biosensors (Hong et al., 2012, Song et al., 2008, Kara et al., 2010a, Kara et al., 2010b).

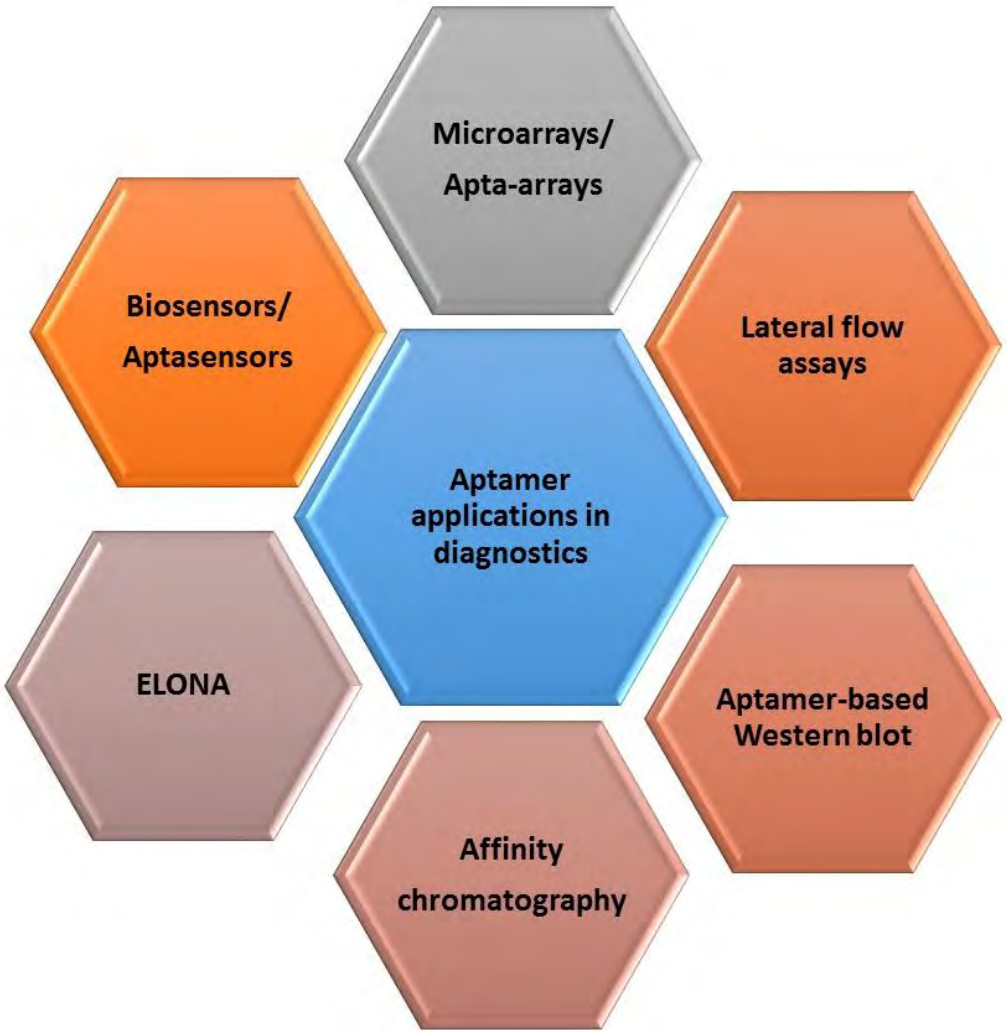

Figure 1.6: Schematic representation of the potential applications of aptamers in diagnostics.

A dry-reagent strip biosensor, also called the lateral flow biosensor using both conventional immunoassay and chromatography, has gained attention in clinical diagnostics. In one study this approach was coupled with aptamer-functionalized gold nanoparticles for a proof-of-concept (Xu et al., 2009). Aptamer-functionalized gold nanoparticles were used as probes to detect thrombin in human samples, and this was compared to an antibody-based strip biosensor. The proposed biosensor had a detection limit of 0.6pmol in the presence of other interfering proteins in the serum such as IgM, and outperformed the antibody-based strip in terms of sensitivity and specificity (Xu et al., 2009). In another study, a multiplex aptamer-based microarray

for the simultaneous detection of multiple analytes was developed (Cho et al., 2006). Two DNA and two RNA aptamers were printed on a coated slide and optimize to work simultaneously. In developing multiplexed protein detection microarrays, the critical parameters are the sensitivity, specificity, reproducibility, and signal-to-noise (S/N) ratio (Cho et al., 2006). Companies such as Somalogic and Achemix developed aptamer microarrays for the detection of photoaptamers (which could covalently cross-link bound protein targets) and aptamers associated with cancer proteins (McCauley et al., 2003, Bock et al., 2004).

Tennico and co-workers (2010) developed a bead-based aptamer sandwich assay using microfluidics for the detection and quantification of thrombin (Tennico et al., 2010). This approach enabled a high specificity and reduced costs. In another study using an electrochemical sandwich assay, a single aptamer was used to detect molecules in complex matrices such as lysates and blood, with a limit of detection in micromolar concentration (Zuo et al., 2009). This assay was simple and cost-effective; and performed on a format that was re-usable, making it a potential platform for use at POC (Zuo et al., 2009).

Biosensors that employ aptamers as a recognition element are called aptasensors (O'Sullivan, 2002). Aptasensors have a great promise in biosensing due to their high sensitivity, cost-effectiveness, selectivity, portability and simple instrumentation (Minunni et al., 2004). A typical biosensor will consist of three components, namely, a biological sensing element (that "recognizes/bind" the analyte), a transducing element (which converts the binding/detection into a measurable signal), and a display, which transforms the measured signal (optical/electrical) into a digital format for the end user (Cheng et al., 2009). Several aptasensors have been developed for clinical diagnostics and those include a sandwich assay with electrochemical-based sensor for thrombin detection, a piezoelectric quartz crystal sensor for IgE quantification and a multiplex cancer marker detection system to name a few (McCauley et al., 2003, Centi et al., 2007, Yao et al., 2009). The main

advantage of aptasensors, more so electrochemical aptasesnors, is that the sensitivity can be enhanced by labelling the aptamer-target complex to amplify the signal. Also, these sensors are convenient for on-field applications as they do not require expensive instrumentation (Torres-Chavolla and Alocilja, 2009). To date, the most successful commercialized biosensor still remains the POC glucose meter reader, in various hand-held formats that use disposable reagent cartridges (Turner et al., 1999).

1.9 SIGNIFICANCE OF THE STUDY

The burden of TB in South Africa is steadily increasing; this is partly due to the delay in diagnosis and treatment. Almost 500 000 prevalent cases of TB are treated in SA annually at great cost to the economy and human life. There is a need for an ASSURED POC test to overcome this challenging disease, which has been around for more than a century. The dual epidemic of TB and HIV also poses a great challenge as TB presentation in these patients is atypical. Therefore to help address the challenges presented by TB diagnosis, this study focused on developing an aptamer-based electrochemical biosensor, which would conceptually allow for rapid testing of EPTB, in a high-throughput platform.

1.10 AIMS AND OBJECTIVES OF THE STUDY

The aim of this thesis was to isolate and characterize ssDNA aptamers against IFN-γ for the development of different EPTB diagnostic tools.

Thus, the objectives of the study were to:

- isolate aptamers binding to IFN-γ with high affinity and specificity;
- determine binding kinetics of IFN-γ aptamers with desirable functional properties such as high specificity; and
- incorporate the selected candidate aptamers into different diagnostic platforms.

1.11 SCOPE AND STRUCTURE OF THE THESIS

Chapter 2 describes the optimisation of the SELEX protocol for the isolation of ssDNA aptamers against IFN-γ.

Chapter 3 focuses on the characterisation of the identified aptamers using different assay platforms such as ELONA and surface plasmon resonance (SPR). In addition, bioinformatics tools were used to determine the structural properties of the selected aptamers.

Chapter 4 focuses on the further characterisation of the high-binding aptamers selected for possible use in different downstream application. In this chapter, I further selected one aptamer and performed different assays to characterise it for possible incorporation into a biosensing device.

Chapter 5 summarises the overall key finding and provides recommendations and future work. Limitations of the study are highlighted and a general conclusion of the thesis is made.

CHAPTER 2
ISOLATION OF SINGLE-STRANDED DNA APTAMERS THAT BIND IFN-γ

SUMMARY

EPTB, a form of TB, is challenging to diagnose. Current tests rely on detecting the bacillus, but they perform poorly (e.g. Culture and GeneXpert). IFN-γ is a promising biomarker for EPTB but POC diagnostic tools are lacking. Aptamers (described in detail in chapter 1) have been an attractive technology since their discovery in the early nineties. In this chapter, this approach is investigated using the well-characterised EPTB biomarker; IFN-γ. I generated single-stranded DNA (ssDNA) aptamers using the **S**ystematic **E**volution of **L**igand **Ex**ponential Enrichment process (SELEX). I performed eight rounds of selection and cloned the library into a vector at round 6, where the recovered ssDNA was 50%. Using standard molecular biology protocols, the final recovered pool was cloned, sequenced and screened for binding. The sequences were aligned and analysed for homologous residues, and to identify related aptamers using a phylogenetic tree. Up to 60% conservation within the 49-nucleotide random region was found, and the consensus sequence also identified. Aptamers were also found in clusters on the phylogenetic tree. Five clusters and 2 sub-clusters were identified. Some aptamers were found in duplicate and others appeared distantly related. Fifty four aptamers were screened for binding using Enzyme-linked Oligonucleotide Assay (ELONA), and 75% (41/60) significantly bound IFN-γ. Six of the 41 aptamers that significantly bound IFNγ were randomly selected for further characterisation through binding kinetics studies to determine their respective affinities. Their respective secondary structures were also determined using bioinformatics tools and *Mfold* algorithms.

2.1 INTRODUCTION

The presence of HIV makes EPTB even more challenging to diagnose, and the incidence of EPTB is almost 5 times higher in those infected with HIV (Sharma and Mohan, 2004). In South Africa, where the prevalence of HIV in high, this suggests that EPTB is the leading cause of morbidity and mortality (Karstaedt, 2013, Karstaedt and Bolhaar, 2014). Clinical presentations of EPTB are diverse (Sharma SK, 2004). It has poor prognosis, and acid fast bacilli (AFB) smears are seldom positive (less than 5% of cases) (Escudero, 1990, Epstein et al., 1987). This results in delayed diagnosis, late treatment initiation (Golden and Vikram, 2005) and therefore poor clinical outcome. Because EPTB is paucibacillary, biomarkers are an important avenue of research. Biomarker discovery has focused more on pulmonary tuberculosis and not so much on the disseminated forms of TB (Fortún et al., 2014). Furthermore, several studies highlight how the turnaround time of the current existing diagnostic tools do not assist in early treatment initiation as they are cumbersome, laborious and expensive, with most only having moderate sensitivity (Dinnes et al., 2007, Pai et al., 2009, Gupta et al., 2010). POC tests are needed because a same day clinical outcome will be achieved where a patient does not have to go away before treatment is initiated. However, even though POC tests are available, their biggest disadvantage is that they are far away from the patients. Studies have shown that even though tests are available at the point of care, patients' initiation on treatment is delayed (MacPherson et al., 2014, Theron et al., 2014). This makes the development of novel and accurate diagnostic tools, which may supplement or replace existing methods, a necessity (Geojith et al., 2011).

Nucleic acid amplification tests (NAATs) have been attractive diagnostic tools for the last decade. The main advantages are the increased sensitivity, specificity and the turnaround time of these tests. The GeneXpert MTB/RIF assay (Cepheid, Sunnyvale, CA, USA), which is a newer NAAT technology, has been shown to have overall good specificity and sensitivity, at 100% and 98% respectively, in pulmonary TB (Blakemore et al., 2010, Helb et al., 2010). This technology has also been used to diagnose some forms of EPTB. On pericardial TB, it showed specificity and sensitivity of 100%:63%, 59%:62%, respectively, and in TB meningitis 99.5%:95%

(Patel et al., 2013, Nhu et al., 2014). On pleural TB the performance was poor (sensitivities 23%; 47% and specificities of 98%; 94%) in independent studies carried out in South Africa recently (Meldau et al., 2014, Scott et al., 2014). The latest WHO report on the performance of GeneXpert MTB/RIF assay on diagnosing EPTB shows that most studies showed poor to moderate sensitivities with good specificity (WHO, 2013). So, even with NAATs improved tools for diagnosis of some types of EPTB, especially pleural TB are needed. A lack of good biomarkers has contributed to the delay of the development of POC tests for diagnosing EPTB. One of the most studied biomarkers is adenosine deaminase (ADA), an enzyme that catalyses the conversion of adenosine to inosine. This marker was first tested for its usefulness in diagnosing patients with pleural tuberculosis in 1987 and was also demonstrated to be a fairly simple test to perform (Piras et al., 1978). These tests, however, have moderate sensitivity and specificity (Greco et al., 2003, Goto et al., 2003). Interferon gamma (IFN-γ), a pro-inflammatory cytokine that is produced by T-helper (CD4) cells and cytotoxic T-cells was discovered and its functions reviewed (Boehm et al., 1997, Wheelock, 1965). It has recently been shown to be a promising biological marker for the diagnosis of EPTB with both high sensitivity and specificity (Jiang et al., 2007, Eldin, 2012, Dheda et al., 2009). When used in an ELISA format, this marker has a specificity of 76-100%, but the sensitivity ranges from 11-77% (Steingart et al., 2007). Based on this evidence, I explored molecules known to have both good specificity and sensitivity, here after referred to as aptamers. These molecules are small (8-25 kDa) compared to their counterparts, antibodies, which are ±150 kDa in size. In addition, due to their small size, they bind their targets with high specificity and affinity, hence they are preferred over antibodies (Jayasena, 1999).

Aptamers for TB have previously been isolated using targets like MPT64, ESAT6:CFP10, EsxG, lipoarabinomannan (LAM), H37Rv bacteria and IFN-γ (Rotherham et al., 2012, Qin et al., 2009, Tang et al., 2014, Ngubane et al., 2014, Cao et al., 2014, Chen et al., 2007, Pan et al., 2014, Balasubramanian et al., 1998). These aptamers were used for both therapeutic and diagnostic purposes. Both Rotherham et al (2012) and Tang et al (2014) isolated ESAT6:CFP10 aptamers with a sensitivity and specificity of 100% and 68%, and 100% and 94%, respectively,

using clinical samples for the diagnosis of pulmonary tuberculosis (Rotherham et al., 2012, Tang et al., 2014). Lee and co-workers (1996) and Balasubaramanian et al (1998) isolated an IFN-γ aptamer to study its effect on the structure of IFN-γ and further demonstrated its inhibitory factor. On the other hand, a recent study by Cao et al raised an IFN-γ aptamer to use in an immunological platform using intracellular cytokine staining (ICS) for the assessment of T-cell reactivity (Lee et al., 1996, Balasubramanian et al., 1998, Cao et al., 2014). Interferon gamma has been shown to be significantly increased in pleural tuberculosis compared to other infectious diseases that illicit an immune response (Jiang et al., 2007, Dheda et al., 2009, Eldin, 2012) . Thus, this chapter describes the development of novel ssDNA IFN-γ aptamers for the detection of pleural TB, with the intention to detect unstimulated IFN-γ in a complex matrix such as pleural fluid.

2.2 MATERIALS AND METHODS

2.2.1 Isolation of aptamers against interferon gamma protein

2.2.1.1 Recombinant interferon gamma protein

Recombinant human interferon gamma (rIFN-γ) was purchased from Biocom Biotech Inc. (Pretoria, South Africa). One milligram of lyophilised rIFN-γ was re-suspended in 1ml of distilled water to bring the final concentration to 1 mg/ml. The concentration was measured using the bicinchoninic acid (BCA) assay (Pierce, Thermo Scientific, USA) (Adilakshami and Laine, 2002, Fischer, 1999, Prozialeck, 2002, Roberts, 2002) as described in detail below (**Section 2.2.1.1.1**). The size and quality of IFN-γ was confirmed on a sodium dodecyl sulphate-polyacrylamide gel electrophoresis (SDS-PAGE).

2.2.1.2 Quantification of interferon gamma concentration by BCA

The BCA assay is a sensitive colorimetric assay based on the reduction of Cu^{2+} to Cu^{+} by proteins. The BCA protein assay kit (Thermo Scientific Pierce, Rockford, IL, USA) was used to quantify total protein for all experiments. Briefly, serial dilutions (125-2000 µg/ml) from standards of bovine serum albumin (BSA), using distilled water were used to generate a standard curve. Crude protein was prepared and 10 µl of all samples, plus 200 µl of working reagent were loaded onto a non-protein binding 96-well plate (Corning, Adcock and Ingram, South Africa) and incubated at 37 °C for 30 min. The plate was cooled to room temperature and the absorbance measured within 10 minutes (min) at 562 nm using a Multiskan-Go microplate reader (Thermo Fisher Scientific, Rockford, IL, USA). Unknown concentration of the interferon gamma was extrapolated by fitting a linear regression line.

2.2.1.3 Analysis of protein by sodium dodecyl sulphate-polyacrylamide gel electrophoresis

In order to validate the molecular weight and determine the purity of the protein, an SDS-PAGE was used. SDS is an amphipathic detergent, known to bind to protein in a non-covalent manner. It also causes proteins to denature and dissociate from each other, while also conferring a negative charge. To separate the protein, a 17%

resolving gel was prepared as outlined in **Table S2.1**. The gel was poured to two-thirds of a gel casting system (Biorad Laboratories, CA, USA), and the remaining space was filled with 100% ethanol (Merck, Darmstadt, Germany) to ensure an even surface while setting. After setting, the ethanol was poured off and the 4% stacking gel (**Table S2.2**) layered on top of the resolving gel.

2.2.1.4 Aptamer libraries

The first step in Systematic Evolution of Ligand by Exponential enrichment (SELEX) process (**Figure 2.1**) was to create a pool of variant sequences from which RNA or DNA ligands of relatively high affinity for target proteins can be selected. A library comprised of a central randomized region of 20-80 nucleotides, flanked by constant regions, which are used as primer annealing sites for the selection is commonly used for SELEX. The length of the random region determines the complexity of the library. Therefore, a library with a random region of about 20 nucleotides will yield 4^{20} unique sequences (Sassanfar and Szostak, 1993, Jayasena, 1999). The molecular diversity of a library depends on the number of randomized nucleotide positions. In theory, a library with a 40nt random region is represented by 1.2×10^{24} individual sequences, simply put $4^{40} = 1.2 \times 10^{24}$. Typically, libraries of 10^{14}- 10^{16} of ssDNA fragments are preferred (Marshall and Ellington, 2000, Pan and Clawson, 2009).

Usually, shorter random regions are preferred as they are just as efficient, cost-effective and much better manageable (Jayasena, 1999). It is not uncommon though to use libraries with longer random regions (up to 120 nucleotides), especially for RNA libraries. They have the ability to form a variable number of different structures and increase the complexity of sequences, increasing the efficiency of the selection method used (Conrad et al., 1996) and providing better opportunities for the identification of aptamers (Marshall and Ellington, 2000). In most cases though, long aptamers end up being truncated as they prove to be cumbersome and unmanageable. Therefore, these aptamers are truncated to yield shorter functional derivatives, as shown by Bock et al, who truncated the human thrombin DNA aptamer comprised

on a 60 nucleotide random region, to a mere 15 nucleotide, which retained the same binding affinity.

For the selection of ssDNA IFN-γ aptamers, a 90mer oligonucleotides library randomized at 49 nucleotide positions and primers were designed and synthesized by Integrated DNA Technology Inc. (Integrated DNA Technology Inc, Iowa, USA). The library used was flanked by constant regions, which were used as primer annealing sites for the selection. The forward primer was modified with biotin at the 5′-end and the reverse with phosphate at the 5′-end. The oligonucleotide library and primer sequences are listed in **Table S2.3**.

2.2.1.5 In vitro selection of ssDNA aptamers

During the selection process, molecules that bind the target with high affinity and specificity will be identified from the thousands of sequences contained in the oligonucleotide library. In most cases selection conditions play a great deal in the properties of the aptamers to be obtained. For example, the number of rounds to be performed depends on the degree of stringency introduced at each round. Furthermore, the type of molecule used as the target, the type of oligonucleotide library, and the partitioning method used all play a great role in the selection process (Stoltenburg et al., 2007). For instance, the conditions can influence the secondary structure, specificity, affinity, stability, and most importantly the dependence or absence thereof of specific ions and salts to promote binding to the target (Irvine et al., 1991).

SELEX consists of three main stages: (i) the incubation of the oligonucleotide library with the target; (ii) the partitioning of target-bound complexes from non-binders; and (iii) the amplification of the target-bound complexes (detailed steps of the selection procedure are presented in Chapter 1, **Figure 1.5**). The procedure consists of several rounds of the three main stages, where an enrichment of several orders of magnitude is expected after each round. On average 5-15 rounds is sufficient to produce good quality aptamers. A standard SELEX protocol was carried out as set-out below.

2.2.1.5.1 Incubation of interferon gamma with oligonucleotide library

Prior to the positive selection, the library was incubated with the nitrocellulose membrane in absence of the target (negative selection). This was done to eliminate sequences that specifically bound to the membrane. For the positive selection, 500 pmol of ssDNA library was used in order to obtain a diversity of at least 10^{14} unique sequences. The ssDNA library was refolded in 1X HMCKN selection buffer (20 mM Hepes, 2 mM $MgCl_2$, 2 mM $CaCl_2$, 2 mM KCl, 150 mM NaCl; pH 7.4) by being denatured at 95°C for 3 min, renatured by immediately cooling on ice for 5 min and then left to reach room temperature. This was done to allow the nucleotides to dissociate from other conformations they could possibly be in, and assume their most stable conformation when in selection buffer. Twenty microliters of IFN-γ protein (1 mg/ml) was added and the mixture incubated for an hour at room temperature. Stringent conditions were introduced only after round 3, where the number of washes were increased from one to two. This was after the selection progress showed a steady increase. This was followed by an additional 2 rounds of positive selection, before a negative selection was introduced after round 5. Other stringent conditions such as a change in salt concentration or a decrease in target (IFN-γ) to ssDNA ratio were kept constant throughout the selection process.

2.2.1.5.2 Partitioning of target binders from non-binders

The most critical step in the selection process is the partitioning of target-oligonucleotide binders from non-binders. This can be achieved using different methods as described in detail in a review by Gopinath (2007). The nitrocellulose membrane is commonly used for partitioning (Tuerk C, 1990, Ellington and Szostak, 1990b). It is easy to use as there is no need for the immobilisation of the target on a surface. Since nitrocellulose membranes (Merck, Millipore, Germany) have been shown to bind non-specifically to proteins (Tuerk C, 1990, Schneider et al., 1992), it was crucial that a negative selection be performed prior to each positive selection. Generally this partitioning method is preferred for protein targets (Gopinath, 2007).

The nitrocellulose membrane (Merck, Millipore, Germany) was pre-treated with 0.5 M KOH solution for 20 min at 22°C, rinsed extensively with dH_2O, then soaked in 100 mM Tris-HCl (pH 7.5), and subsequently stored in the same buffer at 4°C. This caused the membrane to be fragile, and caution when handling was necessary. The membrane was soaked in 1X HMCKN selection buffer for an hour. The pre-treated membrane was then locked into a filter disk holder and ssDNA-protein complexes were passed through. This was followed by washing three times with 300 µl 1X HMCKN binding buffer to eliminate all non-specifically bound oligonucleotides. To elute the bound ssDNA-protein complexes, the membrane was transferred to a clean glass plate and cut into 8 pieces using a sterile scalpel blade. The pieces were then transferred into a microcentrifuge tube, and 200 µl of elution buffer (100 mM Sodium citrate, 3 mM EDTA, 7 M urea) added. The solution was heated at 100°C for 5 min to release the bound complexes from the membrane. This was followed by an addition of 600 µl of phenol chloroform (pH 7.9), and an incubation of 25 min before extraction. Subsequently, the aqueous solution was removed and precipitated by adding 150 µl of 3 M sodium acetate (pH 5.2) and 1 ml of 100% ethanol (Merck, Darmstadt, Germany) and stored overnight at -80°C. The next day, the recovered ssDNA was centrifuged at 14 000 rpm for 30 min at 4°C. The supernatant was decanted and the pellet washed once with 70% ethanol, and left to air dry before being re-suspended in 30 µl sterile dH_2O. The ssDNA was quantified using the Nanodrop® ND-100 spectrophotometer v3.0.1 (Thermo Scientific, MA, USA) and the percentage recovery determined.

2.2.1.5.3 Amplification of target-bound pool by PCR

The recovered ssDNA pool was amplified using PCR under mutagenic conditions (**Table S2.4** and **Table S2.5**) in order to increase the variation of the molecules (Cadwell and Joyce, 1994).The unusually high *Taq* polymerase and $MgCl_2$ concentrations increased the error rate of PCR by stabilizing the non-complementary pairs and increasing the pH (Cadwell and Joyce, 1992, Leung et al., 1989). It is crucial however, that this is carried out in an unbiased fashion. Therefore, over amplification needs to be avoided as this only increases the yield, but not the diversity per se. Most of the mutations introduced are point mutations and they are

commonly A→T or T→A substitutions. A pilot PCR was setup in order to determine the minimum number of cycles needed to optimally amplify the pool. A reaction master mix was set-up using 10% of the recovered ssDNA. The master mix was aliquoted equally into four 0.2 ml tubes and PCR performed for 4, 6, 8 and 10 cycles respectively. A non-template control (NTC) was included in every PCR experiment. The samples were subsequently analysed on a 12% non-denaturing PAGE (**Table S2.6**), stained with ethidium bromide, and viewed using ultraviolet (UV) trans-Illuminator GelDoc™ XR system (Biorad Laboratories, CA, USA). Five microliters of low range DNA marker (Fermentas, Thermofisher Scientific Inc., MA, USA) were loaded in order to determine the correct size of the band. PCR reactions were then prepared with the entire ssDNA pool, using the appropriate number of cycles (as determined by the pilot PCR). Products were pooled (including the one used for the pilot PCR) and subsequently purified using the Nucleospin Extract II PCR cleaning kit (Macherey-Nagel, Düren, Germany), as outlined by the manufacturer. The purified dsDNA was quantified using the Nanodrop® ND-100 spectrophotometer v3.0.1 at 260nm (Thermo Scientific, MA, USA).

2.2.1.5.4 Generation of ssDNA by Lambda exonuclease digestion

Single-stranded DNA is required to perform the SELEX, and it is an essential and also important step. The Lambda exonuclease method was used to generate the ssDNA. This method required that the reverse primer of the SELEX be phosphate-labelled at the 5′-end, which will allow the one strand of the double-stranded (dsDNA) to be phosphorylated, then subsequently digested with the lambda exonuclease enzyme. The other strand will thus still be retained.

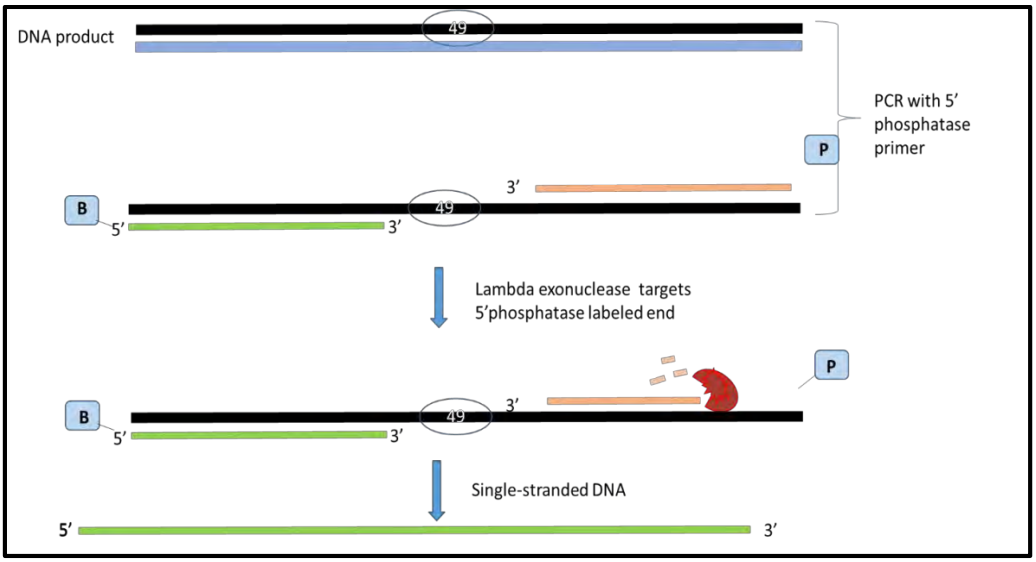

Figure 2.1: The Lambda Exonuclease digestion process.

Lambda exonuclease is a recombinant enzyme that digests a single strand of a duplex DNA in the 5'-3' direction. The 5'-end will be phosphorylated and generating single-stranded DNA. An enzymatic procedure where double stranded DNA is digested to single-stranded DNA by means of the lambda exonuclease enzyme digesting on the 5'-phophate labelled end of the sequence.

About 6.6 µg of the generated dsDNA, was lambda exonuclease digested (**Figure 2.1**) by adding 10 µl of exonuclease buffer (10×) (New England Biolabs® Inc., MA, USA), 6 µl of exonuclease enzyme (50 U) (New England Biolabs® Inc., MA, USA) and water up to a total volume of 100 µl. The reaction mixture was incubated for 4 h at 37°C and terminated by incubating at 72°C for 10 min. The ssDNA was then purified using the Nucleospin Extract II PCR cleaning kit (Macherey-Nagel, Düren, Germany), according to the manufacturer's guidelines, and quantified on the Nanodrop® ND-100 spectrophotometer v3.0.1 at 260nm (Thermo Scientific, MA, USA). A 12% non-denaturing PAGE with a dsDNA product as a control was run to determine the purity and quality of the ssDNA. The enriched ssDNA pool was now ready for the next round of selection.

2.2.2 Cloning and sequencing of ssDNA aptamers

In order to further characterize the aptamers, their sequences had to be known. This was accomplished by cloning the final recovered aptamer pool from the SELEX. After the highest recovery of ssDNA was determined at round six, following an introduction of a negative selection (in the absence of the target protein), the

recovered pool was cloned. First, the pool was amplified and ligated into a pGem-T Easy vector (Promega, WI, USA). The ligation reaction was prepared as outlined in **Table S2.7**, following an incubation step for 1 hour at room temperature with slight agitation. Transformation was carried out by inserting the vector construct into competent *E. coli* TOP10 cells (Invitrogen, CA, USA). Briefly, two microliters of the ligation reaction as set out in **Table S2.7** were added to 50 µl of cells and incubated on ice for 20 min, with occasional mixing. Cells were then heat shocked at 42°C for exactly 45 s, and immediately put back on ice for 2 min. SOC medium (Invitrogen, CA, USA) was added to the cell mixture to a final volume of 1 ml, and incubated at room temperature for 1½ h while shaking. A 100 µl of the mixture was plated onto ampicillin positive nutrient agar plates (Sigma-Aldrich, MO, USA) and incubated overnight at 37°C.

After transformation, 96 colonies were randomly picked and spread onto Luria Broth (LB) agar plates (5% NaCl, 5% yeast extract, 10% tryptone) containing 100 µg/ml of ampicillin (Sigma-Aldrich, MO, USA) and 5-bromo-4-chloro-3-indolyl-β-d-galactopyranoside (X-gal) for blue-white colony screening. Clones were sequenced with M13 universal primers (pUC/M13): primer forward: 5′-CCCAGTCACGACGTTGTAAAACG-3′ ; reverse primer: 5′-AGCGGATAACAATTTCACACAGG-3′ (Inqaba Biotech, Pretoria, South Africa). Glycerol stocks were prepared by making overnight cultures from the 96 randomly picked colonies. The following day the cultures were centrifuged and the pellet and transferred to Eppendorf tubes, and Tween 20 added to the tube. The tubes were snap-freezed using nitrogen and stored at -80°C for future experiments. The analysis of sequences was done using the CLC Sequence Viewer v7.5 (http://www.clcbio.com) (CLC Bio, Aarhus, Denmark), and CLUSTAL W (http://www.ebi.ac.uk/clustalw/) application of BioEdit v7.1.3.0 (Hall, 1999). Sequences were aligned to identify and assess conserved motifs; and to also generate a maximum likelihood tree. Bootstrapped neighbour joining phylogenetic tree with the bootstrap value set to 1000 was generated. The default setting of gap penalties was used.

2.2.3 Binding assay of ssDNA aptamers using the ELONA

ELONA was used to determine the binding of the aptamer to the target, IFN-γ (**Figure 2.2**). This procedure was first described by Drolet and co-workers in1996. A 96-well microtitre plate (Corning, Adcock and Ingram, South Africa) was coated with 10 µg/ml of protein in 10 mM $NaHCO_3$ coating buffer (pH 8.5) using 50 µl per well. The plate was sealed and stored at 4 °C overnight. On the second day, the plate was washed three times with 100 µl of phosphate buffered saline containing 0.05% (v/v) Tween-20 (PBS-T) (pH 7.0) (Sigma-Aldrich, MO, USA) and blocked with 150 µl of 10% (w/v) fat-free milk, then incubated for one hour at 4°C. The plate was washed four times with 100 µl PBS-T and blotted dry after the last wash. Aptamers were prepared at a final concentration of 300 nM and then denatured at 95°C for 3 min, cooled on ice for 5 min, and brought to room temperature before being used. Fifty microliters of each aptamer was added to each well in triplicate.

Three controls were included on each plate. These included the blank (buffer only), aptamer alone control (in absence of IFN-γ) and the IFN-γ-alone control (in absence of aptamer). The plate was sealed and incubated at room temperature for two hours. Then it was washed three times with 100 µl of PBS-T and blotted dry after the last wash. Fifty microliters of Streptavidin-conjugated HRP (diluted 1:10 000 in PBS-T) (Kirkegaard & Perry Laboratories, MD, USA) was added to each well and the plate sealed and incubated at 37°C for two hours. The forward primer used for PCR was modified with biotin at the 5′-end, in order to enable the aptamer to react with the streptavidin-conjugated HRP in this procedure. After two hours, the plate was washed three times with 100 µl of PBS-T and blotted dry after the last wash. The substrate was prepared by adding equal volumes of peroxidase solution and 3, 3′, 5, 5′ tetramethylbenzidine (TMB) solutions (Thermo fisher Scientific, Rockford, USA), and 50 µl was added to each well. A blue colour change was seen almost instantly with the naked eye. The reaction was terminated by using a 2 M sulphuric acid solution, which changed the colour from blue to yellow. The plate was read on a Mulitskan-Go microtitre plate reader (Thermo Scientific, MA, USA) at 450 nm.

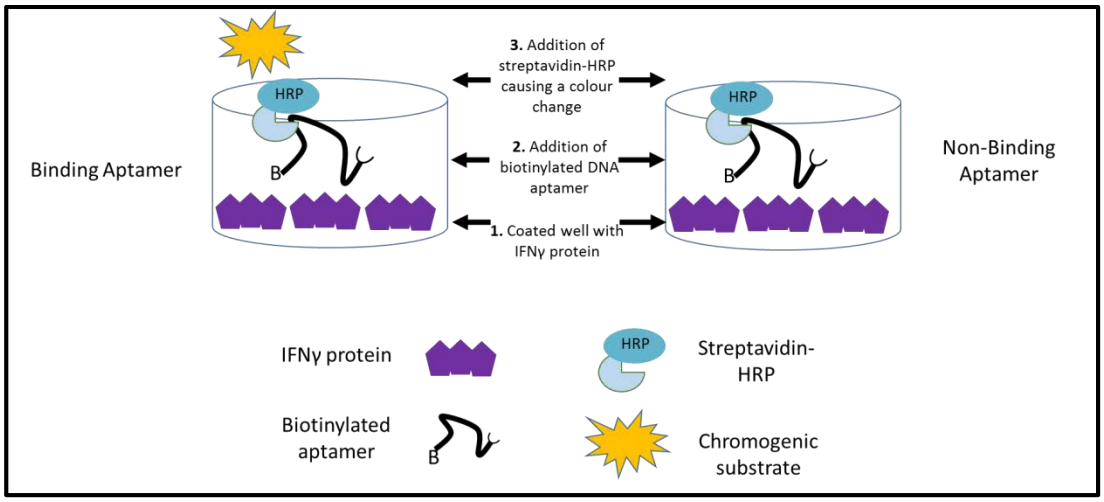

Figure 2.2: Detection of IFN-γ by biotin-conjugated aptamers using ELONA.

In a separate well, IFN-γ was coated and an aptamer introduced after washing and blocking with 10% fat-free milk. A streptavidin-HRP conjugated enzyme was introduced and the TMB chromogenic substrate added before reading at 450nm on a plate reader.

Each aptamer was tested in triplicate, in two independent experiments performed on different days. The repeats were averaged and the standard deviation calculated. The buffer only (blank) was averaged and subtracted from each well, in order to get rid of the background noise. The data was then normalized using the aptamer alone control. The aptamers were then compared to the aptamer alone control using an unpaired two-tailed t-test to determine which aptamers had a significantly higher binding affinity. A p-value of ≤ 0.05 was considered significant.

2.3 RESULTS

2.3.1 Determination of protein concentration for in-vitro selection

2.3.1.1 Concentration of interferon gamma for use in SELEX

In order to use the correct concentration of the target (in this case IFN-γ), in the selection process, the concentration of the stock needs to be determined, such that the correct dilutions are carried out accordingly, to yield the desired final concentration. The expected concentration of IFN-γ was 1000 µg/ml. Therefore, a range of standards between 250-2000 µg/ml was prepared. The unknown concentration was extrapolated and is highlighted in red, on the graph (**Figure 2.3A**). The quality and the size of IFN-γ were determined on a SDS-PAGE (**Figure 2.3B**). The size of IFN-γ measured at 17 kDa, which was the expected size.

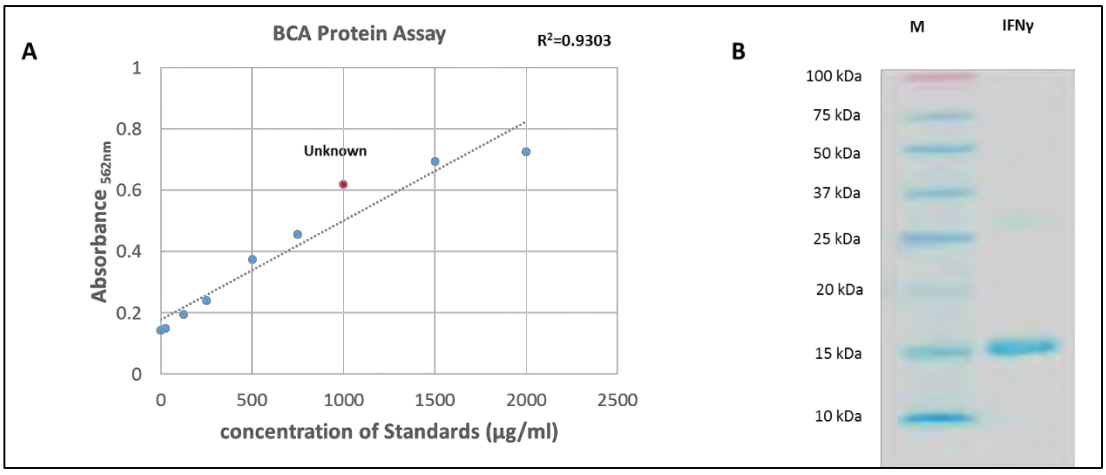

Figure 2.3: A standard curve plotted from the standards used ranging between 0-2000 µg/ml and a 12% sodium dodecyl sulphate-polyacrylamide gel of IFN-γ.

(A) A standard curve was used to extrapolate the concentration of the unknown protein. The closeness of fit determined by adding a linear regression line was calculated and found to be R^2=0.9303. The calculated concentration of the unknown protein was found to be 1.1 mg/ml, using the y=ax+b equation. (B) The reconstituted protein was analysed to confirm the size and the absence of contaminating proteins. The size was determined by using a protein marker (Promega, WI, USA), measuring in kilodaltons (kDa). M: Marker; IFN-γ: interferon gamma protein. IFN-γ is measuring at the appropriate size of 17kDa as indicated by the molecular weight.

2.3.2 Isolation of aptamers against interferon-γ

2.3.2.1 Validation of SELEX library and lambda exonuclease digestion

SELEX was performed as described by Jhaveri and Ellington, (2001) using slight modifications. During each SELEX cycle performed, the recovered pool had to be amplified using PCR. Four to twelve cycles of PCR were done where tubes were removed after every 2 cycles. The recovered pools were subsequently run on a 12% non-denaturing PAGE, followed by staining with ethidium bromide (**Figure 2.4A**). Six cycles of PCR were optimal to amplify the pool. Therefore, the remaining final recovered pool was amplified using 6 cycles of PCR. Over amplification was seen from round 8 to round 12 (**Figure 2.4A**). The non-template control (NTC) showed no presence of any artefacts or contaminants. The product size was the expected 90 bp, as confirmed by the DNA ladder loaded on the far left lane of the gel.

Following the amplification of the recovered pool, the dsDNA was purified and the ssDNA obtained by lambda exonuclease digestion (as described in **Section 2.2.1.4**). After this process, the obtained digested ssDNA was purified accordingly, quantified and validated on a 12% non-denaturing PAGE to ensure complete digestion of the one strand (**Figure 2.5B**). A dsDNA product was included as a control. A slightly higher band is usually seen, should the incubation of the dsDNA and the exonuclease enzyme not be optimal. No higher band was seen for the digested ssDNA.

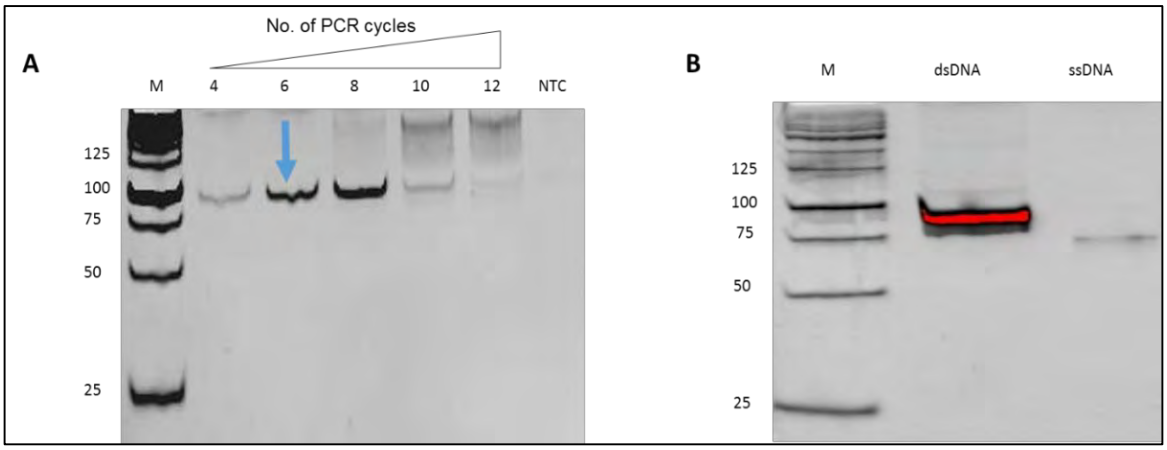

Figure 2.4: Polyacrylamide gels of single stranded DNA and validation following exonuclease digestion.

(A) Amplified product of ssDNA pool after each round of SELEX was validated on a 12% non-denaturing PAGE. A total of 12 PCR cycles were performed and tubes were removed at the 4th cycle, and for each 2nd cycle after that. Lane 1: DNA ladder (25 bp), lane 2: ssDNA at 4 cycles, lane 3: ssDNA at 6 cycles, lane 4: ssDNA at 12 cycles, lane 5: ssDNA at 10 cycles, and lane 6: non-template control (NTC). (B) Validation of ssDNA on 12% non-denaturing PAGE following lambda exonuclease digestion for 4 h at 37°C. The product was purified using Nucleospin ssDNA clean-up kit (Separations), and a special buffer for ssDNA was used. A dsDNA product was included as a control to ensure that no dsDNA was left following the digestion. Lane 1: DNA molecular weight marker, lane 2: double-stranded DNA (dsDNA), lane 3: single-stranded DNA (ssDNA).

2.3.2.2 Recoveries from selection

Six rounds of SELEX were optimal for the positive isolation of IFN-γ binding ssDNA aptamers. Eight rounds were performed, where a gradual increase in recovery was observed from round 1-3 at recoveries of 0.5%, 7% and 22.3% (**Figure 2.5**), epitomising the exponential increase expected to be seen. However, a sudden decrease in percentage recovery was then identified at rounds 4 and 5 (5% and 7%, respectively), which was then followed by an introduction of a negative selection (where non-specific binders to the nitrocellulose membrane were removed). An arrow on the graph was used to indicate where the negative selection was done (**Figure 2.5**). Upon continuation of positive selection, a significant increase was obtained at round 6 with a recovery of 49.9% of ssDNA (**Figure 2.5**). An aliquot of the recovered pool was kept for cloning before continuing with the selection. A decline was observed at rounds 7 and 8 with recoveries of 7% and 13%, respectively (**Figure 2.5**). For this reason it was decided to stop the selection.

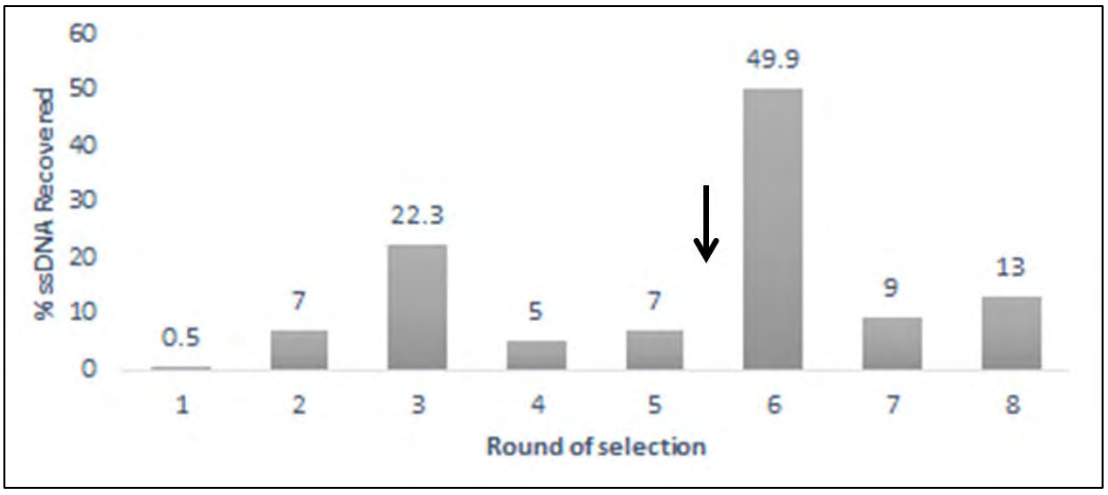

Figure 2.5: The percentage of IFN-γ binding ssDNA pool recovered at each round of SELEX.

Eight rounds of selection were performed and cloning done at round 6, which had the highest recovery of almost 50%. The arrow depicts where the negative selection (in absence of target) was done. A decline was observed at rounds 6 and 7.

2.3.3 Analysis of ssDNA aptamer sequences

2.3.3.1 Sequence alignment

In order to identify sequences of the aptamers, clones were sequenced and subsequently analysed using CLC Sequence Viewer v7.5 (**Figure 2.6**). Some sequences were found in duplicates; A7 and F5, A9 and G6, B2 and G7, E1 and H11, F7 and E2, F3 and G3 (**Figure 2.6**). Aptamer F4 differed by 1 base pair compared to F5 and A7; and aptamers A4 and F8 had a 2 base pair difference, and the rest of the sequences were unique. One aptamer, H9, was found to be 48nt long. This could have been caused by the high error rate of *Taq* polymerase per nucleotide per pass during mutagenic PCR (Cadwell and Joyce, 1994). Some aptamers' sequences had a trail of Ts e.g. G5, B2, and B12. Conservation within the 49mer motif generally ranged between about 30 and 61%; except for bases 24 and 25, with only 8% conservation. The highest conservation was seen at base position 43, at 61%. The flanking sides (forward and reverse primers) had 100% conservation as expected. For a complete alignment with primers (see **Appendix 2C)**. The consensus sequence for the motif is shown in a red box at the bottom of the alignment, and the base percentages and other nucleotide statistics can be found in **Appendix 2D**. Sequences which had incomplete or missing primer sequences; those whose chromatograms

could not be accurately read, those who had chunks of the 49-nucleotides motif missing, and those with the letter "N" were excluded from the multiple alignment.

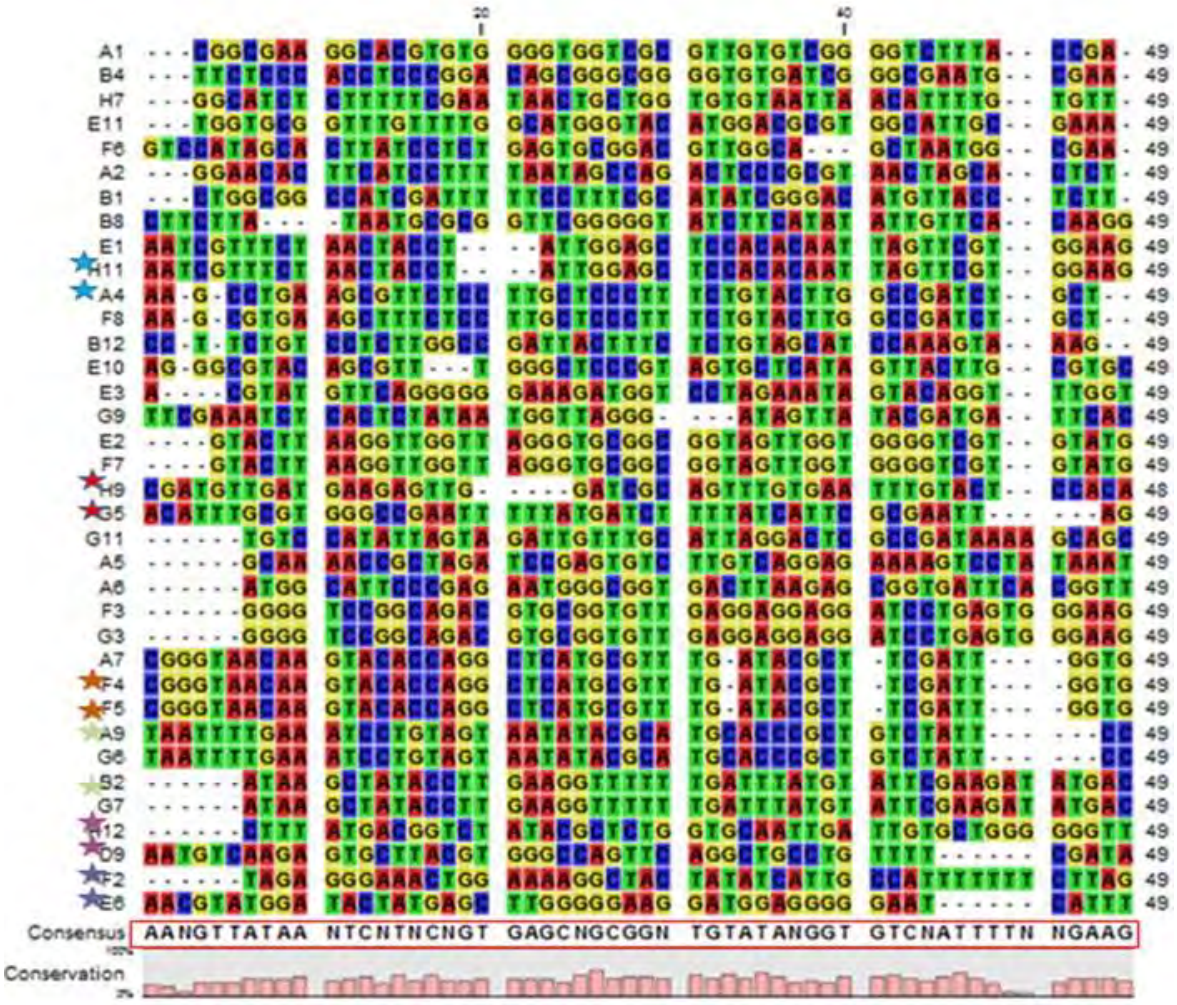

Figure 2.6: The tabular format of a multiple alignment of 36 IFN-γ DNA sequences identified in the 5′-3′ direction.

Sequence identification appear at the beginning of each row and the position of each base is indicated by the numbers at the top of the alignment columns. The number at the end of the sequence indicated the number of nucleotides for each sequence. The level of sequence conservation is shown at the bottom of the alignment in pink, with a scale of 0-100% located on the left. The primers on the flanking sides of the motif, are the most conserved. The red box indicates the consensus sequence of the 49mer motif. Duplicate sequences were identified and are illustrated by matching stars. The gaps represent where the sequences were least conserved.

2.3.3.2 Phylogenetic analysis

An unrooted phylogenetic tree was constructed using CLUSTAL W to compare the divergence of the aligned aptamer sequences. The bootstrap was set to 1000 replicates, which was a means of measuring the phylogenetic accuracy. The aptamers seemed diverse, which could be an indication of increased specificity to IFN-γ. The aptamers shared homology as indicated by the short horizontal branches, which were drawn proportional to the number of base pair difference between two sequences (**Figure 2.7**).

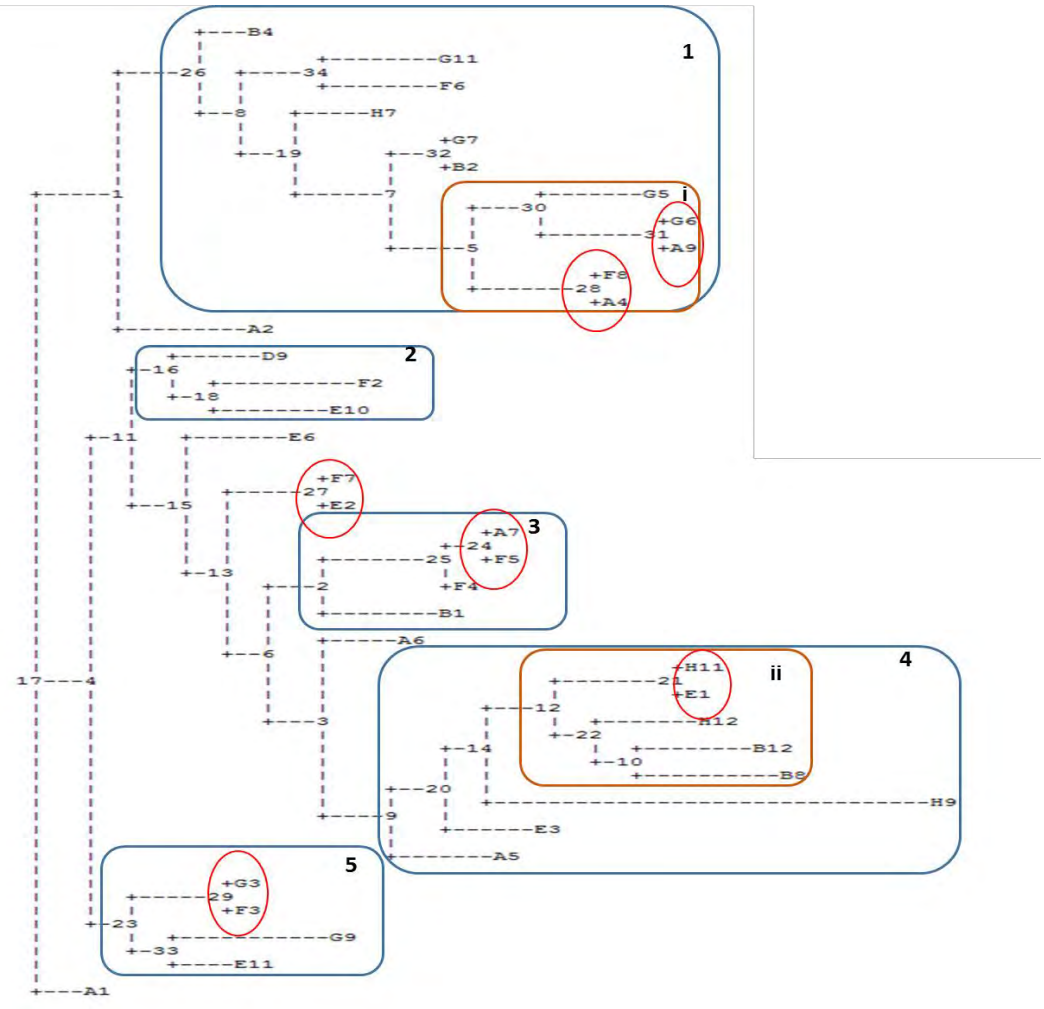

Figure 2.7: A phylogenetic neighbour joining tree following multiple alignment.

The length of branches was directly proportional to the base difference between aptamers. Aptamers that are clustered are grouped (shown in blue rectangles) and sub-clusters are shown in orange. In total, 5 clusters (1, 2, 3 4 and 5) and 2 sub-clusters (i and ii) were found. Six aptamers were duplicated with 2 having 1 and 2 base pair differences.

When the tree was studied closely it was observed that sequences could be clustered into 5 groups, labelled as 1, 2, 3, 4 and 5; and two more sub-clusters, labelled i and ii, were seen within clusters 1 and 4, respectively. One main outlier, aptamer A1 was found. This aptamer branched from the main branch, which suggests that its sequence was the most different from the rest of the other aptamers. Another possibility could be the type of secondary structure that it forms upon binding IFN-γ. The six aptamer duplicates seen in the multiple alignment (**Figure 2.7**), are seen on the tree (in red circles), where they were found on the same position on the branch. Those aptamers were: G6 and A9; G7 and B2; E2 and F7; A7 and F5; E1 and H11; G3 and F3. Aptamers F8 and A4 had a 2 base difference, while aptamer F4 was different with one base to aptamers A7 and F5. Only one of the duplicate aptamers was included in subsequent assays. This neighbour joining tree does not provide details of ancestral sequences. Therefore, the ancestral history of the sequences that were contained in the final recovered pool is not known.

2.3.4 ELONA-based identification of IFN-γ binding aptamers after SELEX

In parallel with the bioinformatic analyses, we used ELONA to measure the binding of the candidate aptamers to IFN-γ. Only one of each duplicated aptamer was included in the screening. Therefore, of the 60 aptamer clones aligned, only 54 were screened following the SELEX (**Figure 2.8**). An aptamer alone control was run for each aptamer and used to normalise the data. Out of the 54 biotinylated ssDNA aptamers screened, 68% (41/60) bound to IFN-γ significantly ($p < 0.05$). Nineteen aptamers bound IFN-γ with $p \leq 0.001$, 13 with $p \leq 0.01$ and 9 with $p \leq 0.05$, when compared to the aptamer alone control (**Figure 2.8**).

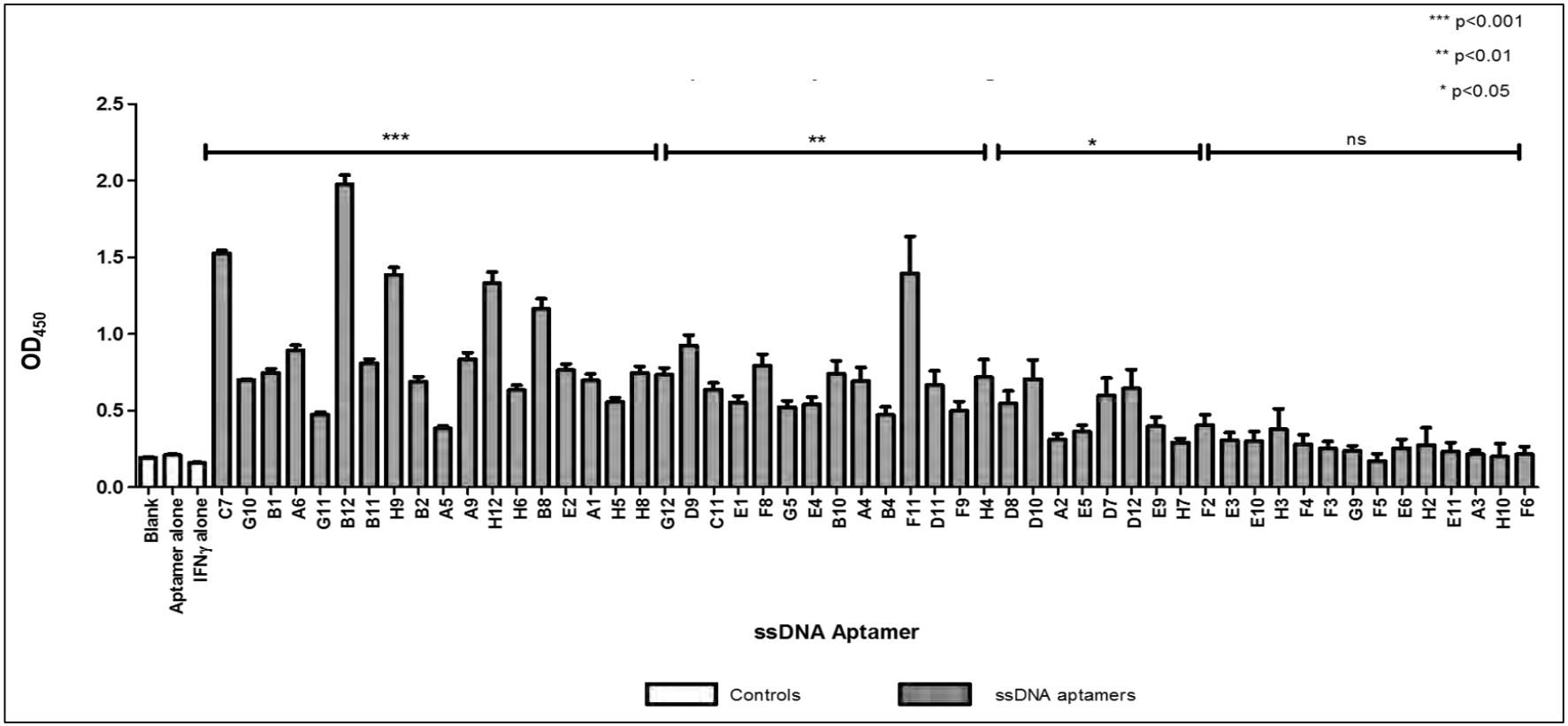

Figure 2.8: Binding of ssDNA aptamers for IFN-γ.

P-values are for comparisons in OD between wells containing IFN-γ and aptamer versus wells containing the aptamer without IFN-γ. Fifty microliters of IFN-γ (1 µg/ml) in HMCKN binding buffer (pH 7.4) was pipetted into a 96-well microtitre plate in triplicate. Individual aptamers (300 nM) were added and three controls, blank (HMCKN binding buffer only), aptamer alone, and IFN-γ alone, were included. An aptamer alone control was included for each aptamer, but only the OD for one (aptamer H12) was shown for illustrative purposes. A two tailed *t*-test was used to determine the p-values. The experiment was done at least twice in triplicates. The error bars denote standard deviations of the duplicate experiments done in triplicates.

2.4 DISCUSSION

This chapter describes the results of the SELEX procedure used for the isolation of IFN-γ binding aptamers, the subsequent analyses of the aptamer sequences and their binding to IFN-γ. The three key findings were: (i) Ninety six aptamers were isolated against IFN-γ; (ii) There was up to 61% homology between aptamers (iii) A total of 41 aptamers bound significantly to IFN-γ when compared to the aptamer alone control ($p<0.05$).

We used SELEX to isolate ssDNA aptamers that bound IFN-γ. Eight rounds were performed with a round of counter selection introduced after round 5. Usually, it is recommended that 6-15 rounds be performed in order to isolate aptamers with high binding affinity and specificity (Jayasena, 1999, Gopinath, 2007). The protocol used proved sufficient after only eight rounds, where an enrichment of 50% was achieved. The recovered ssDNA pool was subsequently cloned and sequenced. Specifically, 96 clones were randomly selected and sequenced. These results are consistent with Bock and co-workers' (1992) experimental approach and findings. Their SELEX against thrombin also achieved an enrichment of ~40% at round five where they cloned (Bock et al., 1992). The percentage increase of 0.01% at round one in the study by (Bock et al., 1992) was comparable to the current study at 0.5%. In another SELEX study that isolated ssDNA aptamers against TB-related protein CFP-10:ESAT-6 final recoveries were between 55% and 68% (Rotherham et al., 2012). Similarly, Barfod et al achieved a recovery of 58% when isolating aptamers against malaria species, plasmodium falciparum (Barfod et al., 2009).

The number of aptamers obtained from the final recovered pool depends on the conditions of the selection process, stringency and the nature of the target molecule used (Nieuwlandt, 2000). It was important to study the different aptamer sequences using bioinformatics tools, which allowed for categorisation of the homologous sequences. Sequencing revealed that the aptamers in the final recovered pool shared sequence homology to one another and the consensus sequence was determined. This

observation suggests that there was a convergent evolution during the SELEX process.

Although there was a degree of homology, some aptamers were distantly related, indicating that they likely had a different mechanism of binding, or they were binding to different epitopes of the IFN-γ. Aptamer H9 had a sequence length of 48nt instead of 49nt. However, this phenomena has been seen before (Wang et al., 2013). Aptamers were found in clusters, which further confirmed their relation as shown on the phylogenetic tree (**Figure 2.8**). The algorithm used in this analysis solely depended on distance, which was calculated to be directly proportional to the number of base difference per sequence (Sleator, 2011, Saitou and Nei, 1987). The motifs identified following the alignment are believed to be involved in the specific target binding of the aptamers (Stoltenburg et al., 2007), where secondary structure predictions can also be determined using the same sequences. This is supported by findings from a study by Gopinath and colleagues (2006b) who isolated an RNA aptamer that bound specifically to the haemagglutinin of influenza B virus, but failed to bind when a new aptamer was developed using the complementary sequence of the original aptamer. It could also be possible that the aptamer with the complementary sequence was assuming a different secondary structure (upon binding target) from the original. This clearly demonstrated that the random region of the original aptamer was responsible for binding (Gopinath et al., 2006b). This is discussed further in **Chapter 3**.

Different binding patterns were observed from duplicate sequences, which can be attributed to the secondary structures that the aptamers conform when binding to IFN-γ. Interestingly, these seemed to be the most abundant candidate aptamers present in the final selection round. The majority of those that bound IFN-γ significantly were found in clusters as seen on the phylogenetic tree (**Figure 2.8**). Additionally, the phylogenetic tree algorithm which was used to perform the analysis of the closely related aptamers was based solely on the sequence and not on the structure of the aptamer. Because the binding of the aptamer to its target is based on

its structure, looking into the analysis of the secondary structures of those specific aptamers could provide further insight. None of the aptamers isolated and sequenced in the current study matched the two previously published IFN-γ aptamers (Balasubramanian et al., 1998, Cao et al., 2014), when their sequences were compared. Thus, Balasubramanian and co-workers (1998) isolated a 26mer IFN-γ aptamer that could alter the structure of the IFN-γ protein. Also, another group most recently developed a 59mer aptamer that could be used to evaluate intracellular IFN-γ generated by lymphocytes (Cao et al., 2014).

2.5 CONCLUSION

Aptamers binding IFN-γ were isolated, their sequence homology analysed and their binding determined. A substantial number of aptamers significantly bound IFN-γ and they shared a degree of homology. Some of these differences could be attributed to the conditions with which the SELEX was carried out. One important limitation is that not the entire final recovered pool was sequenced. Clones were randomly picked and processed for sequencing. As a result this led to only a few sequences being identified. Additionally, some sequences were eliminated due to various reasons discussed in **Section 2.3.2.1**. High-throughput sequencing platforms like Illumina (Schütze et al., 2011, Cho et al., 2010, Guo et al., 2014, Ngubane et al., 2014) are therefore recommended to overcome this limitation as they produce a significantly higher number (thousands-millions) of reads. This can also be coupled with parallel quick binding characterization (Cho et al., 2013). Furthermore, recovered pools at each SELEX cycle could have been sequenced. That would have allowed for the monitoring of the SELEX experiment, which is crucial in maintaining a balance between diversity and good binders.

CHAPTER 3
CHARACTERISATION AND BINDING KINETICS OF APTAMERS TO IFN-γ

SUMMARY

The affinity and stability of aptamers is determined by their 3D structures. In the previous chapter I described 45 ssDNA aptamers that bound significantly to IFN-γ ($p<0.05$). In this chapter, I describe secondary structure prediction of the six aptamers randomly selected from the 45 that bound significantly to IFNγ. This chapter also describes the limit of detection (LOD) and the period of time needed to reach saturation (time-course assays) by each of the six aptamers. Furthermore, I describe the constant rates; association constant (K_a), dissociation constant (K_d), and the equilibrium dissociation constant (K_D) for each aptamer, using surface plasmon resonance (SPR). When predictions of secondary structures were done, each aptamer had a maximum of six possible stable structures they could adopt upon binding IFN-γ. In addition, aptamers A1 and B4 could fold into G-quadruplex structures, which was attributable to their G-rich sequences. Binding efficiency studies revealed a LOD of 10 μg/ml. Moreover, at this specific IFN-γ concentration (10 μg/ml), aptamers A1, B2 and B4 bound in an aptamer concentration-depended manner, whereas aptamers A2, A9, B2 and H12 reached saturation at an aptamer concentration of 75 nM each. The SPR data suggested that most aptamers had high affinity for IFN-γ indicated by their sub-nanomolar K_D. The lowest K_D were 2.06E-10 and 3.90E-10 for aptamers H12 and A9, respectively. The fast association (within 10 min) and saturation after 60 min seen for aptamer H12 correlated to the low K_D from the SPR data.

3.1 INTRODUCTION

Secondary structures of aptamers have been shown to be a dominant element in determining their functionality (Jayasena, 1999). Aptamers assume their structures upon binding to their targets through a "lock and key" mechanism where they organise themselves to fit the target, showing great specificity and high affinity (Gold et al., 1995, Eaton et al., 1995). In addition, aptamers' high discriminatory value allows them to bind their targets with dissociation constants in the sub-nanomolar to picomolar range. Therefore, determining the binding kinetics of the aptamers is crucial in understanding their versatility (Jenison et al., 1994, Stoltenburg et al., 2007, Zimmermann et al., 2000). Assessing kinetics of aptamers allows us the understanding of how rapidly the aptamers and IFN-γ associate and also how soon the aptamers-IFN-γ complex dissociates. The sturdier the bond of the aptamer-ligand, the lower the dissociation constant will be. Therefore, an ideal aptamer would have a fast association rate but a slow dissociation rate, resulting in a aptamer-ligand complex maintained for longer, then subsequently leading to a lower equilibrium dissociation constant (K_D). In return, a low K_D shows higher binding affinity (Stoltenburg et al., 2007). In the case of a point-of-care diagnostic, this phenomenon becomes crucial because the cascade of events (from introducing the biological sample to obtaining a read-out) will be a timed reaction.

Moreover, to measure the binding affinity of aptamers to targets, binding studies using different assays have been employed over the years (Drolet et al., 1996, Cooper, 2003, Tang et al., 2007). This is a very important part of aptamer selection and is usually followed by studying aptamer-target interactions using techniques such as footprinting (Tahiri-Alaoui et al., 2002) and the three-dimensional binding structure is clarified through systems like nuclear magnetic resonance (NMR) spectroscopy (Santini et al., 2009, Baouendi et al., 2012, Foot et al., 2014). The information gathered from these assays assists in determining whether there is accurate binding between the ligand and target and if so, how much binding is

present. Regarding application in clinical medicine, the LOD becomes an important measure as it needs to fall within the biological range of diseased patients.

This chapter assesses whether the candidate IFN-γ aptamers selected for characterisation have the properties of a promising detection molecule which can potentially be incorporated into different point-of-care tests for EPTB. Forty five ssDNA aptamers that significantly bound IFN-γ were isolated. Ten of the aptamers shown to have high binding affinity were initially selected. Of the ten, six with the most unique secondary strutures as determied by *Mfold*, and which were not found within the same cluster on the phylogenetic tree, were selected for further characterisation. Here, I employed ELONA and SPR to determine the binding affinity and dissociation constants (K_D), of the respective six aptamers that significantly bound IFNγ. To further understand the mechanism of binding between the aptamers and IFN-γ, I studied the topologies of the secondary structures using different bioinformatics tools. The characterisation of aptamers was imperative because the aim of this thesis was to identify at least one aptamer that possesses all the necessary properties for the intended downstream application; in this case as detection molecule(s) on a diagnostic platform.

3.2 MATERIALS AND METHOD

3.2.1 *In silico* analysis of selected aptamers using bioinformatic tools

Aptamers form thermodynamic structures in order to bind to their targets with high affinity and specificity (Jayasena, 1999). I performed *in silico* analysis to identify hairpin loops, stems and bulge loops, which are properties of secondary structures known to improve their target affinity and specificity. A web-based software, *Mfold* (http://www.bioinfo.rpi.edu/applications/mfold), was used to predict secondary structures of the 6 selected IFN-γ aptamers. The algorithm calculates the minimum free energy between bases, also considering the stems, loops and bulges (Zuker, 2003). Sequences for the selected aptamers (identified in the sequence alignment in **Chapter 2**, **Section 2.3.2.1**) were added in FASTA format as linear DNA. Secondary structure predictions were done at 37 °C (the physiological temperature of the body), 1 M NaCl, 5% sub-optimality, upper limit of 50 computed folding, maximum interior/ bulge loop size of 30 base pair and maximum asymmetry of interior bulge loop of 30 base pairs. No limits were defined for the distance between base pairs. Predicted secondary structures were analysed carefully in order to identify any similarities in conformation within a particular aptamer, and between one aptamer and the next.

Another common secondary structure conformation known to improve the stability of ssDNA aptamers is the G-quadruplex. The G-quadruplex, also known as a G-quartet or G- tetrad, usually forms in the presence of a guanine (G)-rich nucleotide sequence in a square planar array. They stack themselves by means of strong Hoogsteen hydrogen bonds in that way stabilising the overall molecule (Gellert et al., 1962). The Na^+ and K^+ cations are known to further stabilise the G-quadruplex at physiological temperatures and pH *in vitro* (Burge et al., 2006). The predictions of the G-quadruplex secondary structures were made computationally using a web-based software **Q**uadruplex forming **G**-**R**ich **S**equences (QGRS) Mapper, http://bioinformatics.ramapo.edu/QGRS/ (Kikin et al., 2006). Predictions were done at 150 mM NaCl and 2 mM $MgCl_2$, which are similar to the concentrations of these

cations in the 1X HMCKN binding buffer used during SELEX. Although this *in silico* analysis was a prediction it was necessary to mimic the conditions that were used to select the aptamers. The molecules are more likely to behave in the same way even if the environment is different.

3.2.2 Limit of detection of IFN-γ aptamers

3.2.2.1 Production of ssDNA aptamers

This section describes the purification of DNA aptamers obtained during the SELEX, which were stored in *E.coli* vectors for later usage. Plasmid DNA was purified from stored glycerol stocks and ssDNA prepared. Overnight cultures were prepared and the plasmid DNA isolated using the QIAprep Spin Miniprep purification kit (QIAgen, Hilden Germany) as per the manufacturer's instructions.

The plasmid DNA was quantified, using the Nanodrop® ND-100 spectrophotometer v3.0.1 (Thermo Scientific, MA, USA), and used as template to perform a non-mutagenic PCR (**Chapter 2, Supplementary Table S2.8**). Single-stranded DNA was subsequently prepared as described in **Chapter 2**, **Section 2.2.1.4**. This process produced insufficient ssDNA to carry out all the characterisation assays. Therefore, aptamers synthesised at large scale were purchased from Integrated DNA Technology Inc. (Integrated DNA Technology Inc., Iowa, USA). One batch of the aptamers was biotin-labelled at the 5′-end and the other was unlabelled. The synthesised aptamers were validated to ensure they were the correct size and contained no impurities. This was assessed on a 12% non-denaturing PAGE, stained with ethidium bromide for approximately 3 min and visualised, using ultraviolet (UV) trans-Illuminator GelDoc™ XR system (Biorad Laboratories, CA, USA).

3.2.2.2 Limit of detection of IFN-γ

In order to determine the lowest concentration of IFN-γ to perform functional assays, a titration from 100 µg/ml to 10 µg/ml was done. IFN-γ protein was diluted in 10

mM $NaHCO_3$ to yield final concentrations of 100 µg/ml, 20 µg/ml, 10 µg/ml, and 2 µg/ml. Fifty microliters of each dilution in triplicate was used to coat wells of a 96-well microtitre plate (Corning, Adcock and Ingram, South Africa). The plate was incubated overnight at 4°C. The assay was carried out as described in **Chapter 2**, **Section 2.2.3**. However, a constant 300 nM of aptamer for each IFN-γ concentration was applied. The optical densities of aptamers at each IFN-γ concentration were compared to the IFN-γ-alone control (in absence of aptamer). The experiment was done in triplicate in two independent experiments (n=2).

3.2.2.3 Determining the constant affinity of the aptamers for IFN-γ

Using the IFN-γ concentration determined in the previous assay (**Section 3.2.2.2**), a 2-fold dilution for each aptamer from 300 nM down to 18.75 nM, was performed. The assay was carried out as described in **Chapter 2, Section 2.2.3**, with a minor modification on day 2 where the aptamer was serially diluted 2-fold from 300 nM to yield 150 nM, 75 nM, 37.5 nM and 18.75 nM, and the IFN-γ concentration kept constant at 10 µg/ml. The optical densities of each aptamer at concentrations 150-18.75 nM were compared to their respective at 300 nM. The experiment was done in triplicate in two independent experiments (n=2).

3.2.3 Binding kinetics of aptamers

3.2.3.1 A time course assay to determine the period required for IFN-γ-aptamer complex formation

In order to optimise the minimal time necessary for aptamers to bind IFN-γ, a time-course assay was carried out using ELONA. The optimal concentration of IFN-γ, 10 µg/ml, as determined by the assay described in **Section 3.2.2.2** was used to coat the 96-well microtitre plate (Corning, Adcock and Ingram, South Africa). Aptamers were prepared at 150 nM (the aptamer concentration determined in **Section 3.2.2.3**). Each aptamer was refolded prior to use as previously described in **Chapter 2, Section 2.2.3**. Fifty microliters of each aptamer was added onto the microtitre plate

(Corning, Adcock and Ingram, South Africa) at the following time-points: 120 min, 60 min, 30 min, 20 min and 10 min. The remaining methodology was carried out as described in **Chapter 2, Section 2.2.3**. The optical density of each aptamer at time points 60-10 min was compared to its respective aptamer at 120 min. The experiment was done in triplicate in two independent experiments (n=2).

3.2.3.2 Determining the equilibrium dissociation constant (K_D) of selected aptamers

The BIAcore uses surface plasmon resonance (SPR) technology, which calculates the association and dissociation constants (K_a and K_d), and thus calculates the equilibrium dissociation constant (K_D) (Gonzalez-Fernandez et al., 2012). SPR is a label-free technology that responds to changes in the concentration of molecules at a sensor surface as molecules bind to or dissociate from the surface (**Figure 3.1**). Monitoring of the interacting molecules happens in real time. In order to determine the binding interaction, one molecule is immobilised on the surface of a gold-plated sensor chip using immobilisation chemistry e.g. amine coupling. The other binding molecule, which is in solution, is in a continuous flow at different concentrations usually from lowest to highest. The SPR response hereafter termed response units (RU) is directly proportional to the change in mass concentration close to the surface (Schasfoort and Tudos, 2008).

3.2.3.2.1 Surface preparation for kinetic studies

To study the binding kinetics of each aptamer, the BIAcore™ 3000 (Biacore, Uppsala, Sweden) was used. A CM5 chip (BIAcore, GE Healthcare, UK) containing carboxymethyl groups on the surface was activated through amine-coupling chemistry (Fischer, 2010). The chip was initially primed 3 times using running buffer (1X HMCKN) at a flowrate of 100 µl/min for 20 min. Priming removes preservatives and unwanted particles that may interfere with the immobilisation of IFN-γ. The chip needed to be wet in preparation for the IFN-γ and to moisten the polymer layer (Fischer, 2010). Additionally, the system was primed to ensure that all the residues

remaining in the tubules particularly protein (from previous experiments) was removed as it could interfere by being adsorbed to the surface of the chip during immobilisation of IFN-γ. Two flow cells of the chip were activated using a 1:1 ratio of cross linkers, 0.2 M 1-Ethyl-3-(3-dimehylaminopropyl) carbodiimide hydrochloride (EDC) and 0.5 M N-Hydroxysuccinimide (NHS) (BIAcore, GE Healthcare, UK). IFN-γ (50 μg/ml) was immobilised on 1 flow cell and activated with 10 mM acetate buffer of the appropriate pH for the protein (in this case pH 4.0). To block any remaining activated carboxymethyl groups, 1 M Ethanolamine-hydrochloride-NaOH (pH 8.5) (BIAcore GE Healthcare, UK) was injected over both flow cells. The one flow cell where no protein was immobilised served as a reference blank. The flow rate of 10 μl/min was used and 7 min contact time was allowed.

3.2.3.2.2 Binding kinetic analysis of IFN-γ aptamers

To measure the binding kinetics, aptamers were prepared through serial dilution at concentrations 0.8 nM, 4.6 nM, 27.8 nM, 166.7 nM, and 1 μM using 1X HMCKN buffer (20 mM Hepes, 2 mM MgCl2, 2 mM $CaCl_2$, 2 mM KCl and 150mM NaCl, pH 7.4). Two blanks (without aptamer) were included, one before injection of the lowest concentration and one after injection of the highest concentration to ensure that there would be a suitable blank to normalise the data during each run. 1X HMCKN buffer (running buffer) was filtered through a 0.22 μm filter and de-gassed before use. Filtering and de-gassing the buffer was essential as any small air bubbles or any other small particles found could potentially cause disturbances and negatively affect the experiment. For example, air spikes (seen on the sensorgram) are attributed to the presence of air bubbles in an inadequately or non-degassed running buffer. Aptamers were treated by heating at 95°C for 3 min, immediately cooling on ice for 5 min and left to reach room temperature for 5 min prior to use. The aptamer solutions were centrifuged before being loaded on the instrument as an extra precaution against bubbles. Aptamers were injected over the protein from the lowest to the highest concentration in triplicate across both flow cells at a flow rate of 50 μl/min allowing 2 min of contact time. The aptamers were allowed to

dissociate over 10 min. The surface was regenerated after each cycle, using 20 mM NaOH as a single injection at 30 µl/minute for 30 sec. A pre-needle dip between injections was performed to control for cross contamination. One of the blanks was used to normalise the data. The reference blank was subtracted prior to analysis.

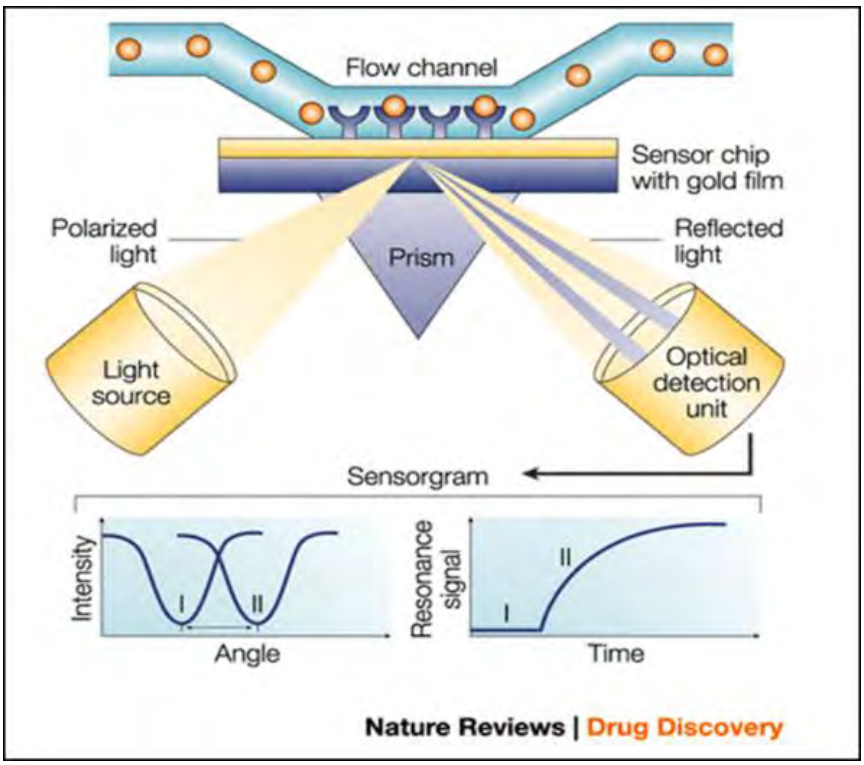

Figure 3.1: A schematic representation of the surface plasmon resonance (SPR) technology.

SPR measures the polarised light at an angle when the protein binds the aptamer and that measurement is referred to as a RU. A protein is immobilised on the sensor chip with a plated gold film. The aptamer is injected over the immobilised protein and the signal response is measured in real time (Cooper, 2003).

3.2.4 Statistical analysis

3.2.4.1 ELONA

Data was analysed using GraphPad Prism version 5.0 software (GraphPad Prism Software Inc. CA, USA), where the statistical analysis was performed by one-way of variance (ANOVA) followed by Bonferonni as a post-hoc test. One-way ANOVA was used to compare different groups (IFN-γ concentrations, aptamer concentrations

and/or time points). Data sets are presented as the mean ± SE. For all tests, data with a p-value of ≤0.05 was considered statistically significant. Each experiment was performed at least twice to ensure reproducibility.

3.2.4.2 SPR

The true values of aptamer binding to IFN-γ were subtracted from the blank reference followed by the analysis, which was done assuming a 1:1 Langmuir model, using BiaEvaluation v4.1 Software (BIAcore, GE Healthcare, UK). The model was used to determine the association rate (K_a), dissociation rate (K_d) and the equilibrium dissociation constant (K_D). A simultaneous fit for K_a/K_d was performed to calculate the K_D. Analysed data was then exported to GraphPad Prism version 5.0 software (GraphPad Prism Software Inc. CA, USA) for plotting of binding curves.

3.3 RESULTS

3.3.1 Structural characterisation of selected aptamers

Predictions of the structures were done using the *Mfold* algorithm. Each aptamer had multiple secondary structure predictions (up to 6 secondary structures). A representative of each aptamer is shown in **Figure 3.2**, which is the structure predicted to be the most stable (as it had the lowest minimum free energy). The minimum free energies (ΔG) are shown in **Table 3.1**. The remaining secondary structures together with the minimum free energies can be found in **Appendix 3.1**. The primer sequences are shown in arrows on the structures where blue arrows represent the forward primer and red arrows represent the reverse primer. When structures were studied closely, primer sequences of most aptamers were found within the bulge-loop with the exception of aptamers A9 and B2, where the forward primer formed part of a stem hairpin loop, and partially so for aptamer B4.

The nucleotides shown to be in contact with the target are usually found within the stem hairpin loops and are usually 10-15 bases long (Gold et al., 2005). Part of the sequence involved in binding was predicted to be within the 49mer motif or random region of the aptamers. All predicted structures for each aptamer had a similar stem hairpin loop with variable lengths of stems, which is highlighted by a black box on the structure (**Figure 3.2**). This is part of 49mer motif, predicted as the portion which interacts with the target as it was observed across all possible secondary structures the aptamer could assume upon binding with its specific target. Aptamer H12 had the least possible structures (it could assume only 2) and contained the longest stem. A low minimum free energy (ΔG=-1.88) was noted for H12, which made it a good candidate for downstream applications as it appeared to be the most stable. Another aptamer forming a long stem was aptamer B4. However, the minimum free energy was not as low (ΔG = -4.81) as H12. The lowest minimum free energy for B4 was ΔG= -4.79, but the structure for this aptamer was not as defined as the rest and thus, not shown as the representative (see **Appendix 3.1**). The remaining aptamers A1, A2, A9 and B2 had fairly short stems forming the stem hairpin loops

with A9 and A2 having the shortest. Furthermore, aptamers A9 and B2 had the lowest free energies amongst all aptamers, which were ΔG =-0.97 and ΔG =-0.94, respectively. Even though aptamer A1 and B4 had slightly increased minimum free energies, ΔG =-5.59 and ΔG =-4.81, they were predicted to have the ability to form a G-quadruplex, which is elaborated further in **Section 3.3.2**.

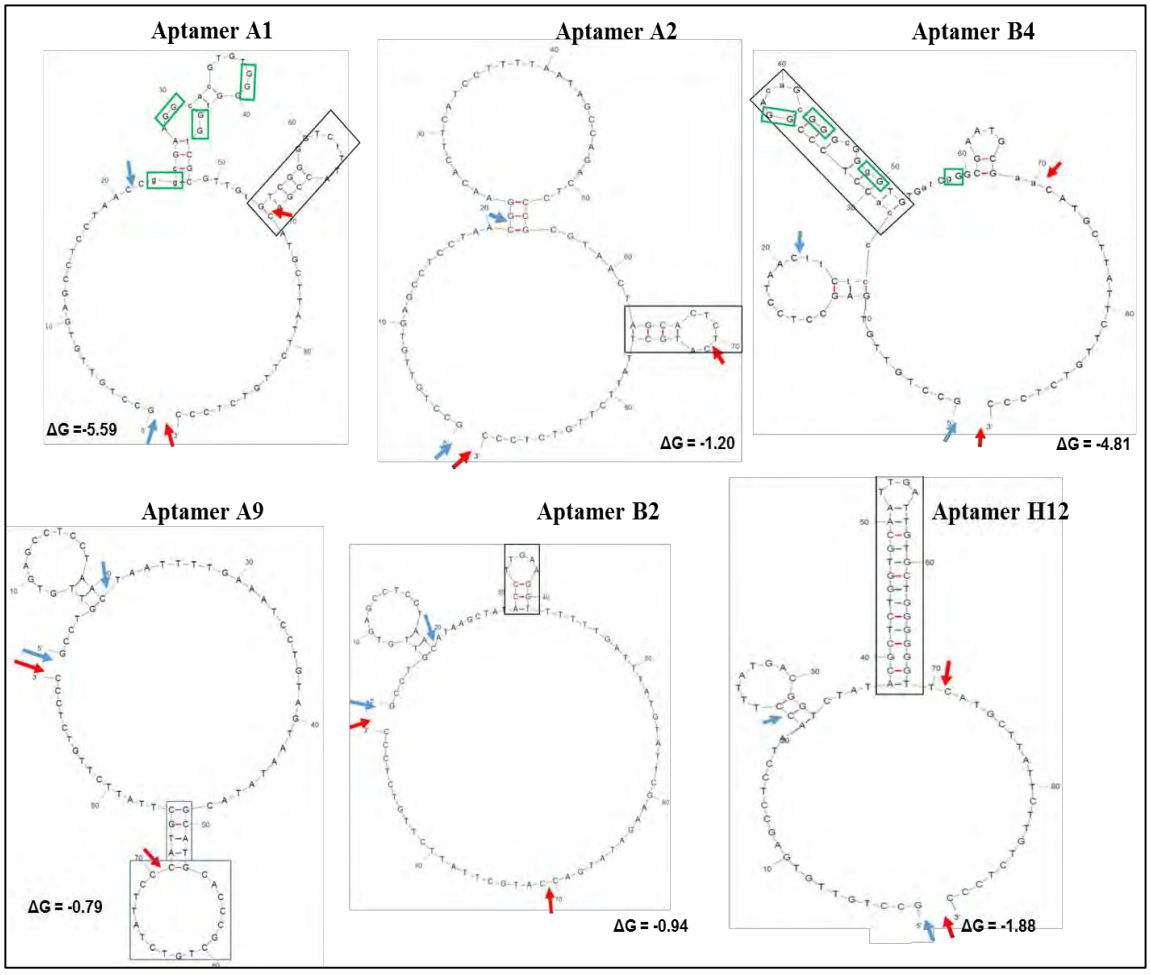

Figure 3.2: Representative secondary structures of the selected IFN-γ aptamers as determined by *Mfold*. GQRS Mapper was used to determined G-quadruplex structures.

The ΔG represents the minimum free energy of each aptamer. Each aptamer had between 2 and 6 possible secondary structures, however, only a representative of each is shown. The forward primer sequence (bases 1-21) is shown by the blue arrows and the reverse primer (bases 71-90) are shown by the red arrows. Common stem loops within each aptamer are depicted using solid black boxes. According to the algorithm used by QGRS mapper software, aptamers A1 and B4 could form G-quadruplexes. The G-bases (in doubles), commonly referred to as G-doublets, which are suggested to take part in forming the G-quadruplex are shown in green boxes. These G-bases had the highest probability as shown by their G-scores, which were 17 and 18 for A1 and B4, respectively.

Table 3.1: The number and minimum free energy of possible secondary strutcures for each aptamer

Aptamer ID	No. of predicted structures	Minimum free energy (ΔG) in kcal/mol
A1	5	−5.59, −5.86, −6.25, −5.72, −5.77
A2	5	−1.20, −2.00, −1.93, −1.64, −1.85
A9	4	−0.97, −1.13, −1.28, −1.78
B2	5	−0.94, −1.09, −1.33, −1.55, −1.84
B4	6	−4.81, −4.91, −5.19, −5.24, −5.72, −4.79
H12	2	−1.88, −2.13

3.3.2 Aptamers A1 and B4 have the ability to form a G-quadruplex

Aptamers were evaluated for their ability to form G-quadruplex structures, using QGRS mapper. Two aptamers A1 and B4 had the ability to form a G-quadruplex with G-scores of 18 and 17, respectively (**Table 3.2**). The G-score, defined as the probability of a molecule to from a G-quadruplex, is calculated based on the size and length of the loops formed by the molecule and the number of guanines present or responsible for forming the G-quadruplex. The scores are dependent on the user's selected maximum QGRS length. The maximum length was 30 nucleotides, which was the default setting used for the analysis. Therefore, the higher the G-score of an aptamer, the more stable it is predicted to be. The highest G-score, using this default setting of 30 nucleotides in length, is 105 in which case a sequence will comprise of 95% of guanine bases. The number of bases responsible for forming the G-quadruplex for aptamer B4 was 24 nucleotides (nt), starting at position 36 on the sequence of the 90nt long aptamer (the full aptamer sequence is shown in the far right column of **Table 3.2**). Aptamer A1 had 22nt forming the structure, starting at position 23 of the full aptamer sequence. To further classify the topology of aptamers B4 and A1, the number and position of the G-tetrads involved in forming the structure was determined (Burge et al., 2006). Both were found to be

unimolecular and contained 2 G-tetrads separated by arbitrary bases in unequal length or composition, which form the loops or gaps (**Figure 3.2**). Structures comprising a higher number of G-tetrads (four) have been shown to be more stable (Kikin et al., 2006). The G-bases predicted to form the G-quadruplex are further annotated on the secondary structures of the aptamers, using green boxes (**Figure 3.2**). The remaining aptamers A2, B2, A9 and H12 did not have the ability to form the G-quadruplex.

Table 3.2: Investigated aptamers that had the ability to form a G-quadruplex structure

Aptamer ID	GQRS position	GQRS length	GQRS	G-score	Sequence
A1	23	22	GGCGAAGGCACGTGT GGGGTGG	17	5′-GCCTGTTGTGAGCCTCCTAAC CGGCGAAGGCACGTGTGGGGT GGTCGCGTTGTGTCGGGGTCTT TACCGACATGCTTATTCTTGTCT CCC-3′
B4	36	24	GGACAGCGGGCGGGG TGTGATCGG	18	5′-CCTGTTGTGAGCCTCCTAACT TCTCCCACCTCCCGGACAGCGG GCGGGGTGTGATCGGGCGAATG CGAACATGCTTATTCTTGTCTCC C-3′

3.3.3 Validation of chemically synthesised aptamers to be used for characterisation assays

During the production of ssDNA aptamers by the lambda exonuclease method (**Chapter 2, Section 2.3.2.1**), it was important that the ssDNA produced be validated for the presence of impurities and contaminants. Also, the correct size had to be confirmed using a low range DNA marker. Additionally, synthesised aptamers were similarly validated (**Figure 3.3**). Two batches of synthesised aptamers were obtained although only the unlabelled aptamers are shown here (**Figure 3.3**). All aptamers were found to be the expected size of 90bp. Aptamer A1 showed multiple bands, which was an indication of the multiple conformations it could adopt. It seemed like

a high concentration was loaded onto the gel for each aptamer, which was indicated by the lower bands seen on the gel.

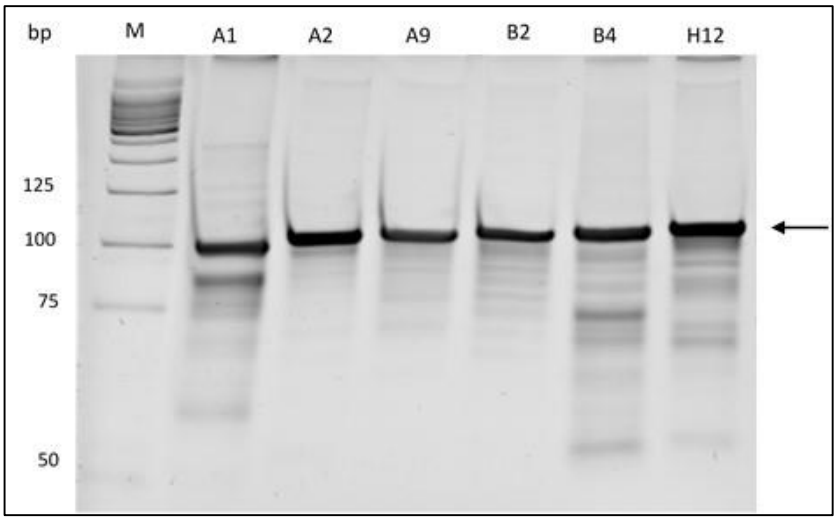

Figure 3.3: Validation of the synthesised aptamers on a 12% non-denaturing PAGE.

Lyophilised **a**ptamer stocks were re-suspended in ddH_2O to a yield a final concentration of 100 µM and then diluted to 100 nM. Synthesised aptamers were run on gel to confirm the correct size of the aptamers and to ensure there were no contaminants present. The gel was run for 1 hour at 100 V and stained with ethidium bromide for approximately 3 min. Lane 1: DNA low range molecular marker, lanes 2-7: Aptamers A1, A2, A9, B2, B4 and H12, respectively. Aptamers were estimated to be around the expected size of 90 bp.

3.3.4 Affinity characterisation of IFN-γ aptamers

3.3.4.1 The limit of detection of IFN-γ

To determine the minimum concentration of IFN-γ that could be accurately detected by the respective aptamers, a limit of detection experiment was performed. The detection limit result contributed to optimising subsequent assays. A dilution gradient ranging from 100 µg/ml to 2 µg/ml of IFN-γ was tested using biotin labelled aptamers at a final concentration of 300 nM (**Figure 3.4**). All aptamers, A1, A2, A9, B2, B4 and H12, bound significantly to IFN-γ ($p \leq 0.001$) at concentrations of 100 µg/ml, 20 µg/ml and 10 µg/ml (**Figure 3.4: B-C**). At a concentration 2 µg/ml of IFN-γ, OD values of aptamers A1, A2, A9 and B4 were undetectable and aptamers

B2 and H12 did not bind significantly (**Figure 3.4: D**). The degree at which the aptamers bound to IFN-γ was dependent on its concentration. The minimum concentration of IFN-γ that all the aptamers could significantly bind was 10 µg/ml. Therefore, this concentration was used in all subsequent assays

.

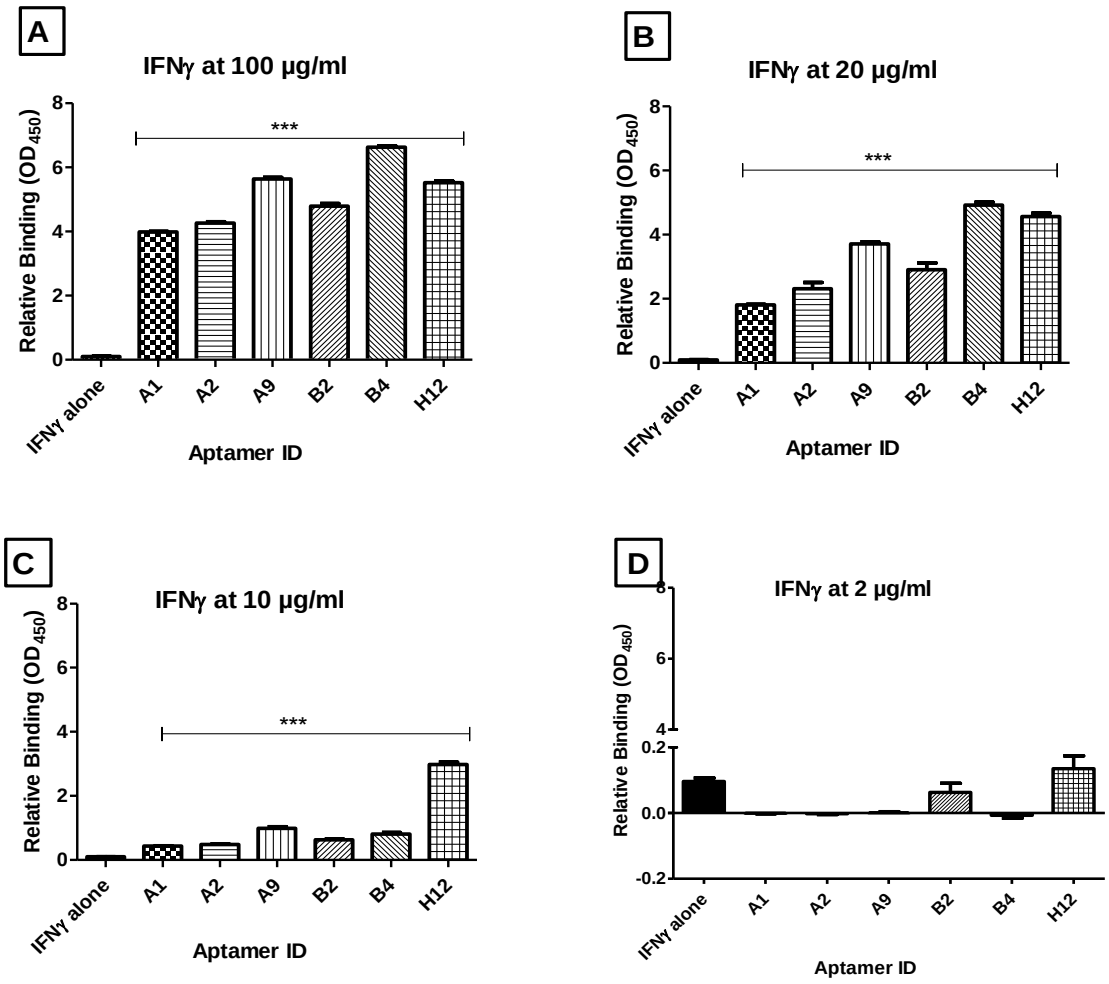

Figure 3.4: Binding of aptamers to IFN-γ.

Aptamers were tested for the lowest concentration of IFN-γ they could detect by ELONA. Varying concentrations of IFN-γ were tested: 100 µg/ml, 20 µg/ml, 10 µg/ml and 2 µg/ml (bar graphs A-D). A blank (buffer only) was included in each experiment and used to subtract the background noise. The binding of aptamers were compared to that of the IFN-γ-alone (absence of aptamer) control using 1-way ANOVA with Bonferroni's post-test, where significant differences were denoted by **=p≤0.01 and ***=p≤0.001.. Data presented are for two independent experiments (n=2) each done in triplicate. Error bars denote mean ± SE.

3.3.4.2 Determination of the minimum concentration of aptamers that bound the minimum concentration of IFN-γ

To determine the minimum and saturation concentrations of the six aptamers that could significantly bind the minimum concentration (10 µg/ml) of IFN-γ determined above, the aptamers were serially diluted and used in ELONA.

A significant reduction in binding ($p \leq 0.001$) was observed at concentrations 18.75-150 nM for aptamer A1 (**Figure 3.5: A**), when compared to binding at 300 nM, which suggested that as the concentration was decreased, the binding was also significantly reduced. A similar pattern was observed for aptamers B4 (Figure 3-5: E) and B2 (**Figure 3.5: D**), where a reduction in binding was seen from a concentration of 75 nM. Significant differences in binding for aptamers B4 (300 nM vs 75 nM and 37.5 nM ($p \leq 0.05$); 300 nM vs 18.75 nM ($p \leq 0.001$)), B2 (300 nM vs. 37nM ($p \leq 0.05$); 300 nM vs. 18.75 nM ($p \leq 0.01$)), and A2 (300 nM vs. 18.75 nM ($p \leq 0.05$)) were observed. No significant differences in binding were seen for aptamers A9 (**Figure 3.5: C**) and H12 (**Figure 3.5: F**). Aptamers A9 and H12 maintained the same binding affinity, regardless of a reduction in aptamer concentration, which indicated that these aptamers possibly reach saturation at 18.75 nM in the presence of 10 µg/ml of IFN-γ. No difference in binding was observed at 300 nM vs. 150 nM for all aptamers with the exception of aptamer A1, which suggested that A1 could be reaching saturation at 150 nM. However, aptamers H12, B2, A9 and A2 reached saturation at 75 nM, as no difference in binding was observed when compared to 300 nM. The data proposes that aptamers A1, B2 and B4 bound IFN-γ in a concentration-dependent manner and a concentration of no more than 150 nM is required for this IFN-γ concentration.

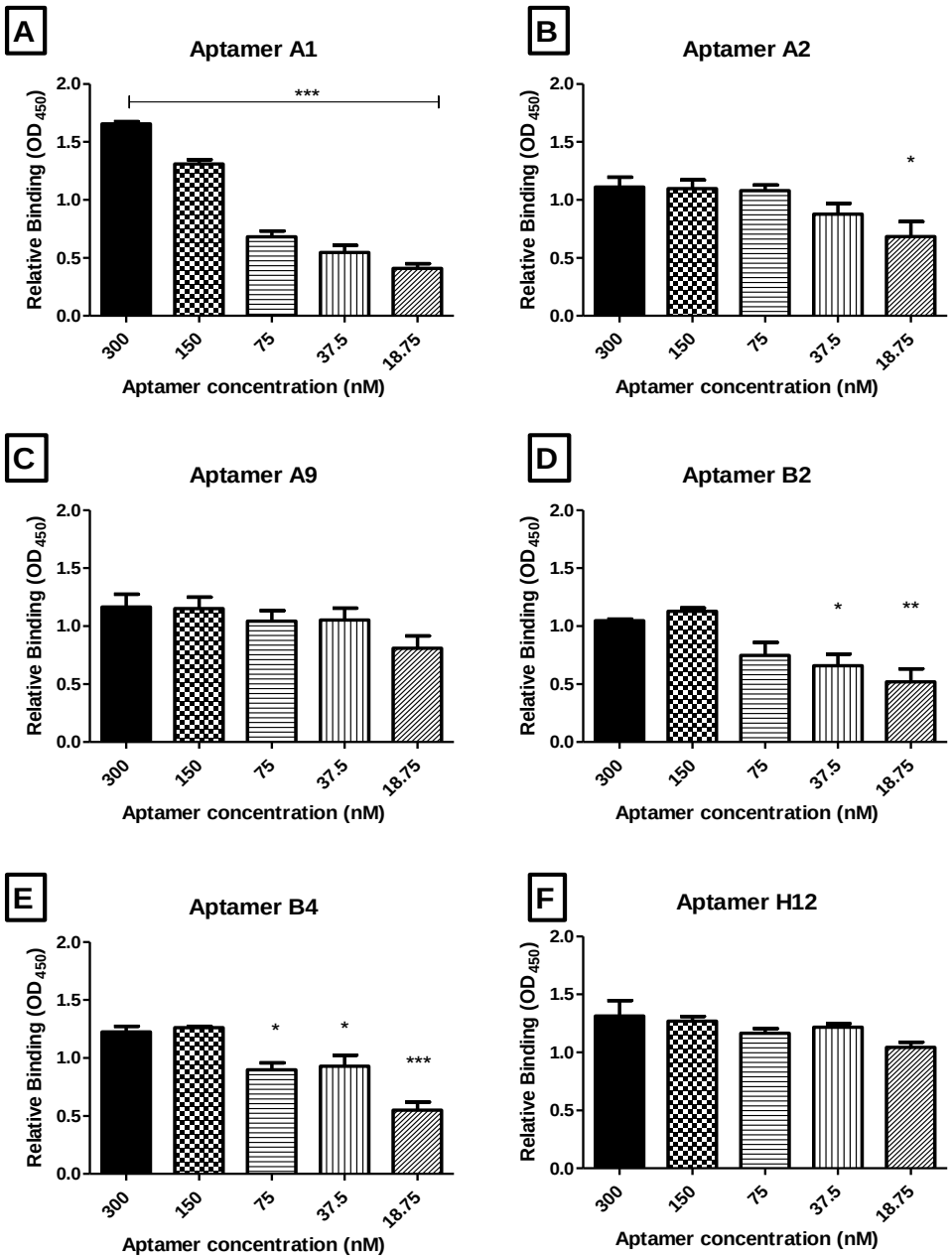

Figure 3.5: Aptamer binding to constant IFN-γ concentration of 10 µg/ml.

Aptamers were tested in a 2-fold serial dilution at 300 nM, 150 nM, 75 nM, 37.5 nM and 18.75 nM, using a constant concentration of IFN-γ of 10 µg/ml. Following the addition of the aptamers at different concentrations, the rest of the parameters were kept constant throughout the assay. The binding of aptamers from 150-18.75 nM was compared to the binding of each aptamer at 300 nM using 1-way ANOVA with Bonferroni's post-test, where significant differences were denoted by *=p≤0.05, **=p≤0.01 and ***=p≤0.001. Data presented are for two independent experiments (n=2) each done in triplicate. Error bars denote mean ± SE.

3.3.5 Binding kinetic studies of selected IFN-γ aptamers

3.3.5.1 A time-course assay to determine highest binding of aptamers

To determine the time necessary to reach the highest binding of aptamers to IFN-γ, a time-course assay was performed, using OD and time via ELONA. Additionally, the method measured the stability of the aptamer-IFN-γ complex over time. Binding of aptamers to IFN-γ was measured at time-points 10, 20, 30, 60 and 120 min. Aptamer and IFN-γ concentrations were kept constant at 150 nM and 10 µg/ml, respectively (**Figure 3.6**). From the previous data (**Section 3.3.4.2**), it seemed possible that some aptamers (H12, A9, B2 and A2) could be reaching saturation at 75 nM. In order to ensure complete saturation, aptamers were tested at 150 nM.

Aptamers A1 and A9 bound IFN-γ in a time-dependent manner. When binding at 60 min was compared to the binding at 120 min for aptamers H12, A1 and B2, no difference in binding was observed, although a significant reduction was seen when compared at 10-30 min (**Figure 3.6**). For A1 at 120 min vs. 10, 20 min, $p \leq 0.01$ and 120 vs. 30 min, $p \leq 0.05$) (**Figure 3.6: A**); B2 120 min vs. 10, 20 & 30 min, $p \leq 0.01$ (Figure 3-6: D) and H12 120 min vs. 10, 30 min, $p \leq 0.001$ and 120 min vs. 20 min, $p \leq 0.01$ (**Figure 3.6: F**). The fact that there was no significant difference at 120 vs. 60 min could be indicative of a slow dissociation rate of the aptamer-IFN-γ complex and the aptamers were thus reaching a plateau at 60 min. The observation suggests that the K_D for these aptamers should be low, at least in the sub-nanomolar range (Kulbachinskiy, 2007). Also observed was a significant reduction in binding at time-points 60 min down to 10 min for aptamers A2 ($p \leq 0.001$) (**Figure 3.6: B**) and A9 ($p \leq 0.001$) (**Figure 3.6: C**); B4 from 10-30 min ($p \leq 0.001$) and also at 60 min ($p \leq 0.05$) (**Figure 3.6: E**), which showed a fast association which kept constant over time. A 1-fold reduction was seen for aptamer A2, which could be attributed to a fast association, followed by a fast dissociation, leading to instability of the aptamer-IFN-γ complex. This phenomenon was predominantly associated with aptamer B2, where the molecules quickly came together (fast association rate), but seemed to decrease slightly in binding when incubated for longer. In contrast, aptamer H12

seemed to stay bound to IFN-γ as time progressed, except for a slight decrease when incubated from 20-30 min (120 vs. 10 min ($p \leq 0.001$), 120 vs. 20min ($p \leq 0.01$), 120 vs. 30min ($p \leq 0.001$) (**Figure 3.6: F**). Aptamers that have a slower dissociation rate, which is usually equivalent to a lower K_D, are preferred. The reason is that it is an indication of the stability of a complex over a longer time period (Jayasena, 1999). From this data, it seems that aptamers H12, A1 and A9 could be good candidates for downstream applications that require one of the molecules to be immobilised on a solid surface. This is further supported by the fast association rate of the aptamers to IFN-γ (in 10 min) and the continued strong bond, which increased over time. Taken together, these results showed that 60 min incubation was sufficient to ensure complete binding of aptamer to IFN-γ.

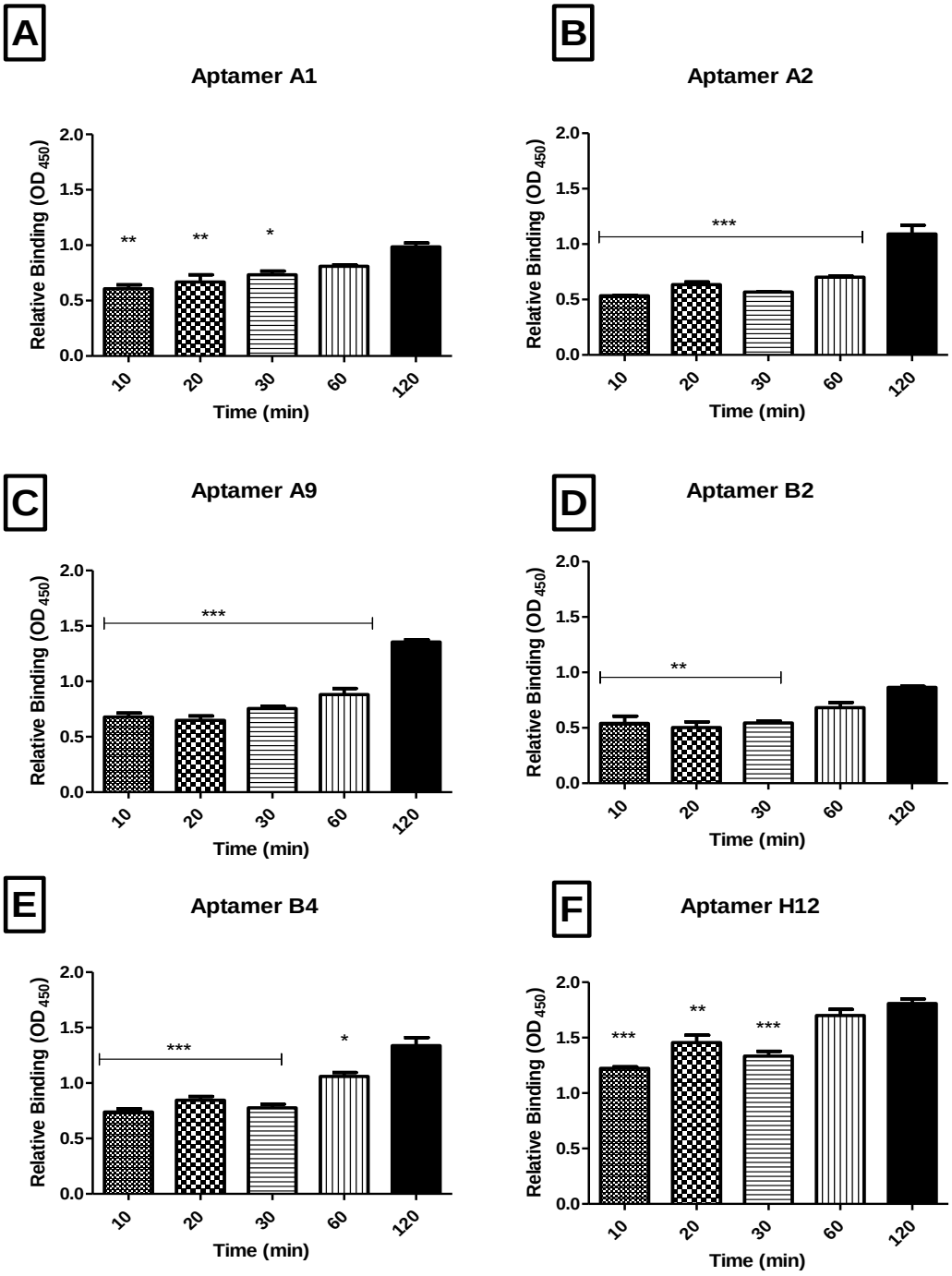

Figure 2.6: Assay to determine how OD450 changes over time at aptamer concentration of 150 nM.

Aptamers at a concentration of 150 nM were incubated at different time points: 120 min, 60 min, 30 min, 20 min and 10 min. Binding of aptamers at variable times was compared to their respective aptamer at 120 min using 1-way ANOVA with Bonferroni's post-test, where significant differences were denoted by *=p≤0.05, **=p≤0.01 and ***=p≤0.001. Data are for two independent experiments (n=2) each done in triplicate. Error bars denote mean ± SE.

3.3.5.2 Surface preparation for determination of kinetics of selected aptamers

To further characterise the aptamer- IFN-γ complexes I used a Biacore 3000. I optimised the immobilisation of IFN-γ using 10 mM acetate buffer at pH 4.0, which was the optimal pH to obtain the highest possible response units (RU). The immobilised IFN-γ bound at 5500 RU at pH 4.0 determined during pH scouting (**Figure 3.7**). A sensorgram, showing the different stages in surface preparation is shown below. In order to prepare the CM5 sensor chip for kinetic measurements, the surface had to be activated with EDC: NHS before immobilising the IFN-γ. All sites during activation, which do not have IFN-γ bound to them, were blocked with ethanolamine, which creates an even surface and prevents protein edging.

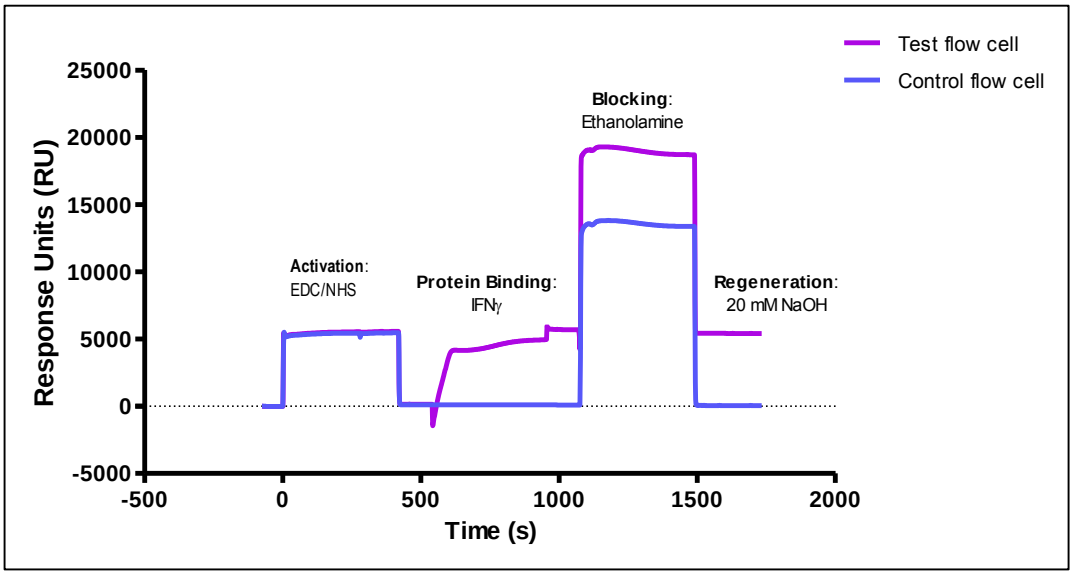

Figure 3.7: A sensorgram showing the immobilisation of IFN-γ on a CM5 sensor chip prior to kinetic analysis.

IFN-γ protein was immobilised using amine coupling chemistry. The chip's carboxyl groups were activated through EDC: NHS, followed by immobilisation of 50 µg/ml of IFN-γ. Activated carboxyl groups sites which had no IFN-γ bound were then blocked with ethanolamine. The surface was regenerated and unbound IFN-γ was removed with 20 mM NaOH. The final immobilised IFN-γ was approximately 5500 RU. The control flow cell was"no protein" control, where no IFN-γ was immobilised to the surface.

3.3.5.3 Determination of the binding kinetics of selected aptamers

The K_D was determined for each aptamer (**Figure 3.8**) and a summary of the kinetic parameters is outlined in **Table 3.3**. The kinetics of the individual aptamers revealed that most of the aptamer bound the target within the low nanomolar to picomolar range (**Figure 3.8**). The kinetic assessment procedure determines association and dissociation constants by fitting the experimental data to a 1:1 molecule interaction model (Langmuir) between molecule A and molecule B. Therefore, for purpose of clarification, K_a is defined as the association rate constant ($M^{-1}s^{-1}$), K_d is the dissociation rate constant (s^{-1}) and K_D is the equilibrium dissociation constant (M), where at equilibrium: association = dissociation.

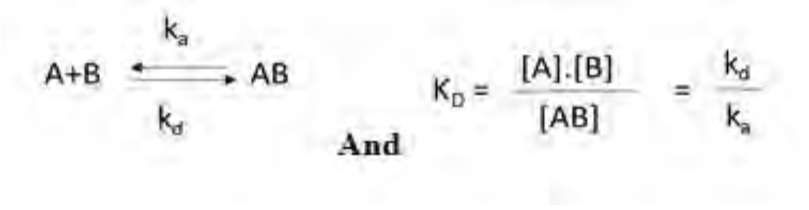

Aptamers with the lowest K_D were A9 and H12 at 3.90E-10 and 2.06E-10, respectively. Both aptamers had a rapid association rate as indicated by their K_a at 2.56E+5 and 2.32E+5, respectively (**Table 3.3**). Aptamers A1, A2, B2 and B4 had a K_D of 5.39E-9, 6.28E-8, 1.94E-8 and 8.61E-9, respectively. Also noted was that A1, A2, B2 and B4 had a K_a 10-fold higher than A9 and H12 (**Table 3.3**). Aptamer A1 also had the ability to form a G-quadruplex structure (see **Section 3.3.2**), which would play a significant role in stabilizing the overall aptamer-IFN-γ complex. Thus, in spite of aptamers A9 and H12 being favoured due to their low K_D, A1 was chosen to be characterised further as it had a low K_D, and the ability to forma G-quadraplex, which are the two characteristics of utmost importance in applications such as biosensors and sandwich assays.

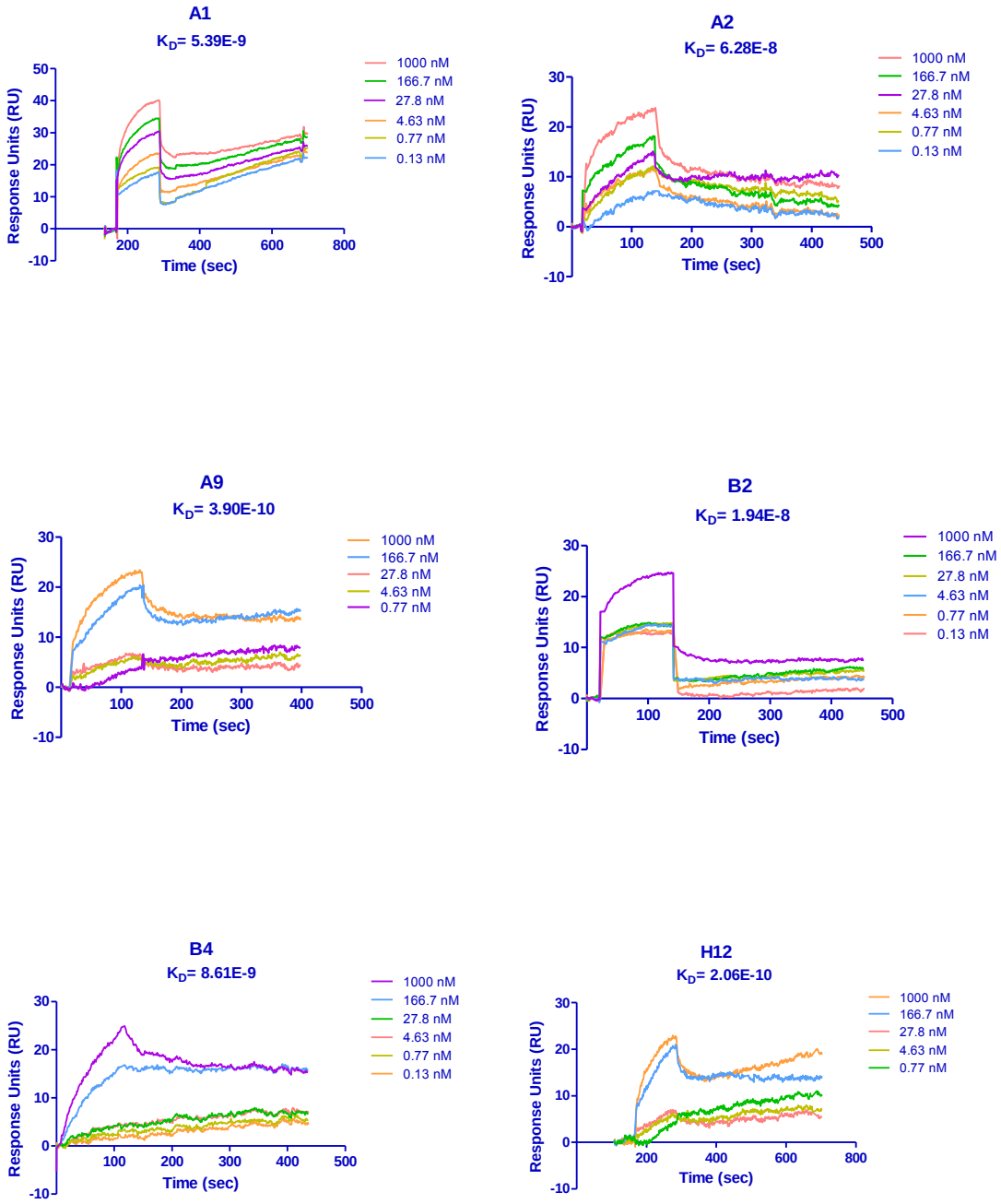

Figure 3.8: Kinetic analysis of aptamer binding to IFN-γ.

SPR technology was used to measure the association and dissociation constant rates and equilibrium dissociation constant of each IFN-γ aptamer. Recombinant IFN-γ was immobilised on a CM5 chip and each aptamer was exposed to the immobilised IFN-γ at varying concentration, ranging from 0.13 nM to 1000 nM. The aptamer concentration is shown on the top right corner of each graph and the K_D is shown at the bottom right corner. The aptamers and the IFN-γ were allowed 7 min contact time before dissociation. To calculate and determine the equilibrium dissociation constant using the association and dissociation constant rates, a 1:1 Langmuir model was assumed using the BIAevaluation v4.1 software.

Table 3.3: Equilibrium dissociation constant (K_D) of IFN-γ aptamers determined through SPR technology

Aptamer ID	Association rate constant [K_a ($M^{-1}s^{-1}$)]	Dissociation rate constant [K_d (s^{-1})]	Equilibrium dissociation constant [K_D (M)]
A1	**3.75E+4**	**2.02E-4**	**5.39E-9**
A2	**3.77E+4**	**2.35E-3**	**6.24E-8**
A9	**2.56E+5**	**9.57E-5**	**3.90E-10**
B2	**5.53E+4**	**1.07E-3**	**1.94E-8**
B4	**6.05E+4**	**5.21E-4**	**8.61E-9**
H12	**1.13E+5**	**2.32E-5**	**2.06E-10**

3.4 DISCUSSION

The previous chapter described the selection and identification of 45 aptamers that significantly bound IFN-γ. In this chapter, I further characterised the six selected aptamers using bioinformatics tools and binding studies. The key findings in this chapter were: (i) the aptamers were predicted to form distinct secondary structures and a G-quadruplex; (ii) The LOD of IFN-γ was 10 μg/ml for all the aptamers; (iii) Aptamers had sub-nanomolar-picomolar K_D.

Subsequent binding studies of the individual aptamers were carried out to determine their affinity to IFN-γ as their downstream application is dependent upon this (Stoltenburg et al., 2007). Firstly, to understand the mechanism of binding and identifying the nucleotides possibly responsible for the specific binding, bioinformatic software (*Mfold* and QGRS Mapper) were used. Each aptamer was predicted to have multiple secondary structures and the minimum free energy ranged from Δ-0.94 to Δ-6.25 kcal/mol.

The aptamers shared structural similarities in that they all contained 2-3 hairpin stem loops within a bigger bulge loop per structure, where aptamer H12 was found to have the longest hairpin stem loop. Within the 2-3 stem hairpin loops, one was common in all predicted derivatives of each aptamer. This hairpin stem loop is set to interact directly with the target thereby enhancing its specificity and high affinity (Jayasena, 1999). The motif was found within the stem hairpin loops, which is apparently where the binding happens as hypothesised (Gold et al., 1995). Gold showed that the full length aptamer had three functional regions, with only about 18-20 bases of the aptamer coming into contact with the target (Gold et al., 1995). Therefore, a portion of the 49mer motif of the IFN-γ aptamers was involved in this regard. Additionally, a small portion of the reverse primers of aptamers A2 and A9 were found to form a stem hairpin loop. The finding was unexpected as the primers are unlikely to interact with the target during binding. Furthermore, the ability of aptamers B4 and A1 to form a G-quadruplex structure confers their increased stability. Although G-

quadruplex structures have been shown to improve stability of aptamers, and a few have been developed over the years, the thrombin-binding aptamer (TBA) remains the only well-characterised G-quadruplex aptamer (Kelly et al., 1996). Also, characteristics of aptamers being able to fold into 3D structures and fold pockets upon binding with their targets has become the foundation of developing biosensors (Zhou et al., 2010, Cao and Chen, 2011, O'Sullivan, 2002). Moreover, none of the previously reported IFN-γ aptamers were able to form G-quadruplexes (Balasubramanian et al., 1998, Cao et al., 2014).

To further characterise the six selected aptamers, their binding affinity to IFN-γ was determined. The lowest detection limit using ELONA was 10 µg/ml. The biological range of IFN-γ in the pleural fluid is estimated to be in picogram concentrations. Therefore, although the LOD was low, the sensitivity of the aptamers can be improved. For example, the aptamers can be conjugated to nanomaterials such as gold nanoparticles to enhance the sensitivity of the assay as it was demonstrated by. Peng and co-workers (2013) using a traditional ELISA. In this study the sensitivity was increased almost 20 times that they could detect as low as 5.6 pg/ml of 7-aminonitrazepam (7-ANZP), which is a primary urinary metabolite of nitazepam (Peng et al., 2013). Despite our reported low sensitivity, similar concentrations (5-10 µg/ml) have been used to conduct binding studies using the ELONA platform (Tang et al., 2014, Martín et al., 2013). In addition, Martin and co-workers (2013) also reported that their aptamers bound Leishmania protein in a concentration-dependent manner, consistent to our findings. Aptamers A9 and H12, in particular, were depicted as good candidates as no differences in binding were observed at the variable concentrations of aptamer. These data suggest that they reached saturation at a low concentration, thus showing a desirable property for an inexpensive point-of-care test.

To further study the stability of the aptamer-IFN-γ complexes, binding kinetic studies were undertaken. All aptamers bound IFN-γ with dissociation constants in the

low nanomolar range, in particular aptamers A9 and H12, had a K_D in the picomolar range, potentially making them ideal molecules for diagnostic applications. This was further supported by their low minimum free energy for their secondary structures. These reported K_D values are in agreement with previous results achieved for other TB aptamers (Balasubramanian et al., 1998, Liu et al., 2010, Rotherham et al., 2012, Ngubane et al., 2014, Tang et al., 2014). Examples include the CSIR 2.19 DNA aptamer to ESAT6-CFP10, which had a K_D=1.6±0.5 nM (Rotherham et al., 2012), EsxG RNA aptamer at K_D=8.04±1.90 nM (Ngubane et al., 2014), DNA aptamer for IFN-γ at K_D=3.11±0.84 nM (Balasubramanian et al., 1998, Liu et al., 2010). This data therefore concurs well with reports that aptamers appear to have binding properties that compare well with antibodies, which also have K_D in the low nanomolar range (Sikarwar et al., 2014, Liu et al., 2014). The low K_D of the aptamers allows them to compete with their antibody counterparts. Perhaps the two molecules (aptamer and antibody) could even be paired together to increase the sensitivity of the IFN-γ aptamers. Although aptamers A9 and H12 did not form G-quadruplex structures, binding kinetics data suggest that they are also good candidates for use in downstream diagnostics applications.

3.5 CONCLUSION

I have identified six ssDNA aptamers that bind IFN-γ with high affinity. The results demonstrate that these selected aptamers can detect IFN-γ on ELONA and SPR platforms. Moreover, the secondary structures correlated with the findings of high binding affinities and enhanced stability as denoted by the long stem hairpin loop. Binding of the aptamers was in the sub-nanomolar range (10^9-10^{10} M), directly showing that these aptamers had high affinity for IFN-γ. The findings suggest that these aptamers can supplement or substitute antibodies (where antibodies have failed on their own). Notwithstanding, the LOD shown in this study IFN-γ suggest that these aptamers in their current form are not desirable for developing a POC test for EPTB, because IFN-γ is found in picogram concentration in clinical samples. This limitation can be overcome by conjugating the aptamers to different nanomaterials as previously done by others with success (Peng et al., 2013).

CHAPTER 4

DETERMINATIONS OF SPECIFICTY OF THE APTAMERS TO IFN-γ, TRUNCATION AND CHARACTERISATION OF DERIVATIVES OF APTAMER A1

SUMMARY

The high degree of specificity often seen in aptamers is a result of the selectivity in SELEX, which eliminates sequences that bind closely related analogues of the target. In this chapter, the six aptamers were further characterised to determine if they are specific to IFN-γ. In addition, the binding of the aptamers to IFN-γ in the presence of an anti-IFN-γ antibody was evaluated. Folding studies were also used to elucidate the importance of aptamer re-folding prior to use in assays.

One aptamer, A1, with desirable properties such as high affinity to IFN-γ and predicated stable secondary structure that form G-quadruplex, was truncated into three derivatives: a 49mer, a 36mer and a 29mer. Their binding affinities were determined and compared to the full length aptamer (90mer). All six full length aptamers showed high specificity for IFN-γ ($p \leq 0.001$). Data from the indirect ELONA using anti-IFN-γ CD66 suggested that aptamer H12 could be used in conjunction with an antibody. In addition, folding studies revealed that the binding of aptamer A1 was significantly increased ($p \leq 0.01$) when used without being re-folded. Binding for the truncated derivatives of A-36mer and 29mer was the same as that of the 90mer. Although the 36mer and 29mer had increased affinity for IFN-γ at 150 nM, only the 49mer truncated derivative was able to detect IFN-γ (10 μg/ml) at a reduced concentration of 18.75 nM. The binding kinetics of the 29mer were performed, and these revealed a 10-fold increment in K_D when compared to the 90mer. The K_D for the 90mer and 29mer were 5.39E-9 and 1.02E-10, respectively. Thus, the aptamers described in this study displayed high specificity for IFN-γ and also demonstrated their capability of being paired with an antibody to develop a sandwich assay. Moreover, truncated derivatives for aptamer A1 maintained the same binding affinity to IFN-γ, comparable to the parental molecule.

4.1 INTRODUCTION

A pre-requisite for a reliable diagnostic test is the ability of the detection molecule to accurately measure the target in the sample. Aptamers have been shown to have these qualities by binding their targets with high affinity and specificity (Eaton et al., 1995, Gold et al., 1995). In this chapter, the six selected aptamers were further characterised to determine their functionality for potential development as diagnostic reagents for EPTB. Specifically, their specificities to IFN-γ and competition with anti-IFN-γ antibody were respectively determined. Moreover, I also truncated aptamer A1 and determined binding kinetics of its derivatives to IFN-γ.

Although aptamers have been reported to rival antibodies in diagnostics application (Jayasena, 1999), antibodies remain widely used in clinical medicine (Ruigrok et al., 2011). Antibody-based assays like ELISA continue to be the most frequently used tests in routine diagnostics. This is mainly due to their ability to recognise their targets with high specificity and affinity. This has been the case for decades despite their drawbacks. For instance, their large and complex structure makes them susceptible to degradation and denaturation. They also have limited stability and modifying them results in loss of sensitivity (Mairal et al., 2008). Their large size (±150 kDa) is also limiting. However, they have been shown to partner well with aptamers (Drolet et al., 1996). Thus the combination of antibodies and aptamers warrants further investigation in developing more robust POC tests.

Aptamers, in contrast, have more attractive qualities. Their size (5-20 kDa), stability and structural properties makes them preferred over their counterparts especially in platforms like biosensors (Jhaveri and Ellington, 2001). Their ability to change structure upon binding with target means they can be used to design sensors that are similar to molecular beacons (Patel et al., 1997, Wang et al., 2005, Yamamoto et al., 2000, Zhou et

al., 2010, Nutiu and Li, 2005, Nutiu and Li, 2004). Their amenability to modification without compromising their affinity and specificity further make them desirable molecules for diagnostic applications. Furthermore, their size allows them to be immobilised in high densities therefore warranting their reusability (Mao et al., 2010). This therefore indicates that one can now picture aptamers as equivalent, and in some ways superior, to antibodies in diagnostics (O'Sullivan, 2002). Likewise, more affordable, rapid and robust POCs can be developed in order to control the TB endemic, especially in developing countries.

The nature of most clinical samples of EPTB, particularly pleural fluid samples is known to be heterogeneous. This is the first major challenge of diagnostics when using pleural fluid even more so for a POC test where one would not be subjected to pre-treating the sample. Furthermore, pleural fluid removed from patients via a pleural tap can sometimes appear bloody or milky, which increases the heterogeneity of the sample due to the presence of red blood cells. The second major challenge is the concentration of IFN-γ found in pleural fluid. Recent work in our laboratory has shown that IFN-γ is available in trace amount (10-250 pg/ml) in pleural fluid (Meldau et al., 2014). Due to other larger proteins present, which are also present in high concentrations, IFN γ is not easily detectable as it is masked by these proteins. For example, albumin is a 150 kDa protein, which is found abundantly in pleural fluid and almost 10-fold larger than IFN-γ, which is only 17 kDa.

In this chapter, I therefore tested the specificity of aptamers to IFN-γ in relation to other proteins abundantly found in the pleural fluid such as albumin. I also evaluated the binding of aptamers to IFN γ in the presence of an anti- IFN-γ antibody. To further prove the versatility of aptamers, I truncated one aptamer called A1 to yield shorter derivatives.

4.2 MATERIALS AND METHODS

All the aptamer preparations, ELONA and methods used to determine the optical density are as previously described in **Chapter 2**, **Section 2.2.3**, unless stated otherwise.

4.2.1 Aptamer specificity testing

Although aptamers can be specific in laboratory settings, when placed in pleural fluid it can be problematic to attain the same specificity due to the reasons stated above. Therefore to test for specificity, mycobacterial and non-mycobacterial molecules were used. The molecules were selected carefully so that they included some proteins present in the pleural fluid as well as other known mycobacterial proteins. The tested proteins included were diverse and are listed in **Table 4.1**. Interleukin 4 (IL-4) and pure protein derivative of tuberculin (PPD) were donated by Mr Anil Pooran and Dr Malika Davids from the Department of Medicine, University of Cape Town. Proteins were tested at a concentration of 10 μg/ml and IFN-γ was included as a positive control. The assay was carried out as previously described in **Chapter 2**, **Section 2.2.3**.

Table 4.1: Investigated proteins and molecules and controls used for specificity testing

Proteins/molecules	Quantity	Positive control	Negative Controls
Interleukin 4 (IL-4)	10 µg/ml	Interferon gamma (IFNγ)	Aptamer-alone (no IFNγ)
Lipoarabinomannan (LAM)			IFNγ-alone
Pure protein derivative of tuberculin (PPD)			IFNγ + Random oligonucleotide
Albumin			Coating buffer only
Glucose			Wash buffer only (TBS)
Casein			Block buffer (10% fat-free milk solution
Bovine serum albumin (BSA)			

*Random oligonucleotide = unrelated DNA aptamer

4.2.2 Aptamer-Antibody sandwich ELONA assay

A sandwich ELISA has been shown to improve sensitivity of the molecule being detected, hence their widespread use in clinical diagnostics (Engvall and Perlmann, 1971). A sandwich ELISA includes capture and detection molecules, respectively. The capture molecule is usually not labelled, while the detection molecule is labelled to allow visualisation and quantification of the reaction. Streptavidin- horseradish peroxidase (HRP) is the most widely used detection agent in ELISA platforms. In this chapter, a sandwich ELONA was optimized using a biotinylated aptamers and a capture anti-IFN-γ monoclonal antibody (donated by Antrum Biotechnologies Inc., South Africa). The two anti-IFN-γ monoclonal antibodies tested were CD119 and CD66 (**Figure 4.1**).

To optimize the sandwich ELONA, 96-well microtitre plates (Corning, Adcock Ingram) were coated with 50 µl of 1 µg/ml CD119 and CD66, respectively. The antibodies were diluted in 10 mM $NaHCO_3$ coating buffer (pH 8.5) and the plates incubated overnight at 4°C. The next day, the plates were washed 3× with 100 µl TBS and blocked with 150 µl 10% blocking buffer (fat-free milk re-suspended in TBS) then incubated for 1 h at 4°C. The plates were washed again with 3× with 100 µl TBS and blotted dry on paper towel after the final wash. IFN-γ protein was diluted in 10 mM $NaHCO_3$ buffer (pH 8.5) and incubated at room temperature for 2 h. Yet again, the plates were washed 3X with 100 µl TBS and blotted dry on paper towel after the final wash. Aptamers were prepared at 150 nM in 1X HMCKN buffer as described in Chapter 2, Section 2.2.3, and 50 µl pipetted into each well. Plates were incubated at room temperature for 2 h and subsequently washed 3X with 1X TBS. A 50 µl of streptavidin HRP was added to each well and incubated for 2 h at 37°C. Plates were washed 3X with TBS and blotted dry before adding 50 µl of chromogenic substrate to each well. Once the reaction turned from clear to blue it was stopped using 2M sulphuric acid, which subsequently turned the reaction from blue to yellow. The plates were immediately read at 450 nm on a microtitre plate reader. To disregard/rule-out non-specific binding an antibody-aptamer negative control was included (as blank) where no IFN-γ was present. This control was used to normalise the data and also test how the binding between the antibody and aptamer would bind in absence of IFN-γ. An antibody-antibody control was included as a positive control in this assay. For purposes of consistency, each experiment (for both CD119 and CD66) was further repeated by an independent researcher (Dr Philippa Randall, University of Cape Town). The repeat experiments were performed on the same day, under the same conditions.

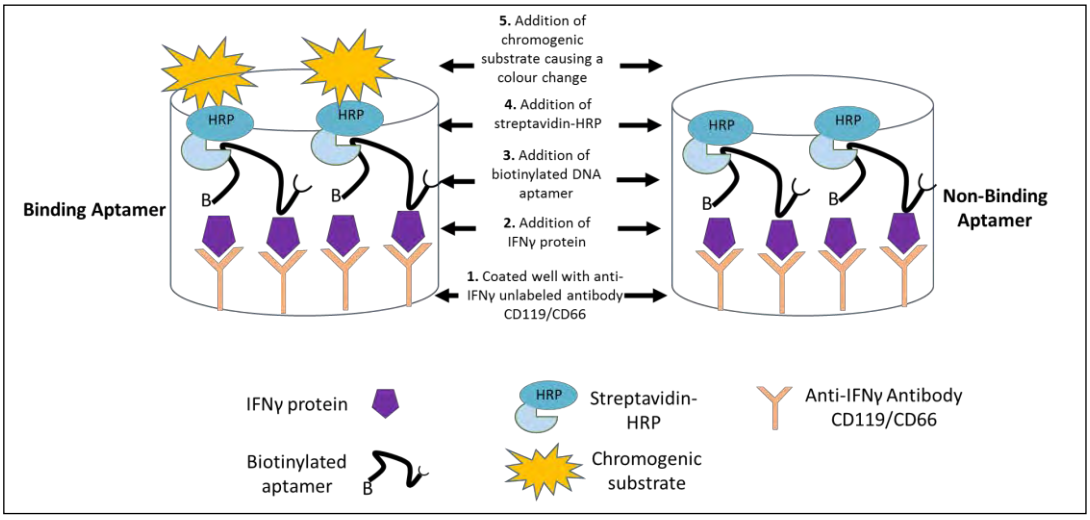

Figure 4.1: Detection of IFN-γ by antibody-aptamer sandwich assay.

Antibodies (CD119 and CD66) were diluted in 10 mM $NaHCO_3$ buffer to 1 µg/ml and used to coat wells of a microtitre plate. IFN-γ was added at 10 µg/ml and subsequently 150 nM refolded biotinylated aptamer. A streptavidin-HRP enzyme was introduced, followed by addition of TMB substrate. The reaction was stopped by using 2 M sulphuric acid before being read on a plate reader at 450 nm. Well on the left (Binding aptamer) shows a positive reaction, where an aptamer bound to IFN-γ and well on the right (Non-binding aptamer) shows a negative reaction, where no binding was observed.

4.2.3 Determining whether aptamer refolding alters binding

Aptamers are predominantly unstructured in solution and only fold into distinct structures upon binding their targets (Hermann and Patel, 2000). Traditionally, aptamers are unfolded prior to being used by heat denaturation and rapid cooling. This is performed in order to ensure that the aptamer is unstructured and thus able to form distinct secondary structures upon binding target. On the contrary, when developing a POC test such as a biosensor that incorporates aptamers (often referred to as an "aptasensor") this step needs to be excluded as it might not be feasible for the intended application. Therefore, to validate if aptamer refolding will be necessary for the IFN-γ aptamers, two batches of aptamers were prepared. Both batches were thawed; one was prepared by denaturing at 95°C for 3 min, cooled on ice for 5 min and brought to room

temperature. The other batch was used as is (in native state). Both batches were tested using an ELONA as previously described in **Chapter 2**, **Section 2.2.3**.

4.2.4 Structural characterisation of full length aptamer A1

4.2.4.1. Truncation of aptamer A1

In-silico truncations of aptamer A1 were performed using *Mfold* http://www.bioinfo.rpi.edu/applications/mfold . The strategy used to perform the truncations was that bases were removed from the 3′-end of the sequence. The guanine bases responsible for forming the G-quadruplex were closer to the 5′-end. Therefore, since this aptamer has the ability to form a G-quadruplex, the bases responsible for forming the structure were not disrupted. The same parameters used to fold the secondary structures were used when folding the truncated derivatives and the predicted binding site. Furthermore, in order to confirm that the G-quadrupplex structures were not disturbed, truncated derivatives were yet again analysed for putative G-quadruplex formation using QGRS Mapper, http://bioinformatics.ramapo.edu/QGRS/ (Kikin et al., 2006).

4.2.4.2. Validation of synthesized apatamer A1 truncated derivatives

The truncated derivatives synthesised on a 200 nM scale and biotin-labelled at the 5′-end were ordered from Biosearch Technologies (CA, USA). The lyophilized derivatives were then re-suspended in ultra-pure distilled water and approximately 100 nM electrophoresed on a 12% native PAGE. The full-length aptamer was included as a positive control. The gel was stained and imaged as described in **Chapter 3**, **Section 3.2.2.1**.

4.2.4.3. Measuring binding of the truncated derivatives vs. full-length

Following validation of the truncated derivatives' size on a gel, their binding efficiencies were determined using an ELONA as previously described (**Chapter 2**, **Section 2.2.3**). Each aptamer at 150 nM was prepared by refolding as previously described prior to use. The reason for using 150 nM was to ensure complete saturation as lower concentrations resulted in decreased binding affinity to IFN-γ (**Chapter 3**, **Section 3.3.4.2**). Two negative controls, Malaria aptamer (27mer) and HIV aptamer (15mer) were included and were donated by Professor Kevin Plaxco (Department of Biochemistry and Chemistry, University of California, Santa Barbara).

4.2.4.4. Binding kinetics of truncated derivatives of aptamer A1 using ELONA

Binding kinetics of truncated derivatives of aptamer A1 were determined using ELONA as previously described in **Chapter 3**, **Section 3.2.2.3**.

4.2.4.5. Binding kinetics of truncated derivatives of aptamer A1 using SPR

In addition, truncated derivative of aptamer A1 were characterised by determining the binding kinetic parameters using SPR as previously described in **Chapter 3**.

4.2.5 Statistical Analyses

Data were analysed as described in **Chapter 3**, **Section 3.2.4**. A paired two-tailed t-test was used for statistically significant data with a p-value of ≤ 0.05.

4.3 RESULTS

4.3.1 Validation of specificity of aptamers to IFN-γ

To test whether the ssDNA aptamers isolated against IFN-γ were specific, I validated them against mycobacterial and non-mycobacterial molecules (listed in **Table 4.1**). The aptamers only bound significantly ($p \leq 0.001$) to IFN-γ and not to any other tested molecules, including those frequently found within the pleural fluid such as albumin and glucose (**Figure 4.2**). Further detail including all controls that were run can be found in **Appendix 4.1**.

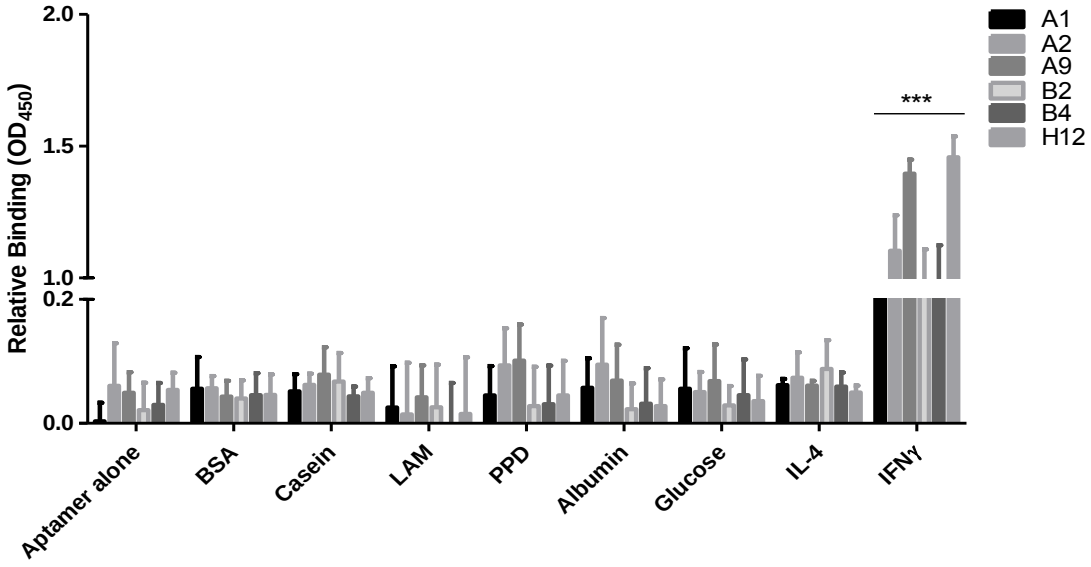

Figure 4.2: Specificity of aptamers to IFN-γ in relation to mycobacterial and non-mycobacterial molecules.

Each aptamer was tested at 150 nM. All the molecules tested were at a final concentration of 10 µg/ml. The mycobacterial molecules tested were; lipoarabinomannan (LAM), interleukin 4 (IL-4), and purified protein derivative (PPD). Some of the proteins found in abundance in the pleural fluid and tested included: albumin and glucose. Casein, an abundant protein found in milk (hereto used as blocking buffer) was also included as a control to rule out the possibility of the protein blocking all the available binding sites. Bovine serum albumin (BSA) was also included as a negative control. Data represent two independent experiments (n=2) each done in triplicate. Error bars denote a mean ± SE and *** denotes $p \leq 0.001$.

4.3.2 Aptamer-Antibody sandwich ELONA

Aptamers are useful in sandwich assays as aptamer-antibody pairs (Drolet et al., 1996, Engvall and Perlmann, 1971). Two anti-IFN-γ monoclonal antibodies, CD119 and CD66, were tested in sandwich ELONA with each aptamer in the presence of IFN-γ. The OD_{450} of each of the antibody-aptamer pairs was less than that of the aptamer-only control (**Figure 4.3**). For aptamer A1, the aptamer-only control had an OD of 1.3062 vs. ODs of 0.3452 ($p \leq 0.001$) and 0.4766 ($p \leq 0.001$) for anti-IFN-γ antibodies CD119 and CD66, respectively (**Figure 4.3A**). Also, aptamers paired with CD66 generally had higher binding than those paired to CD119. For example, aptamer H12 had an OD of 0.802 when paired to CD66 and an OD of 0.463 when paired to CD119 ($p \leq 0.001$) (**Figure 4.3F**). Similarly, aptamer B4 had an OD of 0.5168 when paired with CD66 and an OD of 0.1888 when paired with CD119 ($p \leq 0.001$) (**Figure 4.3D**).

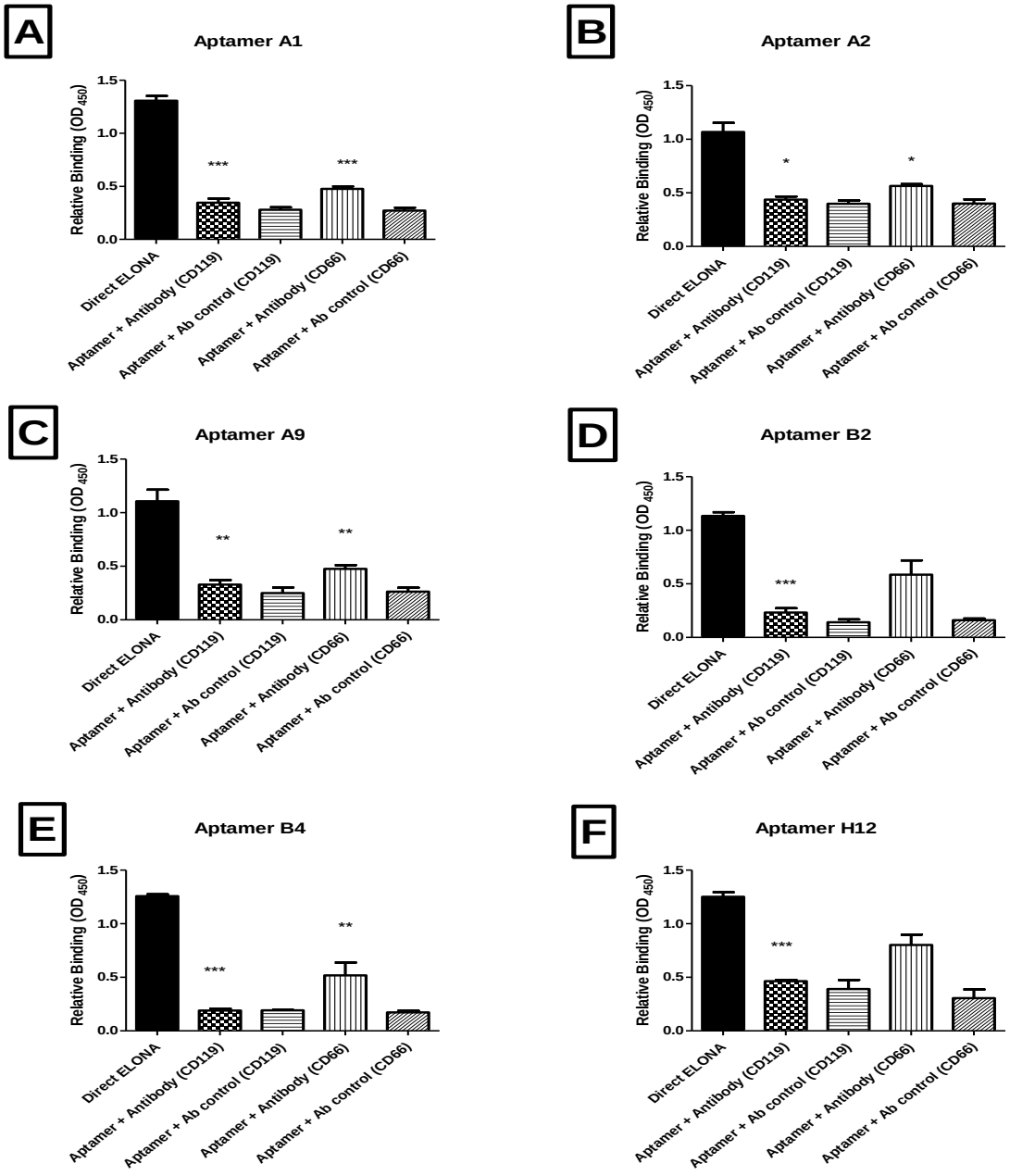

Figure 4.3: An aptamer only (Direct) ELONA vs. aptamer-antibody sandwich ELONA.

Two monoclonal anti- IFN-γ antibodies, CD119 and CD66 were tested for binding IFN-γ in the presence of the aptamer. On separate microtitre plates, wells were coated with 1 µg/ml of either antibody, CD119 or CD66. The IFN-γ and aptamer were then introduced and the binding affinity compared to direct testing of IFN-γ in absence of antibody (direct ELONA). On each plate, each molecule (aptamer or antibody) was tested alone, to rule out contamination. Also added was the aptamer + antibody control (in absence of IFN-γ) for each aptamer. A paired two-tailed t-test was used to determine significance (*$p \leq 0.05$, **$p \leq 0.01$, ***$p \leq 0.001$) between the aptamer only assay and the aptamer-antibody sandwich assay. Data are for two independent experiments repeats (n=2) each done in triplicate. Results are presented as mean ± SE. The error bars represented the difference in the arithmetic means of optical densities at 450 nm measured in triplicate.

4.3.3 Aptamer refolding does not alter binding affinity

Aptamers are usually refolded by denaturation at high temperatures before being used. This is done to ensure that they are linear and thus will be able to assume the active secondary structure upon binding with target. To test whether the refolding step was necessary for IFN-γ aptamers, we tested two batches of each aptamers which were prepared differently. After thawing, one batch was denatured to 95°C followed by cooling (refolded), and the other batch was used directly (native). Aptamer A1 showed a significant ($p \leq 0.01$) difference in binding when refolded compared to when in a native state at OD450, 0.497 vs. 0.828 (**Figure 4.4**). All other aptamers (A2, A9, B2, B4 and H12) showed no significant differences when tested in the two different states. Aptamer A1 illustrated increased binding affinity when it was not refolded, which is ideal for diagnostic applications.

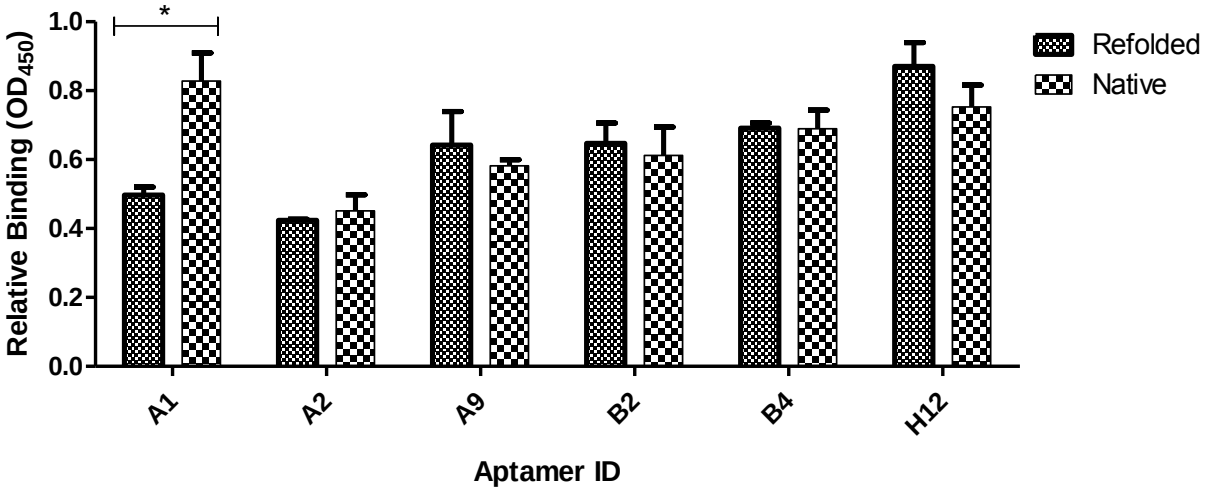

Figure 4.4: Aptamer refolding vs. native state.

Each aptamer was prepared differently and the binding affinity assessed. One batch was denatured at 95°C, rapidly frozen and cooled to room temperature, while the other batch was only thawed and used directly. The two batches were thus tested using an ELONA and their binding affinities compared. A paired two-tailed t-test was used to asses significance between the refolded and native aptamers, where $p \leq 0.05$ was denoted by *. The error bars represented the difference in the arithmetic means of optical densities at 450 nm measured in triplicate.

4.3.4 Structural characterisation of aptamer A1

4.3.4.1. Truncation of aptamer A1

Aptamer A1 was truncated and optimized for future incorporation into the biosensor for EPTB, due to its affinity to IFN-γ, the ability to bind IFN-γ significantly better in its native form and propensity to form G-quadruplexes. It was truncated into three derivatives, where the one showing the best efficiency was chosen for further characterisation. The full-length (90mer) was truncated to 49mer, 36mer and 29mer derivatives, respectively (**Figure 4.5**). When the derivatives were compared to the 90mer, they all shared a common 25nt double stem hairpin loop (**Figure 4.5**). Additionally, the 49mer and 36mer had two secondary structure predictions hereto referred to as truncation 1 (T1) and truncation 2 (T2), with minimum free energies of T1=Δ-1.93; T2=Δ-5.08 and T1=Δ-1.93; T2=Δ-2.87, respectively. The 29mer only had one predicted structure, with a minimum free energy of Δ-2.87. The common double stem hairpin loop was suspected to be the predicted binding site of the aptamer. Also, this double stem hairpin loop was seen on at least one structure (T1) of the two predictions for truncated derivatives 49mer and 36mer. Furthermore, the minimum free energies for the structures (with the double stem hairpin loop) seemed to increase as the truncated derivative became shorter, from 90mer being Δ-5.59 then to Δ-5.08 for 49mer, then to Δ-2.87 for both 36mer and 29mer.

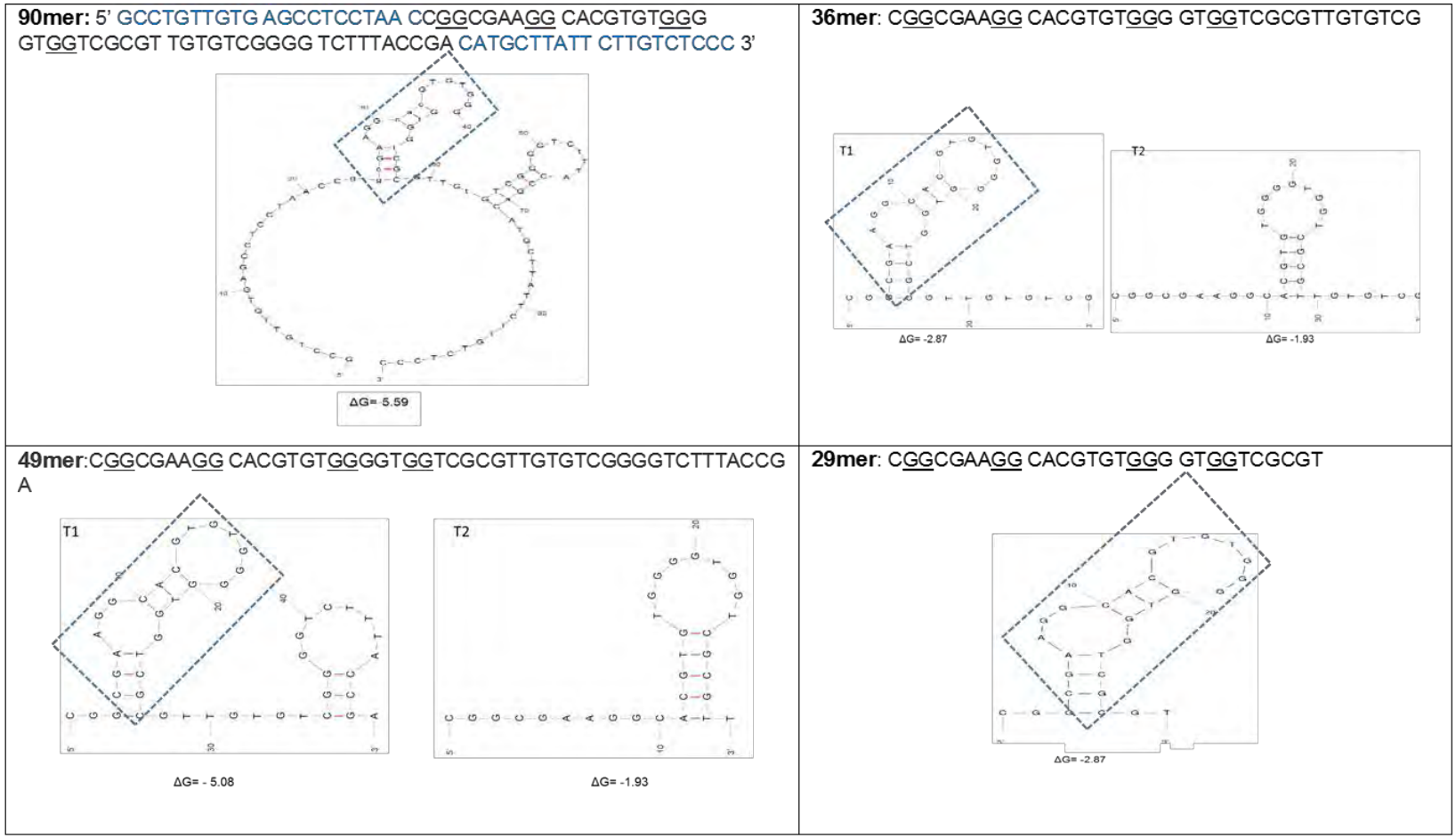

Figure 4.5: Structures and minimum free energies of final truncate derivatives showing preservation of the stable hairpin loop after truncation.

Aptamer A1 was truncated to yield 49mer, 36mer, and 29mer derivatives. The double hairpin loop responsible for binding is highlighted in a blue dashed box, and was found to be present on all the derivatives. The minimum free energies, which gave an indication of the stability of the structure, were found to be 49mer: T1=Δ-1.93; T2=Δ-5.08, 36mer: T1=Δ-1.93; T2=Δ-2.87, 29mer: Δ-2.87, with the 90mer being Δ-5.59. The guanine bases which enabled all truncated derivatives to still have the ability to form a G-quadruplex structure are underlined (shown on each sequence). The aptamer sequences are shown on flanking sides of the 90mer sequence in blue.

4.3.4.2. Confirmation of truncated derivatives forming G-quadruplexes

After truncating aptamer A1 to 49mer, 36mer and 29mer derivatives, they were analysed for putative G-quadruplex formation. As expected, all truncated derivatives could form a G-quadruplex structure (**Table 4.2**). The positions of the bases (GG doublets) responsible for forming the G-quadruplex was the same, from position 2and position 23 of the full length (90mer) parental aptamer. The position of the bases for the 90mer was different because the sequence was longer; it included the primers. The length of the sequence forming the G-quadruplex, for the truncated derivatives and for the 90mer, was found to be the same; containing 22 bases with the same G-score. The G-score of the derivatives and the 90mer was found to be the same at 17, which is expected since the same bases were responsible for the formation of the G-quadruplex for all derivatives.

Table 4.2: Truncated derivatives of aptamer A1 had the ability to form a G-quadruplex structure

Aptamer ID	GQRS position	GQRS length	GQRS	G-score	Sequence
90mer	23	22	GGCGAAGGCACGTGTGGGGTGG	17	5′GCCTGTTGTGAGCCTCCTAACCGGCGAAGGCACGTGTGGGGTGGTCGCGTTGTGTCGGGGTCTTTACCGACATGCTTATTCTTGTCTCCC-3′
49mer	2	22	GGCGAAGGCACGTGTGGGGTGG	17	5′CGGCGAAGGCACGTGTGGGGTGGTCGCGTTGTGTCGGGGTCTTTACCGA-3′
36mer	2	22	GGCGAAGGCACGTGTGGGGTGG	17	5′CGGCGAAGGCACGTGTGGGGTGGTCGCGTTGTGTCG-3′
29mer	2	22	GGCGAAGGCACGTGTGGGGTGG	17	5′GGGCGAAGGCACGTGTGGGGTGGTCGCGT-3′

4.3.4.3. Validation of synthesised truncated derivatives of aptamer A1

All the aptamers were the expected sizes, which was between 20 and 100 bp (**Figure 4.6**). The 90mer appeared as a smear and this was an indication of the multiple possible conformations that it could undergo (**Figure 4.6**). The higher band indicating the formation of a G-quadruplex is supposed to be 4x the number of nucleotides in the sequence. It was noted that the higher band indicative in lane 2 was a contaminant (which was about 90 nucleotides long (equivalent to the 90mer in lane 1), therefore suggestive of a spill-over from lane 1 during aptamer loading onto gel).

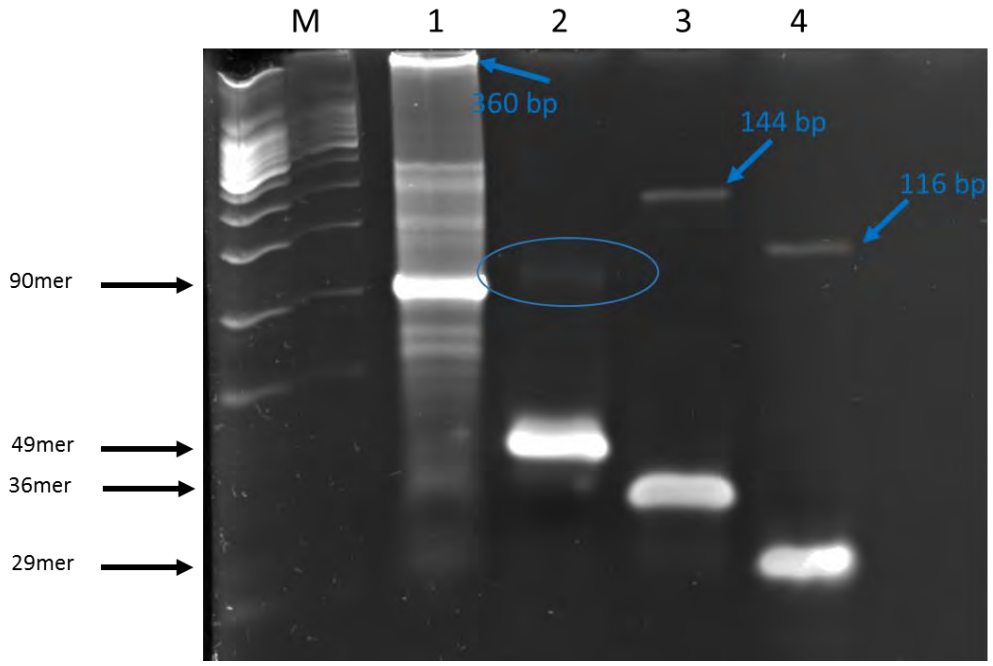

Figure 4.6: A1 truncated derivatives were validated on a 12% non-denaturing PAGE to determine their sizes and topologies.

Truncations of aptamer A1: 49mer, 36mer, and 29mer, were run on a 12% non-denaturing PAGE to determine their sizes, and was compared to the full length 90mer. The lanes were loaded from the largest to the smallest aptamer (lanes 1-4). Lane M: Marker; Lanes 1-4: 90mer, 49mer, 36mer: and 29mer, respectively. The higher bands in lanes 1, 3 and 4 (indicated by blue arrows), are an indication of the aptamer forming a G-quadruplex and their sizes are denoted in blue. A double-stranded DNA marker was used and therefore the sizes of the aptamers are not expected to be accurately displayed on this gel. The motilities of the aptamers however, were about the expected size (between 20 and 100 bp). A faint band seen in lane 2 (denoted with a blue circle) is indicative of a contaminant.

4.3.4.4. Measuring binding efficiencies of full-length vs. truncated derivatives

The binding affinity of the 90mer was compared to the truncated derivatives, 49mer, 36mer and 29mer using an ELONA (**Figure 4.7**). The binding of the 49mer was significantly reduced at OD450 (OD of 49mer = 0.403 vs. 90mer=0.651 ($p \leq 0.01$)) compared to 90mer. No difference in binding was observed for 36mer and 29mer compared to the 90mer (**Figure 4.7**). These data suggested that the 36mer and 29mer derivatives bound IFN-γ comparatively similar to the 90mer. Two aptamer truncated derivatives which are unrelated to TB were used as negative controls (27mer malaria aptamer and a 15mer HIV aptamer) and none of them significantly bound IFN-γ. Since the shortest aptamer that retains functionality is ideal for use in most downstream diagnostic applications, the 29mer was further investigated for such future use.

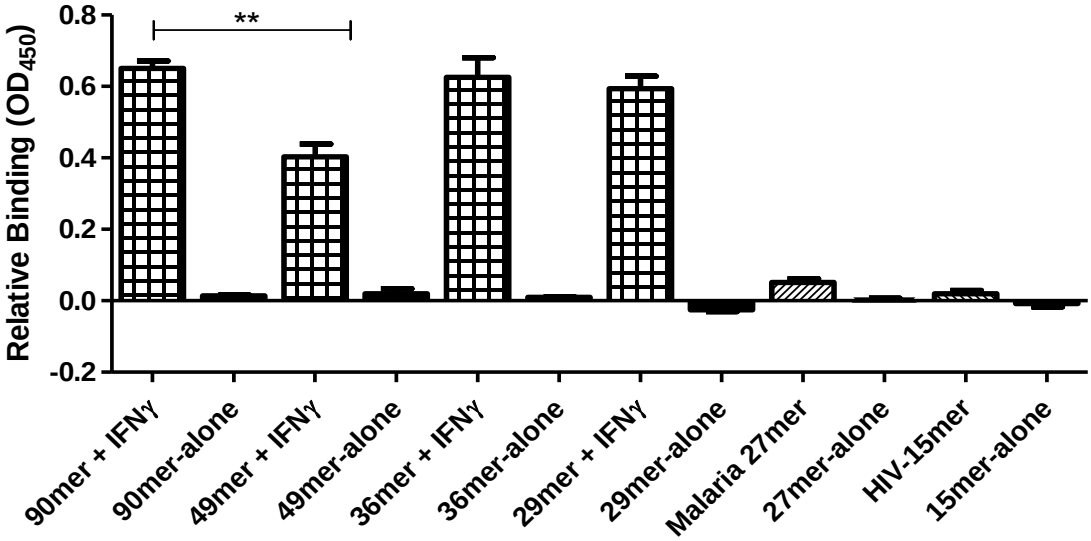

Figure 4.7: Binding of the A1 truncated derivatives compared to the full length parental aptamer and controls.

A paired two-tailed t-test was used to assess significance, ** denotes $p \leq 0.01$. The experiment was performed in triplicate in two independent experiments (n=2). The error bars represented the difference in the arithmetic means.

4.3.4.5. Binding capacity of selected truncated derivatives

The binding capacity of the full length aptamer A1 was investigated using a concentration of 10 µg/ml of IFN-γ. Aptamer A1 was able to significantly bind 10 µg/ml IFN-γ at 18.75 nM. It was therefore necessary to test if these results will be reproduced with truncated derivatives. All the truncated derivatives were assessed and the 90mer included as a positive control (**Figure 4.8**). Only truncated 49mer derivative could significantly bind IFN-γ at 18.75 nM (**Figure 4.8**)

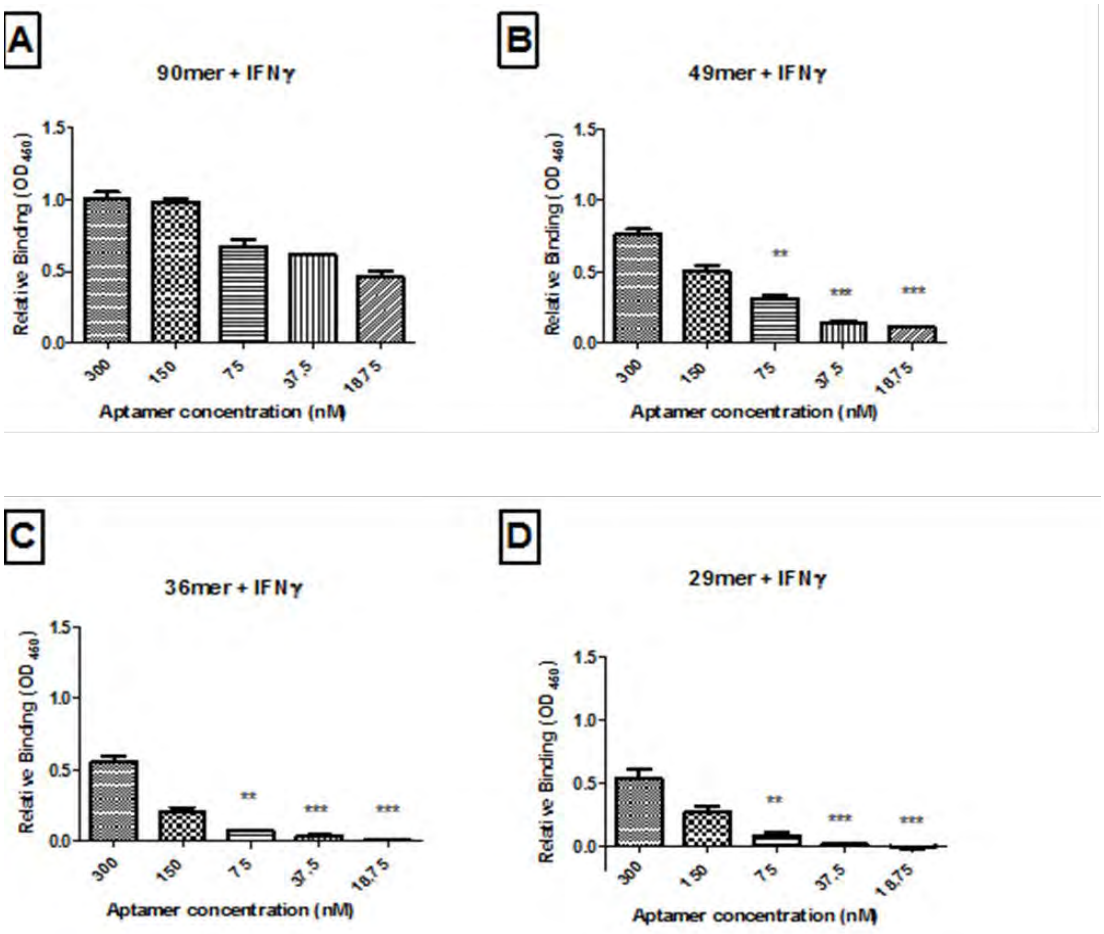

Figure 4.8: Binding of truncated derivatives of aptamer A1 to constant IFN-γ concentration of 10 µg/ml.

Aptamer A1 truncated derivatives were tested in a 2-fold serial dilution at 150 nM, 75 nM, 37.5 nM and 18.75 nM, using a constant concentration of IFN-γ of 10 µg/ml. Following the addition of the aptamers at different concentrations, the rest of the parameters were kept constant throughout the assay. The binding of aptamers from 75-18.75 nM was compared to the binding of each aptamer at 150 nM using 1-way ANOVA with Bonferroni's post-test where significant differences were denoted by *=p≤0.05, **=p≤0.01 and ***=p≤0.001. Data are for two independent experiments (n=2) each done in triplicate. Error bars represent mean ± SE.

4.3.4.6. Binding kinetics of truncated derivative: A1-29mer

In addition to characterising the aptamer A1-29mer for its possible incorporation into an application such as a biosensor, its kinetic parameters including association constant rate (K_a), dissociation constant rate (K_d) and equilibrium dissociation constant (K_D) were determined using SPR (**Figure 4.9**). A large increase in the association constant (K_a) of the 29mer compared to the 90mer, from 3.75E+4 to 1.29E+7 was seen (**Figure 4.9**). Additionally, truncated derivative 29mer dissociated from IFN-γ with a K_d of 1.32E-3, which was an increase from 2.02E-4 calculated for the 90mer (**Table 4.2**). The calculated K_D was found to be 1.02E-10 for the 29mer compared to 5.39E-9 for the 90mer (**Figure 4.9** and **Table 4.2**). This data supported the hypothesis that shorter derivatives of an aptamer can increase the binding affinity and in return produce tighter complexes between the molecules (aptamer) and the target (IFN-γ).

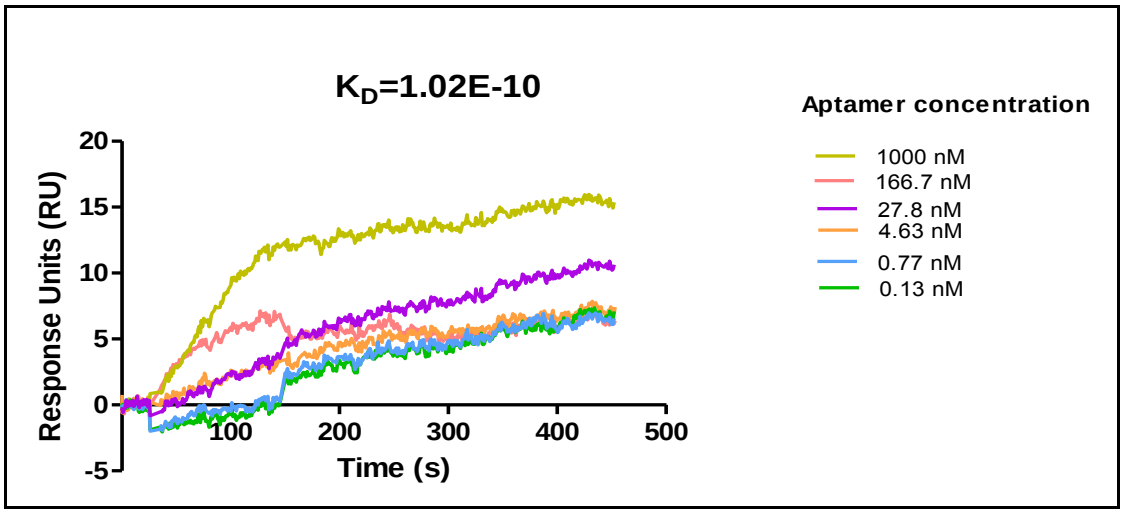

Figure 4.9: Binding kinetics of A1-29mer Biacore.

The equilibrium dissociation constant (K_D) of the 29mer truncated derivative was determined using SPR technology. Recombinant IFN-γ was immobilised on a CM5 chip and each aptamer was exposed to the immobilised IFN-γ at varying concentration, ranging from 0.13 nM to 1000 nM. The aptamer concentration series is shown on the top right corner of each graph and the K_D is shown at the bottom right corner. The aptamers and the IFN-γ were allowed 7 min contact time before dissociation. To calculate and determine the equilibrium dissociation constant using the association and dissociation constant rates, a 1:1 Langmuir model was assumed using the BIAevaluation v4.1 software. The assay was performed in triplicate and the average K_D determined. The K_D was calculated by assuming a 1:1 Langmuir model using the BIAevaluation software package.

Table 4.3: Kinetic parameters of aptamers A1-90mer and A1-29mer truncated derivative

Aptamer ID	Association rate constant [K_a ($M^{-1}s^{-1}$)]	Dissociation rate constant [K_d (s^{-1})]	Equilibrium dissociation constant [K_D (M)]
A1-90mer	**3.75E+4**	**2.02E-4**	**5.39E-9**
A1-29mer	**1.29E+7**	**1.32E-3**	**1.02E-10**

4.4 DISCUSSION

In this chapter, I further characterised the six aptamers and truncated derivatives of aptamer A1. The key findings were: (i) the aptamers were specific to IFN-γ (ii) aptamer-antibody ELONAs had less binding affinity compared to direct (aptamer only) ELONAs; (iii) truncated A1-derivatives had similar free energies and generally kept structural features important for binding; (iv) the truncated A1-29mer derivatives showed increased performance and stability compared to the full length parental molecule.

The most important prerequisites of a good clinical POC diagnostic test are high sensitivity, specificity and rapidity. Aptamers can have specificities and affinities that are comparable to monoclonal antibodies, and in some cases are superior (McKeague et al., 2010, Jayasena, 1999). IFN-γ aptamers raised in this study were found to be highly specific. This was similar to findings reported for other aptamers isolated against *M. Tuberculosis* cell component lipoarabinomannan (LAM) (Pan et al., 2014) and other targets such as *human influenza-B virus*, *Shigella dysenteriae*, *Leshmania infantum* and *Vibrio alginolyticus* (Gopinath et al., 2006a, Tang et al., 2013, Duan et al., 2013, Martín et al., 2013).

None of the IFN-γ aptamers described in this study bound any of the mycobacterial and non-mycobacterial molecules they were tested against. Thus, the aptamers did not significantly bind mycobacterial molecules such as PPD and LAM and human markers made in response to mycobacterial infection such as IL-4. Interestingly, the aptamers also did not bind molecules known to be present in abundance in the pleural fluid such as albumin and glucose. Although previous work by others has described isolation of aptamers against IFN-γ; specificity of the aptamers was not determined (Balasubramanian et al., 1998). However, a recent study demonstrated good specificity of a DNA aptamer isolated against IFN-γ for its intracellular measurement in an

immunoassay (Cao et al., 2014). The aptamer was tested against albumin, since it is a protein well known to be abundant in blood (Cao et al., 2014). Additionally, they used Balasubramanian's aptamer as a control, and that showed binding to albumin, suggesting that it lacked specificity (Cao et al., 2014, Balasubramanian et al., 1998). The results of this study therefore suggest that the aptamers are unlikely to yield false positive results due to non-specific binding. Although not all molecules contained in the pleural fluid were tested, the ability of the aptamers to not cross-react with any of the highly abundant constituents was an encouraging finding.

To address the suboptimal IFN-γ sensitivity reported in Chapter 3, an aptamer-antibody sandwich ELONA was optimised to increase performance. Studies have shown sandwich assays to have the ability to exceed the sensitivity and specificity compared to direct assays (Drolet et al., 1996, Grebenchtchikov et al., 2004). As an example, Drolet and co-workers (1996) performed a sandwich ELONA (using an aptamer and antibody) to detect and quantitate VEGF isoform in serum samples and compared it to an ELISA, which it outperformed yielding a sensitivity of 25pg/ml. In addition, the ELONA had higher OD readings compared to the ELISA in twelve of the 21 (57%) serum samples tested. In a similar study, Shiratori and colleagues reported binding affinities 10-fold higher in a sandwich ELONA compared to a direct assay. Additionally, the direct assay needed a 100-fold more concentration of the virus, to generate a signal similar to the indirect assay (Shiratori et al., 2014). The aptamer-antibody sandwich assay described in this study was, however, outperformed by the direct (aptamer-only) ELONA. The direct ELONA also yielded higher OD values compared to the aptamer-antibody sandwich assay. Binding in the direct format was almost twice that of the sandwich assay (e.g. for aptamers B2 and H12), which was similar to findings reported by others (Shiratori et al., 2014). These findings therefore suggested that the direct assay was more sensitive. Two possibilities could be responsible for this phenomenon. Either there were no epitopes available for both the aptamer and the antibody to bind. For instance, it is obvious that both molecules need to bind the target on two different epitopes in order for the assay to

be a success. Therefore, the target protein needs to be mapped using technologies like nuclear magnetic resonance (NMR) or X-ray crystallography to ensure that both molecules can simultaneously bind. In fact, using two aptamers could actually be a solution. Balogh and co-workers (2010) developed a double-oligonucleotide sandwich (DOS) ELONA for detecting protein in complex virus matrices, which outperformed commercial double-antibody sandwich assay (Balogh et al., 2010). The same approach was reported by Shiratori (Shiratori et al., 2014), and both groups demonstrated improved sensitivities. Alternatively, site directed SELEX can be performed from the beginning, in order to isolate aptamers targeted at certain epitopes (Kulbachinskiy, 2007).

On the other hand, the aptamers could assume a different structure in presence of the antibody. Interestingly, my data suggested that the binding of the aptamers to IFN-γ was not affected by a refolding step except for aptamer A1. This meant that the binding of the aptamers was the same irrespective of whether they were denatured or not. This could be an indication that the aptamers only self-assembled into specific conformations upon binding the target and were not dependent on a denaturation step. Furthermore, the phenomena seen for aptamer A1 could be suggesting that the "unstructured" aptamer in solution can linearize and bind without being denatured. Rotherham et al reported the same results for ESAT6:CFP10 aptamers and this bodes well for the future development of POC clinical diagnostics (Rotherham et al., 2012).

In order to understand the binding mechanisms of aptamers, knowledge of the structure of the aptamer and the predicted binding site are important. Furthermore, not all nucleotide bases of an aptamer are essential for binding. In fact,, structural analysis showed that aptamers can retain their functionality even when the essential bases are removed, provided the structure of the necessary bases does not change (Jayasena, 1999). Truncations are usually performed to remove non-essential nucleotides of an

aptamer sequence, thus increasing sensitivity and specificity and reducing production costs during chemical synthesis. In addition, truncated derivatives are structurally suitable and ideal for incorporations into biosensing platforms.

In this study aptamer A1 was truncated because it had a K_D in the low nanomolar range (5.39E-9), it bound significantly better to IFN-γ, and it had the ability to form a G-quadruplex due to its guanine-rich sequence. This was supported by the evidence showing the ability of full length aptamer A1 to encompass a range of multiple conformations (DNA sizes ~90 nucleotides and ~20 nucleotides) on a non-denaturing PAGE (**Figure 4.6**). Furthermore, the truncated derivatives were also able to form G-quadruplexes which was apparent on this type of gel, thus highlighting their stability. G-quadruplexes can appear as monomeric or multimeric form (Shum and Tanner, 2008). The migration of truncated derivatives 36mer and 29mer was an indication of their multimeric forms. The higher band seen in lanes 1, 3 and 4 is an indication of this. Therefore, the total number of nucleotides of each truncated derivative was multiplied by four in order to accurately identify the G-quadruplex. As such, the expected sizes were 360mer (90x4), 144mer (36x4) and 116mer (29x4) for the 90, 36 and 29mer, respectively (**Figure 4.6**). An interesting observation made was that the 49mer derivative was different in topology from other derivatives and the full length aptamer (based on the different mobilities). The 49mer was monomeric as it ran as a single band, which has been seen in previous studies (Hamilton and Germann, 2011, Shum and Tanner, 2008). Also noted was that the 49mer derivative had reduced binding compared to the full length aptamer and other derivatives (36mer and 29mer) (**Figure 4.7**). The loss in sensitivity could be attributed to the fact it forms a monomeric G-quadruplex, as seen on the non-denaturing PAGE. The topologies of the truncated derivatives can further be confirmed by circular dichroism (CD) studies, which is a widely used technique for this purpose.

Although the binding of the 49mer was reduced compared to the 90mer, the binding affinity of the 36mer and 29mer was similar. Of interest though, was the fact that all truncated derivatives retained the common 25nt double stem hairpin loop, even though the binding affinities differed. Due to the high affinity for IFN-γ that the 29mer had, it was selected to be further characterised for its possible future incorporation into a biosensor. SPR was used to determine the K_D of the truncated aptamer. Indeed, a large increase in the K_a was seen, signifying a very quick "on-rate". In terms of POC tests, this characteristic will be valuable as the process will be a timed reaction. This means that the aptamer-IFN-γ complex will be able to form in less than 10 min. In addition, an improved K_D for the 29mer was also observed. It is possible that this K_D could be inaccurate as the SPR curves did not clearly show the "off-rate" (Figure 4.9) compared to those seen for the full length aptamer A1 (Figure 3.8). It looked like the aptamer-IFN-γ complex was not coming "off"/separating. The size of the aptamer could have contributed to its instability when used in this type of assay. Another group has reported similar findings where truncated derivatives had increased K_D (20 nM to 1.4 nM) compared to their full length counterparts (Nonaka et al., 2010). This further supports the notion that shorter aptamers have better affinities than their longer parental molecules.

4.5 CONCLUSION

I have demonstrated that IFN-γ aptamers are specific and have no cross-reactivity with other molecules common in the pleural fluid like albumin and glucose. Anti-IFN-γ monoclonal antibodies when used in conjunction with aptamers did not improve sensitivity, likely due to shared epitopes. Furthermore, I demonstrated the efficiency of a truncated derivative, A1-29mer, which performed equally well as the 90mer. Moreover, I showed *in silico* that truncated derivatives retained their G-quadruplex structures, which the full-length version had. Taken together, these data could be used as a basis for the future development of these aptamers in diagnostic applications for EPTB.

CHAPTER 5
GENERAL DISCUSSION AND CONCLUSION

5.1 SUMMARY OF FINDINGS

This study described the generation and characterisation of aptamers for the detection of IFN-γ (a clinically important biomarker for the diagnosis of extra-pulmonary TB) using SELEX technology. To date, there are limited diagnostics for pleural TB: i) ADA colorimetric assay; ii) culture; and iii) smear microscopy. These tests, however, have low sensitivity and consequently result in false negatives thereby missing many individuals with EPTB. Even the newest NAAT technology like the GeneXpert has sub-optimal sensitivity of only ~20% in EPTB cases (Meldau et al., 2014, Friedrich et al., 2011, Moure et al., 2012). This therefore warranted the need to develop a POC test with high sensitivity and specificity.

Eight iterative rounds of selection were performed where a pool recovered from the sixth round (which had the highest recovery) was cloned and sequenced. Sixty aptamer candidates were identified, which shared sequence homology and a consensus sequence was determined. Forty five candidate aptamers specifically bound IFN-γ. Six aptamers were randomly selected for further characterisation.

The six selected aptamers bound IFN-γ with high affinity and specificity. Their structural characteristics comprised of long hairpin stem loops, which contributed to their increased affinity. The stability of the aptamers (aptamers A1 and B4) was enhanced by their ability to form G-quadruplex structures, which is a feature of high performance aptamers commonly used in biosensors and microfluidic devices (Song et al., 2008, Hong et al., 2012, O'Sullivan, 2002, Willner and Zayats, 2007, Zhou et al., 2010, Xu et al., 2009). Of importance was the ability of all aptamers to discriminate against other mycobacterial molecules and non-mycobacterial molecules including those contained in the pleural fluid. This finding showed minimal cross reactivity of proteins

within the pleural fluid, although it could not be established if the pH and salt content will potentially affect the binding of aptamers in the pleural fluid sample (Banerjee and Nilsen-Hamilton, 2013).

This study confirmed that the aptamers have high affinity for their targets in the low nanomolar range, which is similar to that of antibodies. Their size and ability to form different structures, however, can result in an even lower dissociation constant (picomolar range). Aptamers A9 and H12 bound IFN-γ in the picomolar range at 206 pM and 390 pM, respectively. The LOD was found to be 10 μg/ml for all the six aptamers, which is similar to other studies that have created aptamers to *Vibrio alginolyticus* and *Leishmania infantum* (Tang et al., 2014, Martín et al., 2013). IFN-γ is, however, found in picogram concentrations in pleural fluid. Recent work using an "in-house" ELISA-like assay determined the biological range of IFNy in individuals with pleural TB to be as low as 110 pg/ml (Meldau et al., 2014). Therefore the inability of the aptamers to detect IFN-γ in this biological range could pose a challenge as they have high specificity but reduced sensitivity. In view of this finding, I paired the aptamers with an anti-IFN-γ antibody with the expectation of achieving an improved LOD since sandwich assays have been shown to have high sensitivity (Drolet et al., 1996, Grebenchtchikov et al., 2004). The data showed no improvement in signal when the sandwich assay (aptamer-antibody) was compared to the performance of the aptamer only assay. This could mean two things: (i) Either the aptamer and antibody competed for the same epitope on IFN-γ, hence the decreased signal, or (ii) only the antibody is binding. These findings provide evidence of the potential of aptamers to be used in diagnostic platforms.

To validate if truncations could improve the binding affinity to IFN-γ, one aptamer was selected. Aptamer H12 was a likely candidate as it had the qualities one would selected for in terms of specificity, affinity and stability. However, this aptamer was not a putative G-quadruplex forming aptamer, which is important for devices based on

biosensor or microfluidic technologies. The lack of this characteristic favoured truncation of aptamer A1, whose performance was within the acceptable standards. The truncated derivatives were tested and their bindings favourably compared to the full length aptamer. Thus, the binding affinity of the truncated derivatives was not superior to the full length, but rather remained the same, which is in agreement with other reports (Rockey et al., 2011). Binding kinetics of the truncated derivative A1-29mer revealed an improved K_D further supporting the hypothesis that non-essential bases of aptamers can be removed without compromising functionality (Baouendi et al., 2012).

In this study, a novel truncated DNA aptamers that bound IFN-γ with high affinity in the low nanomolar range was discovered. This is supported by the fact that all truncated derivatives retained the 25nt double stem loop, which is hypothesised to be the actual binding site of the aptamer. Furthermore, all truncated derivatives could still form G-quadruplex structures, which could further be characterised by CD, X-ray crystallography, and/or NMR, in order to understand further their topologies prior to using them in downstream diagnostic applications.

5.2 IMPLICATIONS OF THIS STUDY

Since the announcement of the pipeline of developing novel technologies to curb the TB epidemic by the World Health Organisation, great strides have been made in the field. About 25% of the TB population has EPTB and this prevalence escalates to almost 50% in HIV-AIDS endemic populations (Sharma and Mohan, 2004). Although many successful advances have been made in the diagnosis of PTB since the development of the GeneXpert, it has proved unhelpful in the diagnosis of EPTB. Recent work including findings from our group and others showed that using GeneXpert to diagnose EPTB had low sensitivity (~20%) (Meldau et al., 2014, Friedrich et al., 2011, Moure et al., 2012, Porcel et al., 2013). Even when using other specimens for EPTB i.e. cerebrospinal fluid

(CSF) and urine for diagnosis with the same technology, the sensitivity was still sub-optimal (Hillemann et al., 2011, Patel et al., 2013).

Since the discovery of IFN-γ as a biomarker for EPTB diagnosis, there is still a lack of POC tests on the market. A University of Cape Town (UCT) spin-off company, Antrum Biotech Inc. has developed a diagnostic test for pleural TB (Meldau et al., 2014). This is an antibody-based assay. The drawbacks associated with these antibodies, however, have driven researchers to look elsewhere for molecules that will overcome the challenges faced by antibodies or maybe even surpass them by performance. In particular more sensitive and rapid assays are required to detect IFN-γ for incorporation into POC assays e.g. lateral flow assays. The aptamer technology has thus been the most recently explored avenue in this regard i.e. likely to have better sensitivity but more importantly short binding times of minutes compared to hours for ELISA thus shortening assay time. Hence, the current project was undertaken.

It has been shown that the performance of aptamers could possibly surpass those of antibodies (Jayasena, 1999) in a number of assays (Kulbachinskiy, 2007) thus possibly creating a niche of their own in diagnostic applications. The amenability of aptamers makes them attractive for specific applications such as biosensors and microarrays, where modifications are vital. Aptamers have been shown to retain their sensitivity post modification. Thus, the aptamers described in this study could be incorporated into an aptasensor and improve their sensitivity by coupling the sensor with an electrochemical readout, which will enhance the signal. With the properties that aptamers come with including their stability, robustness and ease of manufacturing, they are set to change the field of diagnostics. To develop a diagnostic kit, or any other POC device, good sensitivity and specificity cannot be compromised upon. Aptamers have this ability. Even though desired sensitivity levels are sometimes a challenge to achieve, the signal can always be amplified using technologies such as electrochemistry, or gold

nanoparticles. PCR could alternatively be a simple method to use. Other potential advantages include reducing assay time thus reducing overall turnaround time.

5.3 LIMITATIONS OF THIS STUDY

I. Overall limit of detection

The LOD for IFN-γ using the aptamers was 10 µg/ml. ELISA tests used to detect IFN-γ in pleural fluid samples, however, have sensitivity levels in the picomolar range. The lower than expected sensitivity of the aptamers could possibly be attributed to the artefacts of the SELEX protocol, such as PCR bias and the starting concentration of the IFN-γ or less stringent conditions when performing the SELEX.

PCR amplification bias could have played a role in the loss of identifying high affinity binding aptamers, by preferentially enriching sequences which were more abundant but with decreased affinity. The most abundant aptamers will be PCR amplified more efficiently and could result in the loss of other sequences. A way to mitigate this would be to sequence an aliquot from each recovered pool at every round to ensure that high-affinity binders were carried through to the next round. To date, these mitigating steps have not been required during a SELEX protocol as aptamers with high sensitivity have been produced against various targets e.g. cocaine aptamer, and their LOD are the same order of magnitude as that reported here. Nevertheless, despite this suboptimal LOD, this is the first study to isolate IFN-γ aptamers for the diagnosis of EPTB. None of the two IFN-γ aptamers described in literature were assessed for this (Balasubramanian et al., 1998, Cao et al., 2014, Lee et al., 1996).

Another possible contribution to the suboptimal LOD was that aptamers should have been isolated against IFN-γ in the biological range (picogram levels). This could have also been introduced as a stringency method (decreased concentration at later rounds) during the selection process. Due to the large variations in the concentration of IFN-γ in biological samples (Meldau et al., 2014), and the information obtained from this project, future studies can be designed to select aptamers using picomolar concentrations of IFN-γ.

II. Only a subset of aptamer clones were sequenced and not the entire final recovered pool

Due to resources available at the time of this study, after the SELEX reached a plateau the final recovered pool was cloned and only 96 randomly picked colonies were sequenced. Additionally, some sequences were eliminated for various reasons discussed in Chapter 2. In future studies, to overcome this limitation, one would design the study so that high-throughput sequencing platforms like Illumina (Schütze et al., 2011, Cho et al., 2010, Guo et al., 2014) would be used as they produce a significantly higher number (thousands-millions) of reads. Nevertheless, the number of sequences screened is similar to other studies. For example, Cao and co-workers (2014), Ferreira and co-workers (2008) and Rotherham et al (2012) analysed 96, 100 and 104 clones, respectively (Cao et al., 2014, Ferreira et al., 2008, Rotherham et al., 2012).

III. Clinical validation not done

While a clinical validation could have strengthened the study, it should be noted that numerous studies on aptamers exclude a clinical validation (Ngubane et al., 2014, Gopinath et al., 2006a, Grozio et al., 2013). A small set of clinical samples were tested for pleural TB. However, the sensitivity could not be determined

(data not shown). The experiment failed, and I hypothesised that it could have been for one of the following reasons:

- The aptamer could have been unable to detect the low levels of IFN-γ in the pleural fluid.
- The aptamers could have been undergoing degradation due to the presence of nucleases in the pleural fluid. Neither the oligonucleotide library used for the SELEX nor the aptamers were labelled in order to prevent nuclease degradation.
- The aptamers could have adopted different conformations once in pleural fluid, mainly because of the Na^+, K^+ concentrations and pH, which could have been different from the buffer used during SELEX.

Future work will hopefully address these possibilities.

IV. Exclusion of structurally-related proteins for specificity testing

It is acknowledged that a structurally-related protein to IFN-γ, such as interferon–alpha (IFN-α) would have added more value as a control to the specificity data. This is important because aptamers have been shown to be highly specific. Their specificity is attributed to their ability to differentiate between two structurally-related molecules (Eaton et al., 1995, Hermann and Patel, 2000). This control will be included in future specificity assays.

5.4 FUTURE WORK

The aptamers need to be tested in clinical samples in order to establish their validity. Negative pleural fluid samples will be spiked with known concentrations of IFN-γ. A diagnostic accuracy study will then be performed using clinical samples which have already been collected and are currently bio-banked for this purpose, for which we have already received ethical approval. Furthermore, the pH and salt concentrations of the

pleural fluid will be determined, which will assist in optimising the conditions in the buffers when repeating the SELEX using a different approach. We will select new aptamers using recombinant IFN-γ and perform rounds of counter-selection against other proteins e.g. albumin, which is abundantly present in the pleural fluid. To ensure that the newly developed aptamers will be highly sensitive in diagnosing pleural TB, I will optimise for detection in the biological range (picogram levels). Firstly, I will use a modified library to perform the selection. The nucleotide library will be modified with an NH_2-group to make the bases nuclease resistant (Nimjee et al., 2005b, Bruce E, 1997).The random region size will remain unchanged (as 49mer) since longer regions have been shown to allow better opportunities of identifying "winning" aptamers mainly due to the many conformations they can adopt (Marshall and Ellington, 2000). Although other researchers prefer to develop short aptamers which need not to be truncated later, I prefer the former.

The new approach will also include the monitoring of the evolution of the SEELX. Simply put, I will sequence (Illumina sequencing) an aliquot from each recovered pool of every SELEX round, and I will perform alignments and phylogenetic studies to study the evolution of sequences. Furthermore, binding studies to determine the dissociation constant using SPR (Biacore 3000) will be performed for every other SELEX round where the concentration of IFN-γ will be kept constant and the pool diluted in varying concentrations.

5.5 CONCLUSION

I have successfully generated aptamers that bind IFN-γ with high affinity and specificity. Six candidate aptamers were characterised, and while inclusion with an antibody in a sandwich assay did not improve binding affinity, the K_D of aptamer A1 was improved upon truncation. This implies that it is a good candidate for possible incorporation into a biosensing device, especially because of its ability to form a G-quadruplex. The aptamers generated here are, although highly specific, are unable to detect IFN-γ in the biologically meaningful range. Recommendations on future work include coupling aptamers described in these study, such as A1 and its truncated derivatives to gold nanoparticles to increase their sensitivity; in tandem isolate next generation aptamers under more stringent conditions that mimic the physiological environment and concentration of IFN-γ in pleural fluids.

REFERENCES

ADILAKSHAMI, T. & LAINE, R. O. 2002. Ribosomal protein S25 mRNA partners with MTF-1 and La tp rpovide a p53-mediated mechanism for survival or death. . *J Biol Chem,* 277**,** 4147-51.

AL-OTAIBI, A., ALMUNEEF, M. & HAMEED, T. 2012. An unusual combination of extrapulmonary manifestations of tuberculosis in a child. *Journal of Infection and Public Health,* 5**,** 203-206.

ASAI, R., NISHIMURA, S. I. & TAKAHASHI, K. 2003. DNA aptamers that recognize fluorophore using on-chip screening in combination with an in silico evolution. *Nucleic Acids Symposium Series,* 3**,** 321-322.

BALASUBRAMANIAN, V., NGUYEN, L. T., BALASUBRAMANIAN, S. V. & RAMANATHAN, M. 1998. Interferon-γ-Inhibitory Oligodeoxynucleotides Alter the Conformation of Interferon-γ. *Molecular Pharmacology,* 53**,** 926-932.

BALOGH, Z., LAUTNER, G., BARDÓCZY, V., KOMOROWSKA, B., GYURCSÁNYI, R. E. & MÉSZÁROS, T. 2010. Selection and versatile application of virus-specific aptamers. *The FASEB Journal,* 24**,** 4187-4195.

BANALES, J. L., PINEDA, P. R., FITZGERALD, J. M., RUBIO, H., SELMAN, M. & SALAZAR-LEZAMA, M. 1991. ADenosine deaminase in the diagnosis of tuberculous pleural effusions. a report of 218 patients and review of the literature. *Chest,* 99**,** 355-357.

BANERJEE, J. & NILSEN-HAMILTON, M. 2013. Aptamers: multifunctional molecules for biomedical research. *Journal of Molecular Medicine,* 91**,** 1333-1342.

BANG, G. S., CHO, S. & KIM, B.-G. 2005. A novel electrochemical detection method for aptamer biosensors. *Biosensors and Bioelectronics,* 21**,** 863-870.

BAOUENDI, M., COGNET, J. A. H., FERREIRA, C. S. M., MISSAILIDIS, S., COUTANT, J., PIOTTO, M., HANTZ, E. & HERVÉ DU PENHOAT, C. 2012. Solution structure of a truncated anti-MUC1 DNA aptamer determined by mesoscale modeling and NMR. *FEBS Journal,* 279**,** 479-490.

BARFOD, A., PERSSON, T. & LINDH, J. 2009. In vitro selection of RNA aptamers against a conserved region of the Plasmodium falciparum erythrocyte membrane protein 1. *Parasitology Research,* 105**,** 1557-1566.

BARTHELMEBS, L., JONCA, J., HAYAT, A., PRIETO-SIMON, B. & MARTY, J.-L. 2011. Enzyme-Linked Aptamer Assays (ELAAs), based on a competition format for a rapid and sensitive detection of Ochratoxin A in wine. *Food Control,* 22**,** 737-743.

BATES, M., O'GRADY, J., MAEURER, M., TEMBO, J., CHILUKUTU, L., CHABALA, C., KASONDE, R., MULOTA, P., MZYECE, J., CHOMBA, M., MUKONDA, L., MUMBA, M., KAPATA, N., RACHOW, A., CLOWES, P., HOELSCHER, M., MWABA, P. & ZUMLA, A. 2013. Assessment of the Xpert MTB/RIF assay for diagnosis of tuberculosis with gastric lavage aspirates in children in sub-Saharan Africa: a prospective descriptive study. *The Lancet Infectious Diseases,* 13**,** 36-42.

BEMER, P., PALICOVA, F., RÜSCH-GERDES, S., DRUGEON, H. B. & PFYFFER, G. E. 2002. Multicenter Evaluation of Fully Automated BACTEC Mycobacteria Growth Indicator Tube 960 System for Susceptibility Testing of Mycobacterium tuberculosis. *Journal of Clinical Microbiology,* 40**,** 150-154.

BENDAYAN, D., HENDLER, A., LITMAN, K. & POLANSKY, V. 2012. The role of interferon-gamma release assays in the diagnosis of active tuberculosis. *Isr Med Assoc J. ,* 14**,** 107-10.

BERGMANN, J. S. & WOODS, G. L. 1997. Mycobacterial growth indicator tube for susceptibility testing of Mycobacterium tuberculosis to isoniazid and rifampin. *Diagnostic Microbiology and Infectious Disease,* 28**,** 153-156.

BIANCHINI, M., RADRIZZANI, M., BROCARDO, M. G., REYES, G. B., GONZALEZ SOLVEYRA, C. & SANTA-COLOMA, T. A. 2001. Specific oligobodies against ERK-2 that recognize both the native and the denatured state of the protein. *J Immunol Methods,* 252**,** 191-7.

BLAKEMORE, R., STORY, E., HELB, D., KOP, J., BANADA, P., OWENS, M. R., CHAKRAVORTY, S., JONES, M. & ALLAND, D. 2010. Evaluation of the Analytical Performance of the Xpert MTB/RIF Assay. *J. Clin. Microbiol.,* 48**,** 2495-2501.

BOCK, C., COLEMAN, M., COLLINS, B., DAVIS, J., FOULDS, G., GOLD, L., GREEF, C., HEIL, J., HEILIG, J. S., HICKE, B., NELSON HURST, M., HUSAR, G. M., MILLER, D., OSTROFF, R., PETACH, H., SCHNEIDER, D., VANT-HULL, B., WAUGH, S., WEISS, A., WILCOX, S. K. & ZICHI, D. 2004. Photoaptamer arrays applied to multiplexed proteomic analysis. *PROTEOMICS,* 4**,** 609-618.

BOCK, L. C., GRIFFIN, L. C., LATHAM, J. A., VERMAAS, E. H. & TOOLE, J. J. 1992. Selection of single-stranded DNA molecules that bind and inhibit human thrombin. *Nature,* 355**,** 564-566.

BOEHM, U., KLAMP, T., GROOT, M. & HOWARD, J. C. 1997. CELLULAR RESPONSES TO INTERFERON-γ. *Annual Review of Immunology,* 15**,** 749-795.

BOEHME, C. C., NABETA, P., HILLEMANN, D., NICOL, M. P., SHENAI, S., KRAPP, F., ALLEN, J., TAHIRLI, R., BLAKEMORE, R., RUSTOMJEE, R., MILOVIC, A., JONES, M., O'BRIEN, S. M., PERSING, D. H., RUESCH-GERDES, S., GOTUZZO, E., RODRIGUES, C., ALLAND, D. & PERKINS, M. D. 2010. Rapid Molecular Detection of Tuberculosis and Rifampin Resistance. *New England Journal of Medicine,* 363**,** 1005-1015.

BRODY, E. N. & GOLD, L. 2000. Aptamers as therapeutic and diagnostic agents. *Reviews in Molecular Biotechnology,* 74**,** 5-13.

BRODY, E. N., WILLIS, M. C., SMITH, J. D., S., J., D., Z. & L., G. 1999. The use of aptamers in large arrays for molecular diagnostics. *Mol Diagn,* 4**,** 381-8.

BRUCE E, E. 1997. The joys of in vitro selection: chemically dressing oligonucleotides to satiate protein targets. *Current Opinion in Chemical Biology,* 1**,** 10-16.

BRUNO, J. G. 1997. In VitroSelection of DNA to Chloroaromatics Using Magnetic Microbead-Based Affinity Separation and Fluorescence Detection. *Biochemical and Biophysical Research Communications,* 234**,** 117-120.

BURGE, S., PARKINSON, G. N., HAZEL, P., TODD, A. K. & NEIDLE, S. 2006. Quadruplex DNA: sequence, topology and structure. *Nucleic Acids Research,* 34**,** 5402-5415.

BURKE, D. H. & WILLIS, J. H. 1998. Recombination, RNA evolution, and bifunctional RNA molecules isolated through chimeric SELEX. *RNA,* 4**,** 1165-75.

CADWELL, R. C. & JOYCE, G. F. 1992. Randomization of genes by PCR mutagenesis. *Genome Research,* 2**,** 28-33.

CADWELL, R. C. & JOYCE, G. F. 1994. Mutagenic PCR. *Genome Research,* 3**,** S136-S140.

CAO, B., HU, Y., DUAN, J., MA, J., XU, D. & YANG, X.-D. 2014. Selection of a Novel DNA Aptamer for Assay of Intracellular Interferon-Gamma. *PLoS ONE,* 9**,** e98214.

CAO, S. & CHEN, S.-J. 2011. Physics-based de novo prediction of RNA 3D structures. *The journal of physical chemistry. B,* 115**,** 4216-4226.

CARSON, D. A. & SEEGMILLER, J. E. 1976. Effect of adenosine deaminase inhibition upon human lymphocyte blastogenesis. *Journal of Clinical Investigation,* 57**,** 274-282.

CENTI, S., TOMBELLI, S., MINUNNI, M. & MASCINI, M. 2007. Aptamer-Based Detection of Plasma Proteins by an Electrochemical Assay Coupled to Magnetic Beads. *Analytical Chemistry,* 79**,** 1466-1473.

CHEN, F., ZHOU, J., LUO, F., MOHAMMED, A.-B. & ZHANG, X.-L. 2007. Aptamer from whole-bacterium SELEX as new therapeutic reagent against virulent Mycobacterium tuberculosis. *Biochemical and Biophysical Research Communications,* 357**,** 743-748.

CHEN, Q., WU, J., ZHANG, Y., LIN, Z. & LIN, J.-M. 2012. Targeted isolation and analysis of single tumor cells with aptamer-encoded microwell array on microfluidic device. *Lab on a Chip,* 12**,** 5180-5185.

CHENG, A. K. H., SU, H., WANG, Y. A. & YU, H.-Z. 2009. Aptamer-Based Detection of Epithelial Tumor Marker Mucin 1 with Quantum Dot-Based Fluorescence Readout. *Analytical Chemistry,* 81**,** 6130-6139.

CHENG, V., YEW, W. & YUEN, K. 2005. Molecular diagnostics in tuberculosis. *European Journal of Clinical Microbiology & Infectious Diseases,* 24**,** 711-720.

CHINTU, C. 2007. Tuberculosis and human immunodeficiency virus co-infection in children: management challenges. *Paediatric Respiratory Reviews,* 8**,** 142-147.

CHO, E. J., COLLETT, J. R., SZAFRANSKA, A. E. & ELLINGTON, A. D. 2006. Optimization of aptamer microarray technology for multiple protein targets. *Analytica Chimica Acta,* 564**,** 82-90.

CHO, M., OH, S. S., NIE, J., STEWART, R., RADEKE, M. J., EISENSTEIN, M., COFFEY, P. J., THOMSON, J. A. & SOH, H. T. 2015. Array-based Discovery of Aptamer Pairs. *Analytical Chemistry,* 87**,** 821-828.

CHO, M., SOO OH, S., NIE, J., STEWART, R., EISENSTEIN, M., CHAMBERS, J., MARTH, J. D., WALKER, F., THOMSON, J. A. & SOH, H. T. 2013. Quantitative selection and parallel characterization of aptamers. *Proceedings of the National Academy of Sciences,* 110**,** 18460-18465.

CHO, M., XIAO, Y., NIE, J., STEWART, R., CSORDAS, A. T., OH, S. S., THOMSON, J. A. & SOH, H. T. 2010. Quantitative selection of DNA aptamers through microfluidic selection and high-throughput sequencing. *Proceedings of the National Academy of Sciences,* 107**,** 15373-15378.

CHUSHAK, Y. & STONE, M. O. 2009. In silico selection of RNA aptamers. *Nucleic Acids Res,* 37**,** e87.

CITARTAN, M., GOPINATH, S. C. B., TOMINAGA, J., TAN, S.-C. & TANG, T.-H. 2012. Assays for aptamer-based platforms. *Biosensors and Bioelectronics,* 34**,** 1-11.

COLLETT, J. R., CHO, E. J. & ELLINGTON, A. D. 2005. Production and processing of aptamer microarrays. *Methods,* 37**,** 4-15.

CONNELL, T. G., ZAR, H. J. & NICOL, M. P. 2011. Advances in the Diagnosis of Pulmonary Tuberculosis in HIV-Infected and HIV-Uninfected Children. *The Journal of Infectious Diseases,* 204**,** S1151-S1158.

CONRAD, R. C., GIVER, L., TIAN, Y. & ELLINGTON, A. D. 1996. [20] In vitro selection of nucleic acid aptamers that bind proteins. *In:* JOHN, N. A. (ed.) *Methods in Enzymology.* Academic Press.

COOPER, M. 2003. Label-free screening of bio-molecular interactions. *Analytical and Bioanalytical Chemistry,* 377**,** 834-842.

CORRAL, I., QUEREDA, C., NAVAS, E., MARTÍN-DÁVILA, P., PÉREZ-ELÍAS, M. J., CASADO, J. L., PINTADO, V., COBO, J., PALLARÉS, E., RUBÍ, J. & MORENO, S. 2004. Adenosine deaminase activity in cerebrospinal fluid of HIV-infected patients: limited value for diagnosis of tuberculous meningitis. *European Journal of Clinical Microbiology and Infectious Diseases,* 23**,** 471-476.

COULTER, L. R., LANDREE, M. A. & COOPER, T. A. 1997. Identification of a new class of exonic splicing enhancers by in vivo selection. *Mol Cell Biol,* 17**,** 2143-50.

COX, J. C., RUDOLPH, P. & ELLINGTON, A. D. 1998. Automated RNA Selection. *Biotechnology Progress,* 14**,** 845-850.

CRAFT, D. W., JONES, M. C., BLANCHET, C. N. & HOPFER, R. L. 2000. Value of Examining Three Acid-Fast Bacillus Sputum Smears for Removal of Patients Suspected of Having Tuberculosis from the "Airborne Precautions" Category. *Journal of Clinical Microbiology,* 38**,** 4285-4287.

DAVIES, P. D. & PAI, M. 2008. The diagnosis and misdiagnosis of tuberculosis [State of the art series. Tuberculosis. Edited by I. D. Rusen. Number 1 in the series]. *The International Journal of Tuberculosis and Lung Disease,* 12**,** 1226-1234.

DAVIS, J. L., HUANG, L., WORODRIA, W., MASUR, H., CATTAMANCHI, A., HUBER, C., MILLER, C., CONVILLE, P. S., MURRAY, P. & KOVACS, J. A. 2011. Nucleic Acid Amplification Tests for Diagnosis of Smear-Negative TB in a High HIV-Prevalence Setting: A Prospective Cohort Study. *PLoS One,* 6**,** e16321.

DENKINGER, C. M., SCHUMACHER, S. G., BOEHME, C. C., DENDUKURI, N., PAI, M. & STEINGART, K. R. 2014. Xpert MTB/RIF assay for the diagnosis of extrapulmonary tuberculosis: a systematic review and meta-analysis. *European Respiratory Journal,* 44**,** 435-446.

DHEDA, K., VAN ZYL-SMIT, R. N., SECHI, L. A., BADRI, M., MELDAU, R., MELDAU, S., SYMONS, G., SEMPLE, P. L., MAREDZA, A., DAWSON, R., WAINWRIGHT, H., WHITELAW, A., VALLIE, Y., RAUBENHEIMER, P., BATEMAN, E. D. & ZUMLA, A. 2009.

Utility of quantitative T-cell responses versus unstimulated interferon-γ for the diagnosis of pleural tuberculosis. *European Respiratory Journal,* 34**,** 1118-1126.

DIACON, A. H., VAN DE WAL, B. W., WYSER, C., SMEDEMA, J. P., BEZUIDENHOUT, J., BOLLIGER, C. T. & WALZL, G. 2003. Diagnostic tools in tuberculous pleurisy: a direct comparative study. *European Respiratory Journal,* 22**,** 589-591.

DINNES, J., DEEKS, J., KUNST, H., GIBSON, A., CUMMINS, E., WAUGH, N., DROBNIEWSKI, F. & LALVANI, A. 2007. A systematic review of rapid diagnostic tests for the detection of tuberculosis infection. *Health Technol Assess,* 11**,** 1-196.

DOBBELSTEIN, M. & SHENK, T. 1995. In vitro selection of RNA ligands for the ribosomal L22 protein associated with Epstein-Barr virus-expressed RNA by using randomized and cDNA-derived RNA libraries. *Journal of Virology,* 69**,** 8027-8034.

DROLET, D. W., MOON-MCDERMOTT, L. & ROMIG, T. S. 1996. An enzyme-linked oligonucleotide assay. *Nat Biotech,* 14**,** 1021-1025.

DUAN, N., DING, X., WU, S., XIA, Y., MA, X., WANG, Z. & CHEN, J. 2013. In vitro selection of a DNA aptamer targeted against Shigella dysenteriae. *Journal of Microbiological Methods,* 94**,** 170-174.

EATON, B. E., GOLD, L. & ZICHI, D. A. 1995. Let's get specific: the relationship between specificity and affinity. *Chemistry & Biology,* 2**,** 633-638.

ELDIN, E. N. O., A. KHAIRY, M. MEKAWY, A H. GHANEM, M K. 2012. Diagnostic value of ex vivo pleural fluid interferon-gamma versus adapted whole-blood quantiferon-TB gold in tube assays in tuberculous pleural effusion. *Ann Thorac Med. ,* 7**,** 220-5.

ELLINGTON, A. D. & SZOSTAK, J. W. 1990a. In vitro selection of RNA molecules that bind specific ligands. *Nature,* 346**,** 818-822.

ELLINGTON, A. D. & SZOSTAK, J. W. 1990b. In vitro selection of RNA molecules that bind specific ligands. *Nature,* 346**,** 818-22.

ELLINGTON, A. D. & SZOSTAK, J. W. 1992. Selection in vitro of single-stranded DNA molecules that fold into specific ligand-binding structures. *Nature,* 355**,** 850-852.

ENGVALL, E. & PERLMANN, P. 1971. Enzyme-linked immunosorbent assay (ELISA). Quantitative assay of immunoglobulin G. *Immunochemistry,* 8**,** 871-4.

EPSTEIN, D. M., KLINE, L. R., ALBELDA, S. M. & MILLER, W. T. 1987. TUberculous pleural effusions. *Chest,* 91**,** 106-109.

ESCUDERO, B. G., CM. CUESTA, CB. MOLINOS, ML. RODRÍGUEZ, RS. GONZÁLEZ, PA. MARTÍNEZ, GJ. 1990. Cytologic and bacteriologic analysis of fluid and pleural biopsy specimens with Cope's needle. Study of 414 patients. *Arch Intern Med,* 150**,** 1190-4.

EULBERG, D., BUCHNER, K., MAASCH, C., AND KLUSSMANN, S. 2005. Development of an automated in vitro selection protocol to obtain RNA-based aptamers: identification of a biostable substance P antagonist. *Nucleic Acid Research,* 33**,** e45.

FAN, L., CHEN, Z., HAO, X.-H., HU, Z.-Y. & XIAO, H.-P. 2012. Interferon-gamma release assays for the diagnosis of extrapulmonary tuberculosis: a systematic review and meta-analysis. *FEMS Immunology & Medical Microbiology,* 65**,** 456-466.

FANNING, A. 1999. Tuberculosis: 6. Extrapulmonary disease. *CMAJ: Canadian Medical Association Journal,* 160**,** 1597-1603.

FERREIRA, C. S. M., PAPAMICHAEL, K., GUILBAULT, G., SCHWARZACHER, T., GARIEPY, J. & MISSAILIDIS, S. 2008. DNA aptamers against the MUC1 tumour marker: design of aptamer–antibody sandwich ELISA for the early diagnosis of epithelial tumours. *Analytical and Bioanalytical Chemistry,* 390**,** 1039-1050.

FISCHER, D., VAN DER WEYDEN, M. B., SNYDERMAN, R. & KELLEY, W. N. 1976. A role for adenosine deaminase in human monocyte maturation. *Journal of Clinical Investigation,* 58**,** 399-407.

FISCHER, M. E. 2010. Amine Coupling Through EDC/NHS: A Practical Approach. *In:* MOL, N. J. & FISCHER, M. J. E. (eds.) *Surface Plasmon Resonance.* Humana Press.

FISCHER, T., ET AL. 1999. Clathrin-coated vesicles bearing GAIP possess GTPase-activating protein activity in vitro. *proc. Natl. Acad. Sci.,* 96**,** 6722-7.

FLORES, L., PAI, M., COLFORD, J. & RILEY, L. 2005. In-house nucleic acid amplification tests for the detection of Mycobacterium tuberculosis in sputum specimens: meta-analysis and meta-regression. *BMC Microbiology,* 5**,** 55.

FOOT, J. N., FERACCI, M. & DOMINGUEZ, C. 2014. Screening protein – Single stranded RNA complexes by NMR spectroscopy for structure determination. *Methods,* 65**,** 288-301.

FORTÚN, J., MARTÍN-DÁVILA, P., GÓMEZ-MAMPASO, E., VALLEJO, A., CUARTERO, C., GONZÁLEZ-GARCÍA, A., RUBÍ, J., PALLARÉS, E. & MORENO, S. 2014. Extra-pulmonary tuberculosis: a biomarker analysis. *Infection,* 42**,** 649-654.

FRIEDRICH, S. O., VON GROOTE-BIDLINGMAIER, F. & DIACON, A. H. 2011. Xpert MTB/RIF Assay for Diagnosis of Pleural Tuberculosis. *Journal of Clinical Microbiology,* 49**,** 4341-4342.

GELLERT, M., LIPSETT, M. N. & DAVIES, D. R. 1962. HELIX FORMATION BY GUANYLIC ACID. *Proceedings of the National Academy of Sciences of the United States of America,* 48**,** 2013-2018.

GEOJITH, G., DHANASEKARAN, S., CHANDRAN, S. P. & KENNETH, J. 2011. Efficacy of loop mediated isothermal amplification (LAMP) assay for the laboratory identification of Mycobacterium tuberculosis isolates in a resource limited setting. *Journal of Microbiological Methods,* 84**,** 71-73.

GIANG, D. C., DUONG, T. N., HA, D. T. M., NHAN, H. T., WOLBERS, M., NHU, N. T. Q., HEEMSKERK, D., QUANG, N. D., PHUONG, D. T., HANG, P. T., LOC, T. H., LAN, N. T. N., DUNG, N. H., FARRAR, J. & CAWS, M. 2015. Prospective evaluation of GeneXpert for the diagnosis of HIV- negative pediatric TB cases. *BMC Infectious Diseases,* 15**,** 70.

GOLD, L., AYERS, D., BERTINO, J., BOCK, C., BOCK, A., BRODY, E. N., CARTER, J., DALBY, A. B., EATON, B. E., FITZWATER, T., FLATHER, D., FORBES, A., FOREMAN, T., FOWLER, C., GAWANDE, B., GOSS, M., GUNN, M., GUPTA, S., HALLADAY, D., HEIL, J., HEILIG, J., HICKE, B., HUSAR, G., JANJIC, N., JARVIS, T., JENNINGS, S., KATILIUS, E., KEENEY, T. R., KIM, N., KOCH, T. H., KRAEMER, S., KROISS, L., LE, N., LEVINE, D., LINDSEY, W., LOLLO, B., MAYFIELD, W., MEHAN, M., MEHLER, R., NELSON, S. K., NELSON, M., NIEUWLANDT, D., NIKRAD, M., OCHSNER, U., OSTROFF, R. M., OTIS, M., PARKER, T., PIETRASIEWICZ, S., RESNICOW, D. I., ROHLOFF, J., SANDERS, G., SATTIN, S., SCHNEIDER, D., SINGER, B., STANTON, M., STERKEL, A., STEWART, A., STRATFORD, S., VAUGHT, J. D., VRKLJAN, M., WALKER, J. J., WATROBKA, M., WAUGH, S., WEISS, A., WILCOX, S. K., WOLFSON, A., WOLK, S. K., ZHANG, C. & ZICHI, D. 2010. Aptamer-Based Multiplexed Proteomic Technology for Biomarker Discovery. *PLoS ONE,* 5**,** e15004.

GOLD, L., B., P., UHLENBECK, O. & YARUS, M. 1995. Diversity of oligonucleotide functions. *Annu Rev Biochem.,* 64**,** 763-97.

GOLDEN, M. P. & VIKRAM, H. R. 2005. Extrapulmonary tuberculosis: an ovweview. *Am Fam Physician,* 72**,** 1761-8.

GONG, Q., WANG, J., AHMAD, K. M., CSORDAS, A., ZHOU, J., NIE, J., STEWART, R., THOMSON, J. A., ROSSI, J. J. & SOH, H. T. 2012. Selection Strategy to Generate Aptamer Pairs that Bind to Distinct Sites on Protein Targets. *Analytical Chemistry,* 84**,** 5365-5371.

GOPINATH, S. 2007. Methods developed for SELEX. *Analytical and Bioanalytical Chemistry,* 387**,** 171-182.

GOPINATH, S. C. B., BALASUNDARESAN, D., AKITOMI, J. & MIZUNO, H. 2006a. An RNA Aptamer That Discriminates Bovine Factor IX from Human Factor IX. *Journal of Biochemistry,* 140**,** 667-676.

GOPINATH, S. C. B., SAKAMAKI, Y., KAWASAKI, K. & KUMAR, P. K. R. 2006b. An Efficient RNA Aptamer against Human Influenza B Virus Hemagglutinin. *Journal of Biochemistry,* 139**,** 837-846.

GOTO, M., NOGUCHI, Y., KOYAMA, H., HIRA, K., SHIMBO, T. & FUKUI, T. 2003. Diagnostic value of adenosine deaminase in tuberculous pleural effusion: a meta-analysis. *Annals of Clinical Biochemistry,* 40**,** 374-381.

GREBENCHTCHIKOV, N., BRINKMAN, A., VAN BROEKHOVEN, S. P. J., DE JONG, D., GEURTS-MOESPOT, A., SPAN, P. N., PETERS, H. A., PORTENGEN, H., FOEKENS, J. A., SWEEP, C. G. J. & DORSSERS, L. C. J. 2004. Development of an ELISA for Measurement of BCAR1 Protein in Human Breast Cancer Tissue. *Clinical Chemistry,* 50**,** 1356-1363.

GRECO, S., GIRARDI, E., MASCIANGELO, R., CAPOCCETTA, G. B. & SALTINI, C. 2003. Adenosine deaminase and interferon gamma measurements for the diagnosis of tuberculous pleurisy: a meta-analysis. *The International Journal of Tuberculosis and Lung Disease,* 7**,** 777-786.

GRECO, S., RULLI, M., GIRARDI, E., PIERSIMONI, C. & SALTINI, C. 2009. Diagnostic Accuracy of In-House PCR for Pulmonary Tuberculosis in Smear-Positive Patients: Meta-Analysis and Metaregression. *J. Clin. Microbiol.,* 47**,** 569-576.

GROZIO, A., GONZALEZ, V. M., MILLO, E., STURLA, L., VIGLIAROLO, T., BAGNASCO, L., GUIDA, L., D'ARRIGO, C., DE FLORA, A., SALIS, A., MARTIN, E. M., BELLOTTI, M. & ZOCCHI, E. 2013. Selection and Characterization of Single Stranded DNA Aptamers for the Hormone Abscisic Acid. *Nucleic Acid Therapeutics,* 23**,** 322-331.

GUO, L. & KIM, D.-H. 2012. LSPR biomolecular assay with high sensitivity induced by aptamer–antigen–antibody sandwich complex. *Biosensors and Bioelectronics,* 31**,** 567-570.

GUO, W. M., KONG, K. W., BROWN, C. J., QUAH, S. T., YEO, H. L., HOON, S. & SEOW, Y. 2014. Identification and Characterization of an eIF4e DNA Aptamer That Inhibits Proliferation With High Throughput Sequencing. *Mol Ther Nucleic Acids,* 3**,** e217.

GUPTA, S., BANDYOPADHYAY, D., PAINE, S. K., BANERJEE, S., BHATTACHARYA, S., GACHHUI, R. & BHATTACHARYA, B. 2010. Rapid identification of mycobacterium species with the aid of multiplex polymerase chain reaction (PCR) from clinical isolates. *Open Microbiol J,* 4**,** 93-7.

HÄGGSTRÖM, M. 2009. Main symptoms of extrapulmonary tuberculosis, as described in the Wikipedia:Tuberculosis article. *Wikimedia Commons,* http://commons.wikimedia.org/wiki/File:Extrapulmonary_tuberculosis_symptoms.svg.

HALL, T. 1999. BioEdit: a user-friendly biological sequence alignment editor and analysis program for Windows 95/98/NT., . *Nucl. Acids. Symp. Ser.,* 41**,** 95-98.

HAMILTON, C. & GERMANN, M. 2011. Folding and base pairing of a fibrinogen specific DNA aptamer. *Colonial Academic Alliance Undergraduate Research Journal,* 2.

HARRIES, A. D., MAHER, D. & NUNN, P. 1998. An approach to the problems of diagnosing and treating adult smear-negative pulmonary tuberculosis in high-HIV-prevalence settings in sub-Saharan Africa. *Bulletin of the World Health Organization,* 76**,** 651-662.

HELB, D., JONES, M., STORY, E., BOEHME, C., WALLACE, E., HO, K., KOP, J., OWENS, M. R., RODGERS, R., BANADA, P., SAFI, H., BLAKEMORE, R., LAN, N. T. N., JONES-LOPEZ, E. C., LEVI, M., BURDAY, M., AYAKAKA, I., MUGERWA, R. D., MCMILLAN, B., WINN-DEEN, E., CHRISTEL, L., DAILEY, P., PERKINS, M. D., PERSING, D. H. & ALLAND, D. 2010. Rapid Detection of Mycobacterium tuberculosis and Rifampin Resistance by Use of On-Demand, Near-Patient Technology. *J. Clin. Microbiol.,* 48**,** 229-237.

HERMANN, T. & PATEL, D. J. 2000. Adaptive Recognition by Nucleic Acid Aptamers. *Science,* 287**,** 820-825.

HESSELBERTH, J., ROBERTSON, M. P., JHAVERI, S. & ELLINGTON, A. D. 2000. In vitro selection of nucleic acids for diagnostic applications. *Reviews in Molecular Biotechnology,* 74**,** 15-25.

HICKE, B. J., MARION, C., CHANG, Y.-F., GOULD, T., LYNOTT, C. K., PARMA, D., SCHMIDT, P. G. & WARREN, S. 2001. Tenascin-C Aptamers Are Generated Using Tumor Cells and Purified Protein. *Journal of Biological Chemistry,* 276**,** 48644-48654.

HILLEMANN, D., RÜSCH-GERDES, S., BOEHME, C. & RICHTER, E. 2011. Rapid Molecular Detection of Extrapulmonary Tuberculosis by the Automated GeneXpert MTB/RIF System. *Journal of Clinical Microbiology,* 49**,** 1202-1205.

HOMANN, M. & GORINGER, H. U. 1999. Combinatorial selection of high affinity RNA ligands to live African trypanosomes. *Nucleic Acids Res,* 27**,** 2006-14.

HONG, P., LI, W. & LI, J. 2012. Applications of Aptasensors in Clinical Diagnostics. *Sensors (Basel, Switzerland),* 12**,** 1181-1193.

HSU, W. H., CHIANG, C. D. & HUANG, P. L. 1993. Diagnostic value of pleural adenosine deaminase in tuberculous effusions of immunocompromised hosts. *Journal of the Formosan Medical Association = Taiwan yi zhi,* 92**,** 668-670.

HÜNNIGER, T., WESSELS, H., FISCHER, C., PASCHKE-KRATZIN, A. & FISCHER, M. 2014. Just in Time-Selection: A Rapid Semiautomated SELEX of DNA Aptamers Using Magnetic Separation and BEAMing. *Analytical Chemistry,* 86**,** 10940-10947.

INOUE, S., SEYAMA, M., MIURA, T., HORIUCHI, T., IWASAKI, Y., TAKAHASHI, J.-I. & TAMECHIKA, E. Multi-layered aptamer array integrated in microfluidic chip for on-site blood analysis. Proc. 15th Int. Conf. Eon Miniatureized Syst. Chem. Life Sci, 2011. 2-6.

IRVINE, D., TUERK, C. & GOLD, L. 1991. Selexion: Systematic evolution of ligands by exponential enrichment with integrated optimization by non-linear analysis. *Journal of Molecular Biology,* 222**,** 739-761.

JAYASENA, S. D. 1999. Aptamers: An Emerging Class of Molecules That Rival Antibodies in Diagnostics. *Clin Chem,* 45**,** 1628-1650.

JENISON, R. D., GILL, S. C., PARDI, A. & POLISKY, B. 1994. High-resolution molecular discrimination by RNA. *Science,* 263**,** 1425-9.

JENSEN, K. B., ATKINSON, B. L., WILLIS, M. C., KOCH, T. H. & GOLD, L. 1995a. Using in vitro selection to direct the covalent attachment of human immunodeficiency virus type 1 Rev protein to high-affinity RNA ligands. *Proceedings of the National Academy of Sciences of the United States of America,* 92**,** 12220-12224.

JENSEN, K. B., ATKINSON, B. L., WILLIS, M. C., KOCH, T. H. & GOLD, L. 1995b. Using in vitro selection to direct the covalent attachment of human immunodeficiency virus type 1 Rev protein to high-affinity RNA ligands. *Proc Natl Acad Sci U S A,* 92**,** 12220-4.

JHAVERI, S. & ELLINGTON, A. 2001. In Vitro Selection of RNA Aptamers to a Small Molecule Target. *Current Protocols in Nucleic Acid Chemistry.* John Wiley & Sons, Inc.

JHAVERI, S., RAJENDRAN, M. & ELLINGTON, A. D. 2000. In vitro selection of signaling aptamers. *Nat Biotechnol,* 18**,** 1293-7.

JIANG, J., SHI, H.-Z., LIANG, Q.-L., QIN, S.-M. & QIN, X.-J. 2007. Diagnostic value of interferon-γ in tuberculous pleurisy*: A metaanalysis. *Chest,* 131**,** 1133-1141.

JOLMA, A., KIVIOJA, T., TOIVONEN, J., CHENG, L., WEI, G., ENGE, M., TAIPALE, M., VAQUERIZAS, J. M., YAN, J., SILLANPÄÄ, M. J., BONKE, M., PALIN, K., TALUKDER, S., HUGHES, T. R., LUSCOMBE, N. M., UKKONEN, E. & TAIPALE, J. 2010. Multiplexed

massively parallel SELEX for characterization of human transcription factor binding specificities. *Genome Research,* 20**,** 861-873.

JÖNSSON, B. & RIDELL, M. 2003. The Cobas Amplicor MTB Test for Detection of Mycobacterium tuberculosis Complex from Respiratory and Non-respiratory Clinical Specimens. *Scandinavian Journal of Infectious Diseases,* 35**,** 372-377.

KARA, P., DE LA ESCOSURA-MUÑIZ, A., MALTEZ-DA COSTA, M., GUIX, M., OZSOZ, M. & MERKOÇI, A. 2010a. Aptamers based electrochemical biosensor for protein detection using carbon nanotubes platforms. *Biosensors and Bioelectronics,* 26**,** 1715-1718.

KARA, P., MERIC, B. & OZSOZ, M. 2010b. Development of a label free IGE sensitive aptasensor based on electrochemical impedance spectrometry. *Combinatorial chemistry & high throughput screening,* 13**,** 578-581.

KARSTAEDT, A. S. 2013. Extrapulmonary tuberculosis among adults: experience at Chris Hani Baragwanath Academic Hospital, Johannesburg, South Africa. *S Afr Med J.,* 104**,** 22-4.

KARSTAEDT, A. S. & BOLHAAR, M. 2014. Tuberculosis in older adults in Soweto, South Africa. *The International Journal of Tuberculosis and Lung Disease,* 18**,** 1220-1222.

KATSAMBA, P. S., PARK, S. & LAIRD-OFFRINGA, I. A. 2002. Kinetic studies of RNA–protein interactions using surface plasmon resonance. *Methods,* 26**,** 95-104.

KAWAKAMI, J., IMANAKA, H., YOKOTA, Y. & SUGIMOTO, N. 2000. In vitro selection of aptamers that act with Zn2+. *J Inorg Biochem,* 82**,** 197-206.

KEEFE, A. D. & CLOAD, S. T. 2008. SELEX with modified nucleotides. *Current Opinion in Chemical Biology,* 12**,** 448-456.

KEEFE, A. D., PAI, S. & ELLINGTON, A. 2010. Aptamers as therapeutics. *Nat Rev Drug Discov,* 9**,** 537-550.

KELLY, J. A., FEIGON, J. & YEATES, T. O. 1996. Reconciliation of the X-ray and NMR Structures of the Thrombin-Binding Aptamer d(GGTTGGTGTGGTTGG). *Journal of Molecular Biology,* 256**,** 417-422.

KENG, L.-T., SHU, C.-C., CHEN, J. Y.-P., LIANG, S.-K., LIN, C.-K., CHANG, L.-Y., CHANG, C.-H., WANG, J.-Y., YU, C.-J. & LEE, L.-N. 2013. Evaluating pleural ADA, ADA2, IFN-γ and IGRA for diagnosing tuberculous pleurisy. *Journal of Infection,* 67**,** 294-302.

KHATI, M., SCHUMAN, M., IBRAHIM, J., SATTENTAU, Q., GORDON, S., AND JAMES, W. 2003. Neutralisation of Infectivity of Diverse R5 Clinical Isolates of Human Immunodeficiency Virus Type 1 by gp120-Binding 2'F-RNA Aptamers. *Journal of Virology,* 77**,** 12692-12698.

KIKIN, O., D'ANTONIO, L. & BAGGA, P. S. 2006. QGRS Mapper: a web-based server for predicting G-quadruplexes in nucleotide sequences. *Nucleic Acids Research,* 34**,** W676-W682.

KIM, D. W., JUNG, S. J., HA, T. K. & PARK, H. K. 2013. Individual and combined diagnostic accuracy of ultrasound diagnosis, ultrasound-guided fine-needle aspiration and polymerase chain reaction in identifying tuberculous lymph nodes in the neck. *Ultrasound in medicine & biology,* 39**,** 2308-2314.

KIM, Y., LIU, C. & TAN, W. 2009. Aptamers generated by Cell SELEX for biomarker discovery. *Biomarkers in Medicine,* 3**,** 193-202.

KIM, Y. C., PARK, K. O., BOM, H. S., LIM, S. C., PARK, H. K., NA, H. J. & PARK, J. H. 1997. Combining ADA, protein and IFN-gamma best allows discrimination between tuberculous and malignant pleural effusion. *Korean J Intern Med. ,* 12**,** 225-31.

KLUSSMANN, S., NOLTE, A., BALD, R., ERDMANN, V. A. & FURSTE, J. P. 1996. Mirror-image RNA that binds D-adenosine. *Nat Biotechnol,* 14**,** 1112-5.

KNECHEL, N. A. 2009. Tuberculosis: Pathophysiology, Clinical Features, and Diagnosis. *Critical Care Nurse,* 29**,** 34-43.

KRENKE, R., SAFIANOWSKA, A., PAPLINSKA, M., NASILOWSKI, J., DMOWSKA-SOBSTYL, B., BOGACKA-ZATORSKA, E., JAWORSKI, A. & CHAZAN, R. 2008. Pleural fluid adenosine deaminase and interferon gamma as diagnostic tools in tuberculous pleurisy. *J physiol Pharmacol,* 59**,** 349-360.

KULBACHINSKIY, A. 2007. Methods for selection of aptamers to protein targets. *Biochemistry (Mosc),* 72**,** 1505-18.

LANG, A. M., FERIS-IGLESIAS, J., PENA, C., SANCHEZ, J. F., STOCKMAN, L., RYS, P., ROBERTS, G. D., HENRY, N. K., PERSING, D. H. & COCKERILL, F. R. 1998. Clinical Evaluation of the Gen-Probe Amplified Direct Test for Detection of Mycobacterium tuberculosis Complex Organisms in Cerebrospinal Fluid. *Journal of Clinical Microbiology,* 36**,** 2191-2194.

LAO, Y.-H., CHIANG, H.-Y., YANG, D.-K., PECK, K. & CHEN, L.-C. 2014. Selection of aptamers targeting the sialic acid receptor of hemagglutinin by epitope-specific SELEX. *Chemical Communications,* 50**,** 8719-8722.

LARAQUE, F., GRIGGS, A., SLOPEN, M. & MUNSIFF, S. S. 2009. Performance of nucleic acid amplification tests for diagnosis of tuberculosis in a large urban setting. *Clin Infect Dis,* 49**,** 46-54.

LAWN, S. D. & ZUMLA, A. I. 2011. Tuberculosis. *Lancet*.

LAYZER, J. M. & SULLENGER, B. A. 2007. Simultaneous Generation of Aptamers to Multiple Gamma-Carboxyglutamic Acid Proteins from a Focused Aptamer Library Using DeSELEX and Convergent Selection. *Oligonucleotides,* 17**,** 1-11.

LEE, J. Y. 2015. Diagnosis and Treatment of Extrapulmonary Tuberculosis. *Tuberculosis and Respiratory Diseases,* 78**,** 47-55.

LEE, P. P., RAMANATHAN, M., HUNT, C. A. & GAROVOY, M. R. 1996. AN OLIGONUCLEOTIDE BLOCKS INTERFERON-γ SIGNAL TRANSDUCTION1. *Transplantation,* 62**,** 1297-1301.

LEIN, A. D. & VON REYN, C. F. 1997. In Vitro Cellular and Cytokine Responses to Mycobacterial Antigens: Application to Diagnosis of Tuberculosis Infection and Assessment of Response to Mycobacterial Vaccines. *The American Journal of the Medical Sciences,* 313**,** 364-371.

LEUNG, D. W., CHEN, E. & GOEDDEL, D. V. 1989. A method for random mutagenesis of a defined DNA segment using a modified polymerase chain reaction. *Technique,* 1**,** 11-15.

LIANG, Q.-L., SHI, H.-Z., WANG, K., QIN, S.-M. & QIN, X.-J. 2008. Diagnostic accuracy of adenosine deaminase in tuberculous pleurisy: A meta-analysis. *Respiratory Medicine,* 102**,** 744-754.

LING, D. I., PAI, M., DAVIDS, V., BRUNET, L., LENDERS, L., MELDAU, R., CALLIGARO, G., ALLWOOD, B., VAN ZYL-SMIT, R., PETER, J., BATEMAN, E., DAWSON, R. & DHEDA, K. 2011. Are interferon-γ release assays useful for diagnosing active tuberculosis in a high-burden setting? *European Respiratory Journal,* 38**,** 649-656.

LIU, S., ZHANG, H., DAI, J., HU, S., PINO, I., EICHINGER, D. J., LYU, H. & ZHU, H. 2014. Characterization of monoclonal antibody's binding kinetics using oblique-incidence reflectivity difference approach. *mAbs,* 7**,** 110-119.

LIU, Y., TULEOUVA, N., RAMANCULOV, E. & REVZIN, A. 2010. Aptamer-based Electrochemical Biosensor for Interferon Gamma Detection. *Analytical chemistry,* 82**,** 8131-8136.

LOU, X., QIAN, J., XIAO, Y., VIEL, L., GERDON, A. E., LAGALLY, E. T., ATZBERGER, P., TARASOW, T. M., HEEGER, A. J. & SOH, H. T. 2009. Micromagnetic selection of aptamers in microfluidic channels. *Proceedings of the National Academy of Sciences of the United States of America,* 106**,** 2989-2994.

MABEY, D., PEELING, R. W., USTIANOWSKI, A. & PERKINS, M. D. 2004. Tropical infectious diseases: Diagnostics for the developing world. *Nat Rev Micro,* 2**,** 231-240.

MACPHERSON, P., HOUBEN, R. M., GLYNN, J. R., CORBETT, E. L. & KRANZER, K. 2014. Pre-treatment loss to follow-up in tuberculosis patients in low-and lower-middle-income countries

and high-burden countries: a systematic review and meta-analysis. *Bulletin of the World Health Organization,* 92**,** 126-138.

MADHI, S. A., HUEBNER, R. E., DOEDENS, L., ADUC, T., WESLEY, D. & COOPER, P. A. 2000. HIV-1 co-infection in children hospitalised with tuberculosis in South Africa. *The International Journal of Tuberculosis and Lung Disease,* 4**,** 448-454.

MAIRAL, T., CENGIZ ÖZALP, V., LOZANO SÁNCHEZ, P., MIR, M., KATAKIS, I. & O'SULLIVAN, C. 2008. Aptamers: molecular tools for analytical applications. *Analytical and Bioanalytical Chemistry,* 390**,** 989-1007.

MALTEZOU, H. C., SPYRIDIS, P. & KAFETZIS, D. A. 2000. Extra-pulmonary tuberculosis in children. *Archives of Disease in Childhood,* 83**,** 342-346.

MAO, X., HUANG, T. J. & HO, C.-M. 2010. The Lab-on-a-Chip Approach for Molecular Diagnostics. *In:* CONTRIBUTORS, WAYNE, W. G., M.D, PH.D, ROBERT, M. N., CHARLES, M. S., FREDERICK, L. K., MD & PHD (eds.) *Molecular Diagnostics.* San Diego: Academic Press.

MARAIS, B. J., BRITTLE, W., PAINCZYK, K., HESSELING, A. C., BEYERS, N., WASSERMAN, E., SOOLINGEN, D. V. & WARREN, R. M. 2008. Use of Light-Emitting Diode Fluorescence Microscopy to Detect Acid-Fast Bacilli in Sputum. *Clinical Infectious Diseases,* 47**,** 203-207.

MARAIS, B. J. & SCHAAF, H. S. 2014. Tuberculosis in Children. *Cold Spring Harbor Perspectives in Medicine,* 4.

MARSHALL, K. A. & ELLINGTON, A. D. 2000. In vitro selection of RNA aptamers. *Methods Enzymol,* 318**,** 193-214.

MARTÍN, M. E., GARCÍA-HERNÁNDEZ, M., GARCÍA-RECIO, E. M., GÓMEZ-CHACÓN, G. F., SÁNCHEZ-LÓPEZ, M. & GONZÁLEZ, V. M. 2013. DNA Aptamers Selectively Target <italic>Leishmania infantum</italic> H2A Protein. *PLoS ONE,* 8**,** e78886.

MARTINEZ, N. & KORNFELD, H. 2014. Diabetes and immunity to tuberculosis. *European journal of immunology,* 44**,** 617-626.

MAYER, G., AHMED, M.-S. L., DOLF, A., ENDL, E., KNOLLE, P. A. & FAMULOK, M. 2010. Fluorescence-activated cell sorting for aptamer SELEX with cell mixtures. *Nat. Protocols,* 5**,** 1993-2004.

MCCAULEY, T. G., HAMAGUCHI, N. & STANTON, M. 2003. Aptamer-based biosensor arrays for detection and quantification of biological macromolecules. *Analytical Biochemistry,* 319**,** 244-250.

MCKEAGUE, M., BRADLEY, C. R., DE GIROLAMO, A., VISCONTI, A., MILLER, J. D. & DEROSA, M. C. 2010. Screening and Initial Binding Assessment of Fumonisin B(1) Aptamers. *International Journal of Molecular Sciences,* 11**,** 4864-4881.

MELDAU, R., PETER, J., THERON, G., CALLIGARO, G., ALLWOOD, B., SYMONS, G., KHALFEY, H., NTOMBENHLE, G., GOVENDER, U., BINDER, A., VAN ZYL-SMIT, R. & DHEDA, K. 2014. Comparison of same day diagnostic tools including Gene Xpert and unstimulated IFN-gamma for the evaluation of pleural tuberculosis: a prospective cohort study. *BMC Pulmonary Medicine,* 14**,** 58.

MENDONSA, S. D. & BOWSER, M. T. 2004. In vitro selection of high-affinity DNA ligands for human IgE using capillary electrophoresis. *Anal Chem,* 76**,** 5387-92.

MILLER, L. P., CRAWFORD, J. T. & SHINNICK, T. M. 1994. The rpoB gene of Mycobacterium tuberculosis. *Antimicrob. Agents Chemother.,* 38**,** 805-811.

MILLROY, L. 2013. Development of lymphocyte specific internalising aptamers. PhD Thesis, University of Witwatersrand, pg 12-13.

MINUNNI, M., TOMBELLI, S., GULLOTTO, A., LUZI, E. & MASCINI, M. 2004. Development of biosensors with aptamers as bio-recognition element: the case of HIV-1 Tat protein. *Biosensors and Bioelectronics,* 20**,** 1149-1156.

MORRIS, K. N., JENSEN, K. B., JULIN, C. M., WEIL, M. & GOLD, L. 1998. High affinity ligands from in vitro selection: Complex targets. *Proceedings of the National Academy of Sciences of the United States of America,* 95**,** 2902-2907.

MOURE, R., MARTÍN, R. & ALCAIDE, F. 2012. Effectiveness of an Integrated Real-Time PCR Method for Detection of the Mycobacterium tuberculosis Complex in Smear-Negative Extrapulmonary Samples in an Area of Low Tuberculosis Prevalence. *Journal of Clinical Microbiology,* 50**,** 513-515.

NAGESH, B. S., SEHGAL, S., JINDAL, S. K. & ARORA, S. K. 2001. EValuation of polymerase chain reaction for detection of mycobacterium tuberculosis in pleural fluid*. *Chest,* 119**,** 1737-1741.

NEGIN, J., ABIMBOLA, S. & MARAIS, B. J. 2015. Tuberculosis among older adults – time to take notice. *International Journal of Infectious Diseases,* 32**,** 135-137.

NGUBANE, N. A. C., GRESH, L., PYM, A., RUBIN, E. J. & KHATI, M. 2014. Selection of RNA aptamers against the M. tuberculosis EsxG protein using surface plasmon resonance-based SELEX. *Biochemical and Biophysical Research Communications,* 449**,** 114-119.

NGUYEN, V.-T., KWON, Y. S., KIM, J. H. & GU, M. B. 2014. Multiple GO-SELEX for efficient screening of flexible aptamers. *Chemical Communications,* 50**,** 10513-10516.

NHU, N. T. Q., HEEMSKERK, D., THU, D. D. A., CHAU, T. T. H., MAI, N. T. H., NGHIA, H. D. T., LOC, P. P., HA, D. T. M., MERSON, L., THINH, T. T. V., DAY, J., CHAU, N. V. V., WOLBERS, M., FARRAR, J. & CAWS, M. 2014. Evaluation of GeneXpert MTB/RIF for Diagnosis of Tuberculous Meningitis. *Journal of Clinical Microbiology,* 52**,** 226-233.

NIEUWLANDT, D. 2000. In vitro selection of functional nucleic acid sequences. *Curr. Issues Mol. Biol.,* 2**,** 9-16.

NIMJEE, S. M., RUSCONI, C. P., HARRINGTON, R. A. & SULLENGER, B. A. 2005a. The potential of aptamers as anticoagulants. *Trends in Cardiovascular Medicine,* 15**,** 41-45.

NIMJEE, S. M., RUSCONI, C. P. & SULLENGER, B. A. 2005b. Aptamers: An Emerging Class of Therapeutics. *Annual Review of Medicine,* 56**,** 555-583.

NITSCHE, A., KURTH, A., DUNKHORST, A., PANKE, O., SIELAFF, H., JUNGE, W., MUTH, D., SCHELLER, F., STOCKLEIN, W., DAHMEN, C., PAULI, G. & KAGE, A. 2007a. One-step selection of Vaccinia virus-binding DNA aptamers by MonoLEX. *BMC Biotechnol,* 7**,** 48.

NITSCHE, A., KURTH, A., DUNKHORST, A., PÄNKE, O., SIELAFF, H., JUNGE, W., MUTH, D., SCHELLER, F., STÖCKLEIN, W., DAHMEN, C., PAULI, G. & KAGE, A. 2007b. One-step selection of Vaccinia virus-binding DNA aptamers by MonoLEX. *BMC Biotechnology,* 7**,** 48-48.

NONAKA, Y., SODE, K. & IKEBUKURO, K. 2010. Screening and Improvement of an Anti-VEGF DNA Aptamer. *Molecules,* 15**,** 215-225.

NORBIS, L., ALAGNA, R., TORTOLI, E., CODECASA, L. R., MIGLIORI, G. B. & CIRILLO, D. M. 2014. Challenges and perspectives in the diagnosis of extrapulmonary tuberculosis. *Expert Review of Anti-infective Therapy,* 12**,** 633-647.

NUTIU, R. & LI, Y. 2004. Structure-Switching Signaling Aptamers: Transducing Molecular Recognition into Fluorescence Signaling. *Chemistry – A European Journal,* 10**,** 1868-1876.

NUTIU, R. & LI, Y. 2005. Aptamers with fluorescence-signaling properties. *Methods,* 37**,** 16-25.

O'SULLIVAN, C. 2002. Aptasensors – the future of biosensing? *Analytical and Bioanalytical Chemistry,* 372**,** 44-48.

OHUCHI, S. P., OHTSU, T. & NAKAMURA, Y. 2006. Selection of RNA aptamers against recombinant transforming growth factor-beta type III receptor displayed on cell surface. *Biochimie,* 88**,** 897-904.

PAGRATIS, N., GOLD, L., SHTATLAND, T. & JAVORNIK, B. 2001. Truncation selex method. Google Patents.

PAI, M., MINION, J., SOHN, H., ZWERLING, A. & PERKINS, M. D. 2009. Novel and Improved Technologies for Tuberculosis Diagnosis: Progress and Challenges. *Clinics in chest medicine,* 30**,** 701-716.

PAI, M., RILEY, L. W. & COLFORD JR, J. M. 2004. Interferon-γ assays in the immunodiagnosis of tuberculosis: a systematic review. *The Lancet Infectious Diseases,* 4**,** 761-776.

PAN, Q., WANG, Q., SUN, X., XIA, X., WU, S., LUO, F. & ZHANG, X. 2014. Aptamer against mannose-capped lipoarabinomannan inhibits virulent Mycobacterium tuberculosis infection in mice and rhesus monkeys. *Mol Ther,* 22**,** 940-51.

PAN, W. & CLAWSON, G. A. 2009. The Shorter the Better: Reducing Fixed Primer Regions of Oligonucleotide Libraries for Aptamer Selection. *Molecules* 14**,** 1353-1359.

PAN, W., XIN, P. & CLAWSON, G. A. 2008. Minimal primer and primer-free SELEX protocols for selection of aptamers from random DNA libraries. *Biotechniques,* 44**,** 351-60.

PANDIE, S., PETER, J., KERBELKER, Z., MELDAU, R., THERON, G., GOVENDER, U., NTSEKHE, M., DHEDA, K. & MAYOSI, B. 2014. Diagnostic accuracy of quantitative PCR (Xpert MTB/RIF) for tuberculous pericarditis compared to adenosine deaminase and unstimulated interferon-gamma in a high burden setting: a prospective study. *BMC Medicine,* 12**,** 101.

PARK, J.-W., TATAVARTY, R., KIM, D. W., JUNG, H.-T. & GU, M. B. 2012. Immobilization-free screening of aptamers assisted by graphene oxide. *Chemical Communications,* 48**,** 2071-2073.

PARK, S.-M., AHN, J.-Y., JO, M., LEE, D.-K., LIS, J. T., CRAIGHEAD, H. G. & KIM, S. 2009. Selection and elution of aptamers using nanoporous sol-gel arrays with integrated microheaters. *Lab on a Chip,* 9**,** 1206-1212.

PATEL, D. J., SURI, A. K., JIANG, F., JIANG, L., FAN, P., KUMAR, R. A. & NONIN, S. 1997. Structure, recognition and adaptive binding in RNA aptamer complexes. *Journal of Molecular Biology,* 272**,** 645-664.

PATEL, V. B., THERON, G., LENDERS, L., MATINYENA, B., CONNOLLY, C., SINGH, R., COOVADIA, Y., NDUNG'U, T. & DHEDA, K. 2013. Diagnostic Accuracy of Quantitative PCR (Xpert MTB/RIF) for Tuberculous Meningitis in a High Burden Setting: A Prospective Study. *PLoS Med,* 10**,** e1001536.

PENG, C., DUAN, X., SONG, S. & XUE, F. 2013. Parts Per Trillion Detection of 7-Aminonitrazepam by Nano-Enhanced ELISA. *International Journal of Molecular Sciences,* 14**,** 19474-19483.

PENG, L., STEPHENS, B. J., BONIN, K., CUBICCIOTTI, R. & GUTHOLD, M. 2007. A combined atomic force/fluorescence microscopy technique to select aptamers in a single cycle from a small pool of random oligonucleotides. *Microsc Res Tech,* 70**,** 372-81.

PERKINS, M. D. & CUNNINGHAM, J. 2007. Facing the crisis: improving the diagnosis of tuberculosis in the HIV era. *J Infect Dis,* 196 Suppl 1**,** S15-27.

PETERSON, E. M., NAKASONE, A., PLATON-DELEON, J. M., JANG, Y., DE LA MAZA, L. M. & DESMOND, E. 1999. Comparison of Direct and Concentrated Acid-Fast Smears To Identify Specimens Culture Positive for Mycobacterium spp. *Journal of Clinical Microbiology,* 37**,** 3564-3568.

PETO, H. M., PRATT, R. H., HARRINGTON, T. A., LOBUE, P. A. & ARMSTRONG, L. R. 2009. Epidemiology of Extrapulmonary Tuberculosis in the United States, 1993–2006. *Clinical Infectious Diseases,* 49**,** 1350-1357.

PIRAS, M. A., GAKIS, C., BUDRONI, M. & ANDREONI, G. 1978. Adenosine deaminase activity in pleural effusions: an aid to differential diagnosis. *British Medical Journal,* 2**,** 1751-1752.

PLATT, M., ROWE, W., WEDGE, D. C., KELL, D. B., KNOWLES, J. & DAY, P. J. R. 2009. Aptamer evolution for array-based diagnostics. *Analytical Biochemistry,* 390**,** 203-205.

PORCEL, J. M., PALMA, R., VALDÉS, L., BIELSA, S., SAN-JOSÉ, E. & ESQUERDA, A. 2013. Xpert® MTB/RIF in pleural fluid for the diagnosis of tuberculosis [Short communication]. *The International Journal of Tuberculosis and Lung Disease,* 17**,** 1217-1219.

PROSKE, D., BLANK, M., BUHMANN, R. & RESCH, A. 2005. Aptamers—basic research, drug development, and clinical applications. *Applied Microbiology and Biotechnology,* 69**,** 367-374.

PROZIALECK, W. C., ET AL. 2002. Chlamydia trachomatic disrupts N-cadherin-dependent cell-cell junctions and sequester β-catenin in human cervical epithelial cells. *Infection and Immunity,* 70**,** 2605-13.

PULTAR, J., SAUER, U., DOMNANICH, P. & PREININGER, C. 2009. Aptamer-antibody on-chip sandwich immunoassay for detection of CRP in spiked serum. *Biosensors and Bioelectronics,* 24**,** 1456-1461.

QIN, L., ZHENG, R., MA, Z., FENG, Y., LIU, Z., YANG, H., WANG, J., JIN, R., LU, J., DING, Y. & HU, Z. 2009. The selection and application of ssDNA aptamers against MPT64 protein in Mycobacterium tuberculosis. *Clinical Chemistry and Laboratory Medicine.*

RAJENDRAN, M. & ELLINGTON, A. D. 2003. In vitro selection of molecular beacons. *Nucleic Acids Res,* 31**,** 5700-13.

RAVIGLIONE, M. C., NARAIN, J. P. & KOCHI, A. 1992. HIV-associated tuberculosis in developing countries: clinical features, diagnosis, and treatment. *Bulletin of the World Health Organization,* 70**,** 515-526.

REDDINGTON, K., O'GRADY, J., DORAI-RAJ, S., MAHER, M., VAN SOOLINGEN, D. & BARRY, T. 2011. Novel multiplex real-time PCR diagnostic assay for identification and differentiation of Mycobacterium tuberculosis, Mycobacterium canettii, and Mycobacterium tuberculosis complex strains. *J Clin Microbiol,* 49**,** 651-7.

REID, D. C., CHANG, B. L., GUNDERSON, S. I., ALPERT, L., THOMPSON, W. A. & FAIRBROTHER, W. G. 2009. Next-generation SELEX identifies sequence and structural determinants of splicing factor binding in human pre-mRNA sequence. *RNA,* 15**,** 2385-2397.

ROBERTS, K. P., ET AL. 2002. A comparative analyis of expression and processing of the rat epididymal fluid and sperm-bound forms of proteins D and E. *Biology of Reproduction,* 67**,** 525-33.

ROCK, R. B., OLIN, M., BAKER, C. A., MOLITOR, T. W. & PETERSON, P. K. 2008. Central Nervous System Tuberculosis: Pathogenesis and Clinical Aspects. *Clinical Microbiology Reviews,* 21**,** 243-261.

ROCKEY, W. M., HERNANDEZ, F. J., HUANG, S.-Y., CAO, S., HOWELL, C. A., THOMAS, G. S., LIU, X. Y., LAPTEVA, N., SPENCER, D. M., MCNAMARA, J. O., ZOU, X., CHEN, S.-J. & GIANGRANDE, P. H. 2011. Rational Truncation of an RNA Aptamer to Prostate-Specific Membrane Antigen Using Computational Structural Modeling. *Nucleic Acid Therapeutics,* 21**,** 299-314.

ROTHERHAM, L. S., MASERUMULE, C., DHEDA, K., THERON, J. & KHATI, M. 2012. Selection and Application of ssDNA Aptamers to Detect Active TB from Sputum Samples. *PLoS ONE,* 7**,** e46862.

ROULET, E., BUSSO, S., CAMARGO, A. A., SIMPSON, A. J. G., MERMOD, N. & BUCHER, P. 2002. High-throughput SELEX-SAGE method for quantitative modeling of transcription-factor binding sites. *Nat Biotech,* 20**,** 831-835.

RUIGROK, V. J., LEVISSON, M., EPPINK, M. H., SMIDT, H. & VAN DER OOST, J. 2011. Alternative affinity tools: more attractive than antibodies? *Biochem J. ,* 436**,** 1-13.

RUSCONI, C. P., SCARDINO, E., LAYZER, J., PITOC, G. A., ORTEL, T. L., MONROE, D. & SULLENGER, B. A. 2002. RNA aptamers as reversible antagonists of coagulation factor IXa. *Nature,* 419**,** 90-94.

REFERENCES

SAITOU, N. & NEI, M. 1987. The neighbor-joining method: a newmethod for reconstructing phylogenetic trees. *Mol Biol Evol,* 4**,** 406-425.

SANTIN, M., MUÑOZ, L. & RIGAU, D. 2012. Interferon-γ Release Assays for the Diagnosis of Tuberculosis and Tuberculosis Infection in HIV-Infected Adults: A Systematic Review and Meta-Analysis. *PLoS ONE,* 7**,** e32482.

SANTINI, G. P. H., COGNET, J. A. H., XU, D., SINGARAPU, K. K. & HERVÉ DU PENHOAT, C. 2009. Nucleic Acid Folding Determined by Mesoscale Modeling and NMR Spectroscopy: Solution Structure of d(GCGAAAGC). *The Journal of Physical Chemistry B,* 113**,** 6881-6893.

SANTOSH, B. & YADAVA, P. K. 2014. Nucleic Acid Aptamers: Research Tools in Disease Diagnostics and Therapeutics. *BioMed Research International,* 2014**,** 13.

SASSANFAR, M. & SZOSTAK, J. W. 1993. An RNA motif that binds ATP. *Nature,* 364**,** 550-553.

SCHASFOORT, R. B. & TUDOS, A. J. 2008. *Handbook of surface plasmon resonance*, Royal Society of Chemistry.

SCHNEIDER, D., TUERK, C. & GOLD, L. 1992. Selection of high affinity RNA ligands to the bacteriophage R17 coat protein. *Journal of Molecular Biology,* 228**,** 862-869.

SCHÜTZE, T., WILHELM, B., GREINER, N., BRAUN, H., PETER, F., MÖRL, M., ERDMANN, V. A., LEHRACH, H., KONTHUR, Z., MENGER, M., ARNDT, P. F. & GLÖKLER, J. 2011. Probing the SELEX Process with Next-Generation Sequencing. *PLoS ONE,* 6**,** e29604.

SCOTT, L. E., BEYLIS, N., NICOL, M., NKUNA, G., MOLAPO, S., BERRIE, L., DUSE, A. & STEVENS, W. S. 2014. Diagnostic Accuracy of Xpert MTB/RIF for Extrapulmonary Tuberculosis Specimens: Establishing a Laboratory Testing Algorithm for South Africa. *Journal of Clinical Microbiology,* 52**,** 1818-1823.

SEFAH, K., YANG, Z., BRADLEY, K. M., HOSHIKA, S., JIMÉNEZ, E., ZHANG, L., ZHU, G., SHANKER, S., YU, F., TUREK, D., TAN, W. & BENNER, S. A. 2014. In vitro selection with artificial expanded genetic information systems. *Proceedings of the National Academy of Sciences of the United States of America,* 111**,** 1449-1454.

SHANGGUAN, D., CAO, Z., MENG, L., MALLIKARATCHY, P., SEFAH, K., WANG, H., LI, Y. & TAN, W. 2008. Cell-specific aptamer probes for membrane protein elucidation in cancer cells. *J Proteome Res,* 7**,** 2133-9.

SHARMA, S. & BANGA, A. 2004. Diagnostic utility of pleural fluid IFN-γ in tuberculosis pleural effusion. *Journal of interferon & cytokine research,* 24**,** 213-217.

SHARMA SK, A. M. A. 2004. Extrapulmonary tuberculosis. *Indian J Med Res,* 120**,** 316-53.

SHARMA, S. K. & MOHAN, A. 2004. Extrapulmonary tuberculosis. *Indian J Med Res,* 120**,** 316-53.

SHARMA, S. K., MOHAN, A. & KADHIRAVAN, T. 2005. HIV-TB co-infection: epidemiology, diagnosis & management. *Indian J Med Res,* 121**,** 550-67.

SHIMOKATA, K., KAWACHI, H., KISHIMOTO, H., MAEDA, F. & ITO, Y. 1982. Local cellular immunity in tuberculous pleurisy. *The American review of respiratory disease,* 126**,** 822-824.

SHIN, J. A., CHANG, Y. S., KIM, H. J., AHN, C. M. & BYUN, M. K. 2015. Diagnostic utility of interferon-gamma release assay in extrapulmonary tuberculosis. *Diagnostic Microbiology and Infectious Disease,* 82**,** 44-48.

SHIRATORI, I., AKITOMI, J., BOLTZ, D. A., HORII, K., FURUICHI, M. & WAGA, I. 2014. Selection of DNA aptamers that bind to influenza A viruses with high affinity and broad subtype specificity. *Biochemical and Biophysical Research Communications,* 443**,** 37-41.

SHUM, K. T. & TANNER, J. A. 2008. Differential Inhibitory Activities and Stabilisation of DNA Aptamers against the SARS Coronavirus Helicase. *ChemBioChem,* 9**,** 3037-3045.

SIKARWAR, B., SHARMA, P. K., SRIVASTAVA, A., AGARWAL, G. S., BOOPATHI, M., SINGH, B. & JAISWAL, Y. K. 2014. Surface plasmon resonance characterization of monoclonal and polyclonal antibodies of malaria for biosensor applications. *Biosensors and Bioelectronics,* 60**,** 201-209.

SINGLA, R., KHAN, N., AL-SHARIF, N., AL-SAYEGH, M. O., SHAIKH, M. A. & OSMAN, M. M. 2006. Influence of diabetes on manifestations and treatment outcome of pulmonary TB patients. *The International Journal of Tuberculosis and Lung Disease,* 10**,** 74-79.

SLEATOR, R. 2011. Phylogenetics. *Archives of Microbiology,* 193**,** 235-239.

SMITH, D., KIRSCHENHEUTER, G. P., CHARLTON, J., GUIDOT, D. M. & REPINE, J. E. 1995. In vitro selection of RNA-based irreversible inhibitors of human neutrophil elastase. *Chem Biol,* 2**,** 741-50.

SONG, S., WANG, L., LI, J., FAN, C. & ZHAO, J. 2008. Aptamer-based biosensors. *TrAC Trends in Analytical Chemistry,* 27**,** 108-117.

SPIGA, F. M., MAIETTA, P. & GUIDUCCI, C. 2015. More DNA–Aptamers for Small Drugs: A Capture–SELEX Coupled with Surface Plasmon Resonance and High-Throughput Sequencing. *ACS Combinatorial Science,* 17**,** 326-333.

STEINGART, K. R., HENRY, M., LAAL, S., HOPEWELL, P. C., RAMSAY, A., MENZIES, D., CUNNINGHAM, J., WELDINGH, K. & PAI, M. 2007. A systematic review of commercial

serological antibody detection tests for the diagnosis of extrapulmonary tuberculosis. *Postgraduate Medical Journal,* 83**,** 705-712.

STEINGART, K. R., HENRY, M., NG, V., HOPEWELL, P. C., RAMSAY, A., CUNNINGHAM, J., URBANCZIK, R., PERKINS, M., AZIZ, M. A. & PAI, M. 2006. Fluorescence versus conventional sputum smear microscopy for tuberculosis: a systematic review. *The Lancet Infectious Diseases,* 6**,** 570-581.

STOLTENBURG, R., NIKOLAUS, N. & STREHLITZ, B. 2012. Capture-SELEX: Selection of DNA Aptamers for Aminoglycoside Antibiotics. *Journal of Analytical Methods in Chemistry,* 2012**,** 415697.

STOLTENBURG, R., REINEMANN, C. & STREHLITZ, B. 2005. FluMag-SELEX as an advantageous method for DNA aptamer selection. *Anal Bioanal Chem,* 383**,** 83-91.

STOLTENBURG, R., REINEMANN, C. & STREHLITZ, B. 2007. SELEX--A (r)evolutionary method to generate high-affinity nucleic acid ligands. *Biomolecular Engineering,* 24**,** 381-403.

SYRETT, H., COLLETT, J. & ELLINGTON, A. 2009. Aptamer Microarrays. *In:* YINGFU, L. & YI, L. (eds.) *Functional Nucleic Acids for Analytical Applications.* Springer New York.

SZETO, K., LATULIPPE, D. R., OZER, A., PAGANO, J. M., WHITE, B. S., SHALLOWAY, D., LIS, J. T. & CRAIGHEAD, H. G. 2013. RAPID-SELEX for RNA Aptamers. *PLoS ONE,* 8**,** e82667.

TAHIRI-ALAOUI, A., FRIGOTTO, L., MANVILLE, N., IBRAHIM, J., ROMBY, P. & JAMES, W. 2002. High affinity nucleic acid aptamers for streptavidin incorporated into bi-specific capture ligands. *Nucleic Acids Research,* 30**,** e45.

TANG, Q., SU, X. & LOH, K. P. 2007. Surface plasmon resonance spectroscopy study of interfacial binding of thrombin to antithrombin DNA aptamers. *Journal of Colloid and Interface Science,* 315**,** 99-106.

TANG, X.-L., ZHOU, Y.-X., WU, S.-M., PAN, Q., XIA, B. & ZHANG, X.-L. 2014. CFP10 and ESAT6 aptamers as effective Mycobacterial antigen diagnostic reagents. *Journal of Infection,* 69**,** 569-580.

TANG, X., ZHENG, J., YAN, Q., LI, Z. & LI, Y. 2013. Selection of aptamers against inactive Vibrio alginolyticus and application in a qualitative detection assay. *Biotechnology Letters,* 35**,** 909-914.

TENNICO, Y. H., HUTANU, D., KOESDJOJO, M. T., BARTEL, C. M. & REMCHO, V. T. 2010. On-Chip Aptamer-Based Sandwich Assay for Thrombin Detection Employing Magnetic Beads and Quantum Dots. *Analytical Chemistry,* 82**,** 5591-5597.

TEURK, C. & GOLD, L. 1990. Systematic Evolution of Ligands by Exponential Enrichment: RNA Ligands to Bacteriophage T4 DNA Polymerase. *Science,* 249**,** 505-510.

THERON, G., PETER, J., VAN ZYL-SMIT, R., MISHRA, H., STREICHER, E., MURRAY, S., DAWSON, R., WHITELAW, A., HOELSCHER, M., SHARMA, S., PAI, M., WARREN, R. & DHEDA, K. 2011. Evaluation of the Xpert(R) MTB/RIF Assay for the Diagnosis of Pulmonary Tuberculosis in a High HIV Prevalence Setting. *Am. J. Respir. Crit. Care Med.***,** 201101-0056OC.

THERON, G., ZIJENAH, L., CHANDA, D., CLOWES, P., RACHOW, A., LESOSKY, M., BARA, W., MUNGOFA, S., PAI, M., HOELSCHER, M., DOWDY, D., PYM, A., MWABA, P., MASON, P., PETER, J. & DHEDA, K. 2014. Feasibility, accuracy, and clinical effect of point-of-care Xpert MTB/RIF testing for tuberculosis in primary-care settings in Africa: a multicentre, randomised, controlled trial. *The Lancet,* 383**,** 424-435.

THIEL, W. H., BAIR, T., PEEK, A. S., LIU, X., DASSIE, J., STOCKDALE, K. R., BEHLKE, M. A., MILLER, F. J., JR. & GIANGRANDE, P. H. 2012. Rapid Identification of Cell-Specific, Internalizing RNA Aptamers with Bioinformatics Analyses of a Cell-Based Aptamer Selection. *PLoS ONE,* 7**,** e43836.

THWAITES, G., FISHER, M., HEMINGWAY, C., SCOTT, G., SOLOMON, T. & INNES, J. 2009. British Infection Society guidelines for the diagnosis and treatment of tuberculosis of the central nervous system in adults and children. *Journal of Infection,* 59**,** 167-187.

TODAR, K. 2008. Mycobacterium tuberculosis and tuberculosis. . *Available at: http://www.textbookofbacteriology.net/tuberculosis.html. Accessed May 19, 2015.*

TORRES-CHAVOLLA, E. & ALOCILJA, E. C. 2009. Aptasensors for detection of microbial and viral pathogens. *Biosensors and Bioelectronics,* 24**,** 3175-3182.

TORTOLI, E., CICHERO, P., PIERSIMONI, C., SIMONETTI, M. T., GESU, G. & NISTA, D. 1999. Use of BACTEC MGIT 960 for Recovery of Mycobacteria from Clinical Specimens: Multicenter Study. *Journal of Clinical Microbiology,* 37**,** 3578-3582.

TORTOLI, E., RUSSO, C., PIERSIMONI, C., MAZZOLA, E., DAL MONTE, P., PASCARELLA, M., BORRONI, E., MONDO, A., PIANA, F., SCARPARO, C., COLTELLA, L., LOMBARDI, G. & CIRILLO, D. M. 2012. Clinical validation of Xpert MTB/RIF for the diagnosis of extrapulmonary tuberculosis. *European Respiratory Journal,* 40**,** 442-447.

TSAI, R. Y. L. & REED, R. R. 1998. Identification of DNA Recognition Sequences and Protein Interaction Domains of the Multiple-Zn-Finger Protein Roaz. *Molecular and Cellular Biology,* 18**,** 6447-6456.

TUERK C, G. L. 1990. Systematic evolution of ligands by exponential enrichment: RNA ligands to bacteriophage T4 DNA polymerase. *Science,* 249**,** 505-510.

TUERK, C. & GOLD, L. 1990. Systematic evolution of ligands by exponential enrichment: RNA ligands to bacteriophage T4 DNA polymerase. *Science,* 249**,** 505-510.

TURNER, A. P. F., CHEN, B. & PILETSKY, S. A. 1999. In Vitro Diagnostics in Diabetes: Meeting the Challenge. *Clinical Chemistry,* 45**,** 1596-1601.

UDDIN, M. K. M., CHOWDHURY, M. R., AHMED, S., RAHMAN, M. T., KHATUN, R., VAN LETH, F. & BANU, S. 2013. Comparison of direct versus concentrated smear microscopy in detection of pulmonary tuberculosis. *BMC Research Notes,* 6**,** 291-291.

VALDÉS, L., ÁLVAREZ, D., SAN JOSÉ, E. & ET AL. 1998. Tuberculous pleurisy: A study of 254 patients. *Archives of Internal Medicine,* 158**,** 2017-2021.

VALDES, L., SAN JOSE, E., ALVAREZ, D. & VALLE, J. 1996. Adenosine deaminase (ADA) isoenzyme analysis in pleural effusions: diagnostic role, and relevance to the origin of increased ADA in tuberculous pleurisy. *European Respiratory Journal,* 9**,** 747-751.

VAN CREVEL, R. & DOCKRELL, H. M. 2014. TANDEM: understanding diabetes and tuberculosis. *The Lancet Diabetes & Endocrinology,* 2**,** 270-272.

VATER, A., JAROSCH, F., BUCHNER, K. & KLUSSMANN, S. 2003. Short bioactive Spiegelmers to migraine-associated calcitonin gene-related peptide rapidly identified by a novel approach: tailored-SELEX. *Nucleic Acids Res,* 31**,** e130.

VILLEGAS, M. V., LABRADA, L. A. & SARAVIA, N. G. 2000. EValuation of polymerase chain reaction, adenosine deaminase, and interferon-γ in pleural fluid for the differential diagnosis of pleural tuberculosis*. *Chest,* 118**,** 1355-1364.

WANG, C., ZHANG, M., YANG, G., ZHANG, D., DING, H., WANG, H., FAN, M., SHEN, B. & SHAO, N. 2003. Single-stranded DNA aptamers that bind differentiated but not parental cells: subtractive systematic evolution of ligands by exponential enrichment. *Journal of Biotechnology,* 102**,** 15-22.

WANG, H., YUE, J., YANG, J., GAO, R. & LIU, J. 2012. Clinical diagnostic utility of adenosine deaminase, interferon-γ, interferon-γ–induced protein of 10 kDa, and dipeptidyl peptidase 4 levels in tuberculous pleural effusions. *Heart & Lung: The Journal of Acute and Critical Care,* 41**,** 70-75.

WANG, J., CAO, Z., JIANG, Y., ZHOU, C., FANG, X. & TAN, W. 2005. Molecular Signaling Aptamers for Real-time Fluorescence Analysis of Protein. *IUBMB Life,* 57**,** 123-128.

WANG, R., ZHAO, J., JIANG, T., KWON, Y. M., LU, H., JIAO, P., LIAO, M. & LI, Y. 2013. Selection and characterization of DNA aptamers for use in detection of avian influenza virus H5N1. *Journal of Virological Methods,* 189**,** 362-369.

WEN, J.-D. & GRAY, D. M. 2004. Selection of genomic sequences that bind tightly to Ff gene 5 protein: primer-free genomic SELEX. *Nucleic Acids Research,* 32**,** e182-e182.

WHEELOCK, E. F. 1965. Interferon-like virus-inhibitor induced in human leukocytes by phytohemagglutinin. *Science,* 149**,** 310-1.

WHITE, R., RUSCONI, C., SCARDINO, E., WOLBERG, A., LAWSON, J., HOFFMAN, M. & SULLENGER, B. 2001. Generation of species cross-reactive aptamers using "toggle" SELEX. *Mol Ther,* 4**,** 567-73.

WHO 2007. TB diagnostic technology and laboratory strengthening-WHO policy: the use of liquid medium for culture and DST. *World Health Organization,* Available from www.who.int/tb/laboratory.

WHO 2010. Roadmap to rolling out Xpert MTB/RIF for rapid diagnosis of TB and MDR-TB. *World Health Organization*.

WHO 2011. Fluorescent light-emitting diode (LED) microscopy for diagnosis of tuberculosis: policy statement. *World Health Organization,* Geneva, Switzerland.

WHO 2012. Global Tuberculosis Report. *World Health Organization*.

WHO 2013. Global tuberculosis Control. *WHO Report,* Available at: www. who.int/tb/publications/golbal_report/en/index.html.

WHO 2014. Global Tuberculosis Report. *World Health Organization*.

WILLNER, I. & ZAYATS, M. 2007. Electronic Aptamer-Based Sensors. *Angewandte Chemie International Edition,* 46**,** 6408-6418.

WLOTZKA, B., LEVA, S., ESCHGFÄLLER, B., BURMEISTER, J., KLEINJUNG, F., KADUK, C., MUHN, P., HESS-STUMPP, H. & KLUSSMANN, S. 2002. In vivo properties of an anti-GnRH Spiegelmer: An example of an oligonucleotide-based therapeutic substance class. *Proceedings of the National Academy of Sciences of the United States of America,* 99**,** 8898-8902.

WU, L. & CURRAN, J. F. 1999. An allosteric synthetic DNA. *Nucleic Acids Research,* 27**,** 1512-1516.

XU, Y., PHILLIPS, J. A., YAN, J., LI, Q., FAN, Z. H. & TAN, W. 2009. Aptamer-Based Microfluidic Device for Enrichment, Sorting, and Detection of Multiple Cancer Cells. *Analytical Chemistry,* 81**,** 7436-7442.

YAMADA, Y., NAKAMURA, A., HOSODA, M., KATO, T., ASANO, T., TONEGAWA, K. & ITOH, M. 2001. Cytokines in pleural liquid for diagnosis of tuberculous pleurisy. *Respiratory Medicine,* 95**,** 577-581.

YAMAMOTO, R., KATAHIRA, M., NISHIKAWA, S., BABA, T., TAIRA, K. & KUMAR, P. K. R. 2000. A novel RNA motif that binds efficiently and specifically to the Tat protein of HIV and inhibits the trans-activation by Tat of transcription in vitro and in vivo. *Genes to Cells,* 5**,** 371-388.

YAO, C., QI, Y., ZHAO, Y., XIANG, Y., CHEN, Q. & FU, W. 2009. Aptamer-based piezoelectric quartz crystal microbalance biosensor array for the quantification of IgE. *Biosensors and Bioelectronics,* 24**,** 2499-2503.

YAO, C., ZHU, T., QI, Y., ZHAO, Y., XIA, H. & FU, W. 2010. Development of a Quartz Crystal Microbalance Biosensor with Aptamers as Bio-recognition Element. *Sensors (Basel, Switzerland),* 10**,** 5859-5871.

ZAR, H. J., CONNELL, T. G. & NICOL, M. 2010. Diagnosis of pulmonary tuberculosis in children: new advances. *Expert Review of Anti-infective Therapy,* 8**,** 277-288.

ZHOU, J., BATTIG, M. & WANG, Y. 2010. Aptamer-based molecular recognition for biosensor development. *Analytical and Bioanalytical Chemistry,* 398**,** 2471-2480.

ZIMMERMANN, G. R., WICK, C. L., SHIELDS, T. P., JENISON, R. D. & PARDI, A. 2000. Molecular interactions and metal binding in the theophylline-binding core of an RNA aptamer. *RNA,* 6**,** 659-667.

ZUKER, M. 2003. Mfold web server for nucleic acid folding and hybridization prediction. *Nucleic Acids Research,* 31**,** 3406-3415.

ZUO, X., XIAO, Y. & PLAXCO, K. W. 2009. High Specificity, Electrochemical Sandwich Assays Based on Single Aptamer Sequences and Suitable for the Direct Detection of Small-Molecule Targets in Blood and Other Complex Matrices. *Journal of the American Chemical Society,* 131**,** 6944-6945.

APPENDICES

APPENDIX 2A: Methods supplementary material

Table S2.1: Protocol of 17% resolving gel

Contents for resolving gel (17%)	10 ml
1.5 M Tris-HCl [Sigma], pH 8.8 (0. 1% SDS) [Sigma]	2.5 ml
Acrylamide/Bis-acrylamide (40% w/v) [Sigma]	4.25 ml
Ammonium persulfate (APS) 10% (w/v) [Sigma]	100 µl
Tetramethylethylenediamine (TEMED) [Thermoscientific]	10 µl
ddH_2O	3.14 ml

Table S2.2: Protocol of 4% stacking gel

Components of stacking gel (4%)	5 ml
0.5 M Tris-HCl (Sigma), pH 6.8, (0.1%) SDS (Sigma)	1 ml
Acrylamide/Bis-acrylamide (40% w/v)	500 µl
Ammonium per sulfate (APS) 10% (w/v)	50 µl
TEMED [Thermoscientific]	5 µl
ddH_2O	3.45 ml

Table S2.3: Sequences of primers and the library that was used for the SELEX

	Sequences in 5'-3' direction
Forward primer (5'-biotin modified)	GCCTGTTGTGAGCCTCCTAAC
Reverse primer (5'-phosphate modified)	GGGAGACAAGAATAAGCATG
Library	GCCTGTTGTGAGCCTCCTAAC(N49)CATGCTTATTCTTGTCTCCC

Table S2.4: Mutagenic PCR set-up protocol using Go-Taq kit (Promega, WI, USA)

PCR Component	1x reaction
5x Go Taq Buffer	220 µl
MgCl2 [3.5 mM]	154 µl
dNTPs [0.2 mM]	22 µl
SELEX Forward primer [100 µM]	5 µl
SELEX Forward primer [100 µM]	5 µl
Go Taq	5.5 µl
ddH_2O up to 700 µl	640.5 µl

Table S2.5: Cycling protocol for mutagenic PCR

Cycling conditions	1x reaction	
Initial Denaturation	95 °C for 3 min	1 Cycle
Denaturation Annealing Extension	95 °C for 1 min 54 °C for 1 min 72 °C for 1 min:30 sec	20 Cycles
Final Extension Hold	72 °C for 8 min 4 °C	1 Cycle Indefinitely

Table S2.6: Protocol for a 12% non-denaturing polyacrylamide gel

Gel components	10 ml
10x TBE buffer	1 ml
Acrylamide/Bis-acrylamide (40% w/v) [Sigma]	3 ml
Ammonium persulfate (APS) 10% (w/v) [Sigma]	100 µl
Tetramethylethylenediamine (TEMED) [Thermoscientific]	10 µl
ddH_2O	4.9 ml

Table S2.7: Set-up of ligation reaction

Reagent	10 µl
2X Ligation buffer	5 µl
pGEM-T Easy vector (50ng/ µl)	1 µl
T4 DNA Ligase	1 µl
PCR product (100ng/ µl)	1 µl
ddH_2O (3 units)	2 µl

Table S2.8: Non-mutagenic PCR protocol using Go-Taq kit (Promega. WI, USA)

PCR Component	1x reaction
5X Go Taq Buffer	140 µl
MgCl2 [1.5 mM]	42 µl
dNTPs [0.2 mM]	22 µl
SELEX Forward primer [1 µM]	7 µl
SELEX Forward primer [1 µM]	7 µl
Go Taq	3.5 µl
ddH_2O up to 700 µl	478.5 µl

Table S2.9: Cycling conditions for non-mutagenic PCR

Cycling step	Temperature and time	Number of cycles
Initial Denaturation	95°C for 3 min	1 cycle
Denaturation	95°C for 30 seconds	
Annealing	54°C for 30 seconds	20 cycles
Extension	72°C for 30 seconds	
Final Extension	72°C for 8 min	1 cycle

APPENDIX 2B: Protocol for bulking-up of ssDNA for determining binding affinity by ELONA

Production of ssDNA to determine the aptamer-target binding affinities

In order to produce DNA to use for aptamer screening, PCR reactions were prepared by making an emulsion of each colony. A colony was scraped using a sterile pipette tip and inoculated into 25 µl of distilled water using a PCR 96-well plate (Corning, Adcock and Ingram, South Africa). The plate was then put into a PCR machine and heated at 95 °C for 10 min, to burst the cells. Three millilitre PCRs were performed under non-mutagenic conditions (Table S2.8 and S2.9). The sufficient product produced allowed for sufficient ssDNA to be produced following lambda exonuclease digestion (as described in section 2.2.1.4). The final products (ssDNA) were purified using the Nucleospin PCR cleaning kit (Macherey-Nagel, Düren, Germany), as per the manufacturer's instructions. The products were further analysed on a 12% non-denaturing PAGE (Table S2.6), to validate the quality, and to ensure that all the dsDNA was completely digested. The quantity was determined using the Nanodrop® ND-100 spectrophotometer (Thermo Scientific, MA, USA).

APPENDIX 2C: The tabular format of a multiple alignment of 36 IFNγ DNA sequences identified in the 5'-3' direction. The 49nt random region is flanked by primers, which were 100% conserved.

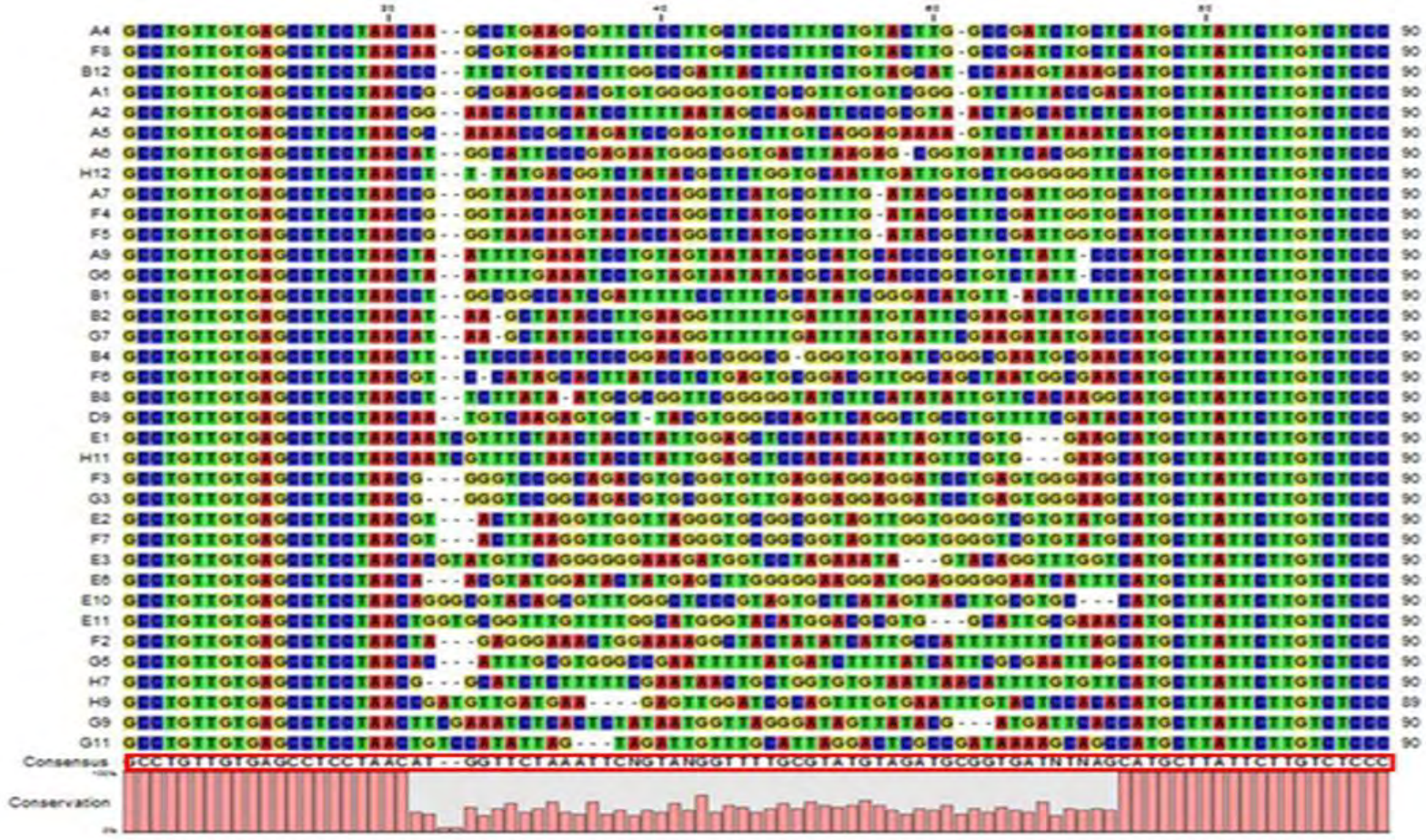

APPENDIX 2D: Nucleotide Sequence Statistics calculated using the CLC Sequence Viewer

1.1 Sequence information

Information	A1	A2	A4	A5	A6	A7	A9	B1	B2	B4	B8	B12	D9	E1	E2	E3	E6	E10	E11	F2	H7	H9	H11	H12	F3	F4	F5	F6	F7	F8	G3	G5	G6	G7	G9	G11
Sequence type	DNA	DNA	DNA	DNA	DNA	DNA	DNA	DNA	DNA	DNA	DNA	DNA	DNA	DNA	DNA	DNA	DNA	DNA	DNA	DNA	DNA	DNA	DNA	DNA	DNA	DNA	DNA	DNA	DNA	DNA	DNA	DNA	DNA	DNA	DNA	DNA
Length	49bp	49bp	49bp	49bp	49bp	49bp	49bp	49bp	49bp	49bp	49bp	49bp	49bp	49bp	49bp	49bp	49bp	49bp	49bp	49bp	49bp	48bp	49bp	49bp	49bp	49bp	49bp	49bp	49bp	49bp	49bp	49bp	49bp	49bp	49bp	49bp
Organism	Not available	Not available	Not available	Not available	Not available	Not available	Not available	Not available	Not available	Not available	Not available	Not available	Not available	Not available	Not available	Not available	Not available	Not available	Not available	Not available	Not available	Not available	Not available	Not available	Not available	Not available	Not available	Not available	Not available	Not available	Not available	Not available	Not available	Not available	Not available	Not available
Name	A1	A2	A4	A5	A6	A7	A9	B1	B2	B4	B8	B12	D9	E1	E2	E3	E6	E10	E11	F2	H7	H9	H11	H12	F3	F4	F5	F6	F7	F8	G3	G5	G6	G7	G9	G11
Description	Not available	Not available	Not available	Not available	Not available	Not available	Not available	Not available	Not available	Not available	Not available	Not available	Not available	Not available	Not available	Not available	Not available	Not available	Not available	Not available	Not available	Not available	Not available	Not available	Not available	Not available	Not available	Not available	Not available	Not available	Not available	Not available	Not available	Not available	Not available	Not available
Modification Date	Not available	Not available	Not available	Not available	Not available	Not available	Not available	Not available	Not available	Not available	Not available	Not available	Not available	Not available	Not available	Not available	Not available	Not available	Not available	Not available	Not available	Not available	Not available	Not available	Not available	Not available	Not available	Not available	Not available	Not available	Not available	Not available	Not available	Not available	Not available	Not available
Weight (single-stranded)	15.369 kDa	14.976 kDa	14.988 kDa	15.202 kDa	15.313 kDa	15.208 kDa	15.036 kDa	15.027 kDa	15.209 kDa	15.221 kDa	15.179 kDa	15.004 kDa	15.214 kDa	15.11 kDa	15.493 kDa	15.4 kDa	15.465 kDa	15.207 kDa	15.366 kDa	15.204 kDa	15.159 kDa	14.948 kDa	15.11 kDa	15.267 kDa	15.525 kDa	15.208 kDa	15.208 kDa	15.193 kDa	15.493 kDa	15.003 kDa	15.525 kDa	15.153 kDa	15.036 kDa	15.209 kDa	15.164 kDa	15.19 kDa
Weight (double-stranded)	30.32 kDa	30.311 kDa	30.314 kDa	30.309 kDa	30.314 kDa	30.313 kDa	30.307 kDa	30.312 kDa	30.302 kDa	30.321 kDa	30.309 kDa	30.31 kDa	30.312 kDa	30.308 kDa	30.315 kDa	30.31 kDa	30.311 kDa	30.316 kDa	30.314 kDa	30.305 kDa	30.305 kDa	29.891 kDa	30.308 kDa	30.312 kDa	30.32 kDa	30.313 kDa	30.313 kDa	30.314 kDa	30.315 kDa	30.313 kDa	30.32 kDa	30.306 kDa	30.307 kDa	30.302 kDa	30.305 kDa	30.308 kDa

1.2 Counts of nucleotides

Nucleotide	A1	A2	A4	A5	A6	A7	A9	B1	B2	B4	B8	B12	D9	E1	E2	E3	E6	E10	E11	F2	H7	H9	H11	H12	F3	F4	F5	F6	F7	F8	G3	G5	G6	G7	G9	G11
Adenine (A)	5	13	6	17	11	11	13	7	15	8	10	10	10	14	6	14	14	7	8	15	10	12	14	7	9	11	11	11	6	6	9	11	13	15	15	14
Cytosine (C)	10	16	16	10	9	11	12	14	5	15	9	14	10	11	4	5	4	12	7	7	7	7	11	8	7	11	11	12	4	15	7	8	12	5	8	9
Guanine (G)	22	7	10	11	17	14	7	10	9	18	12	8	14	9	23	17	19	16	19	10	10	13	9	16	25	14	14	14	23	10	25	10	7	9	9	11
Thymine (T)	12	13	17	11	12	13	17	18	20	8	18	17	15	15	16	13	12	14	15	17	22	16	15	18	8	13	13	12	16	18	8	20	17	20	17	15
C + G	32	23	26	21	26	25	19	24	14	33	21	22	24	20	27	22	23	28	26	17	17	20	20	24	32	25	25	26	27	25	32	18	19	14	17	20
A + T	17	26	23	28	23	24	30	25	35	16	28	27	25	29	22	27	26	21	23	32	32	28	29	25	17	24	24	23	22	24	17	31	30	35	32	29

1.3 Frequencies of nucleotides

Nucleotide	A1	A2	A4	A5	A6	A7	A9	B1	B2	B4	B8	B12	D9	E1	E2	E3	E6	E10	E11	F2	H7	H9	H11	H12	F3	F4	F5	F6	F7	F8	G3	G5	G6	G7	G9	G11
Adenine (A)	0.102	0.265	0.122	0.347	0.224	0.224	0.265	0.143	0.306	0.163	0.204	0.204	0.204	0.286	0.122	0.286	0.286	0.143	0.163	0.306	0.204	0.250	0.286	0.143	0.184	0.224	0.224	0.224	0.122	0.122	0.184	0.224	0.265	0.306	0.306	0.286
Cytosine (C)	0.204	0.327	0.327	0.204	0.184	0.224	0.245	0.286	0.102	0.306	0.184	0.286	0.204	0.224	0.082	0.102	0.082	0.245	0.143	0.143	0.143	0.146	0.224	0.163	0.143	0.224	0.224	0.245	0.082	0.306	0.143	0.163	0.245	0.102	0.163	0.184
Guanine (G)	0.449	0.143	0.204	0.224	0.347	0.286	0.143	0.204	0.184	0.367	0.245	0.163	0.286	0.184	0.469	0.347	0.388	0.327	0.388	0.204	0.204	0.271	0.184	0.327	0.510	0.286	0.286	0.286	0.469	0.204	0.510	0.204	0.143	0.184	0.184	0.224
Thymine (T)	0.245	0.265	0.347	0.224	0.245	0.265	0.347	0.367	0.408	0.163	0.367	0.347	0.306	0.306	0.327	0.265	0.245	0.286	0.306	0.347	0.449	0.333	0.306	0.367	0.163	0.265	0.265	0.245	0.327	0.367	0.163	0.408	0.347	0.408	0.347	0.306
C + G	0.653	0.469	0.531	0.429	0.531	0.510	0.388	0.490	0.286	0.673	0.429	0.449	0.490	0.408	0.551	0.449	0.469	0.571	0.531	0.347	0.347	0.417	0.408	0.490	0.653	0.510	0.510	0.531	0.551	0.510	0.653	0.367	0.388	0.286	0.347	0.408
A + T	0.347	0.531	0.469	0.571	0.469	0.490	0.612	0.510	0.714	0.327	0.571	0.551	0.510	0.592	0.449	0.551	0.531	0.429	0.469	0.653	0.653	0.583	0.592	0.510	0.347	0.490	0.490	0.469	0.449	0.490	0.347	0.633	0.612	0.714	0.653	0.592

APPENDIX 3A: Secondary structure predictions

Aptamer A1

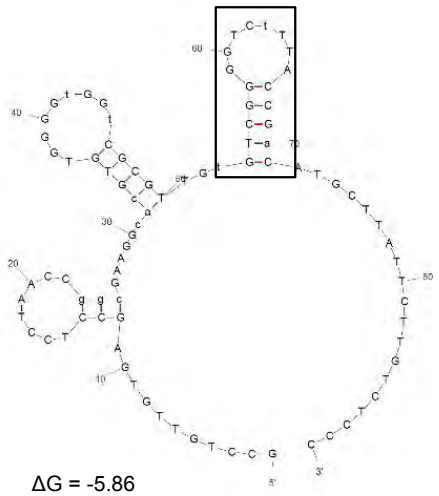

ΔG = -5.86

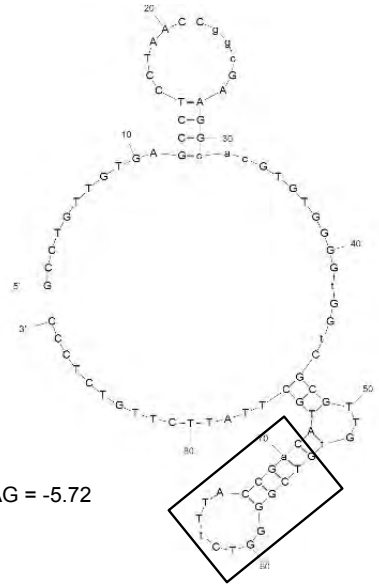

ΔG = -5.72

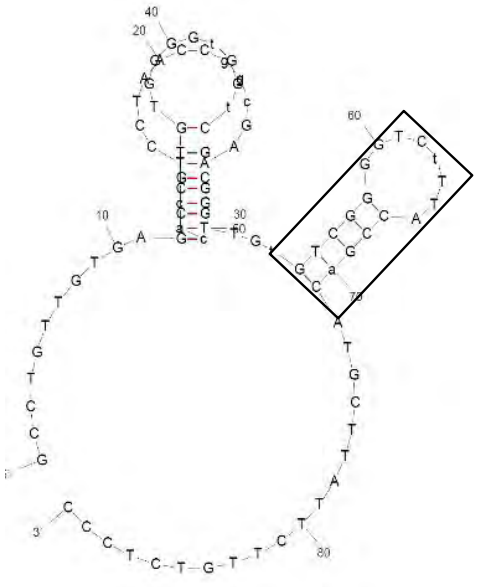

ΔG = -6.25

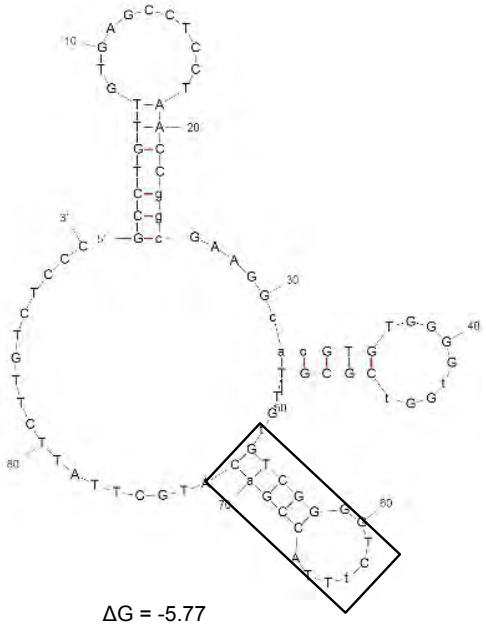

ΔG = -5.77

Aptamer A2

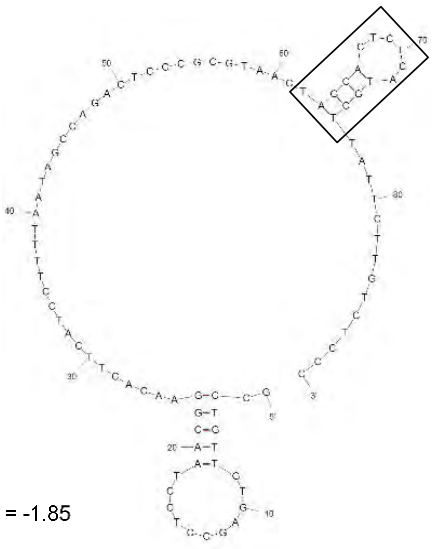

ΔG = -1.85

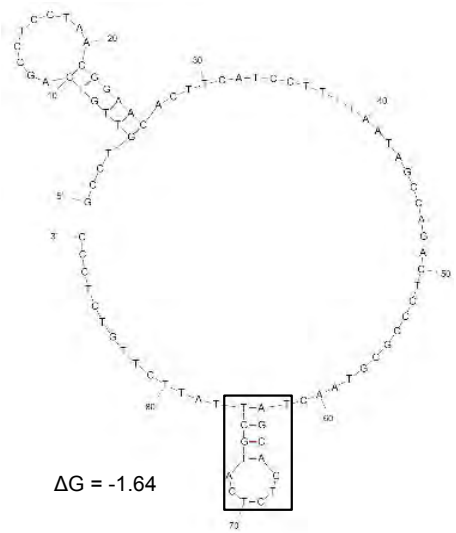

ΔG = -1.64

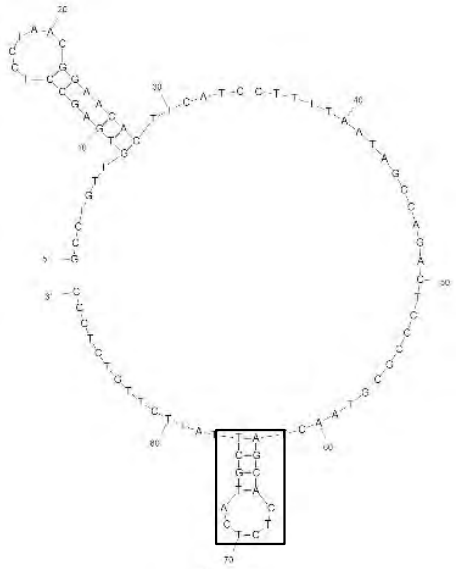

ΔG = -1.93

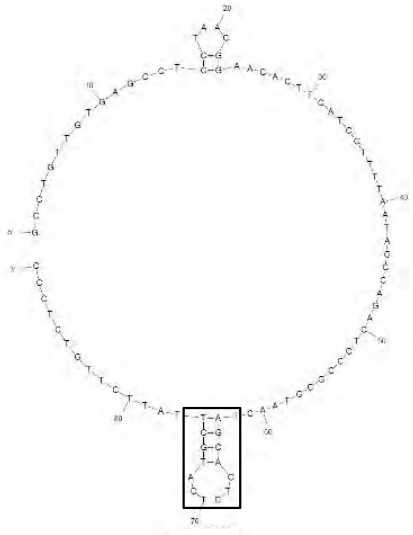

ΔG = -2.00

Aptamer A9

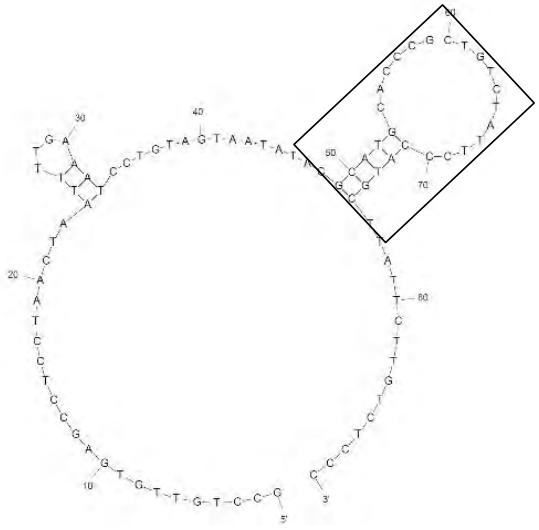

ΔG = -1.13

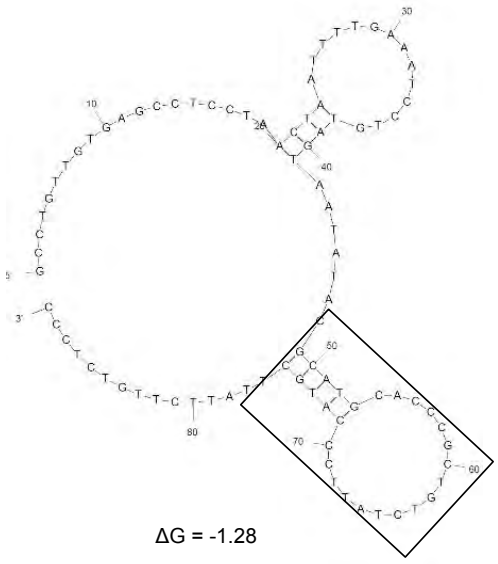

ΔG = -1.28

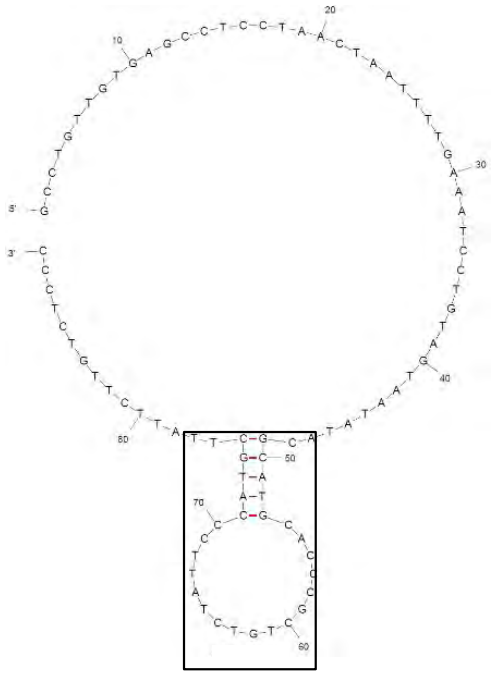

ΔG = -1.78

Aptamer B2

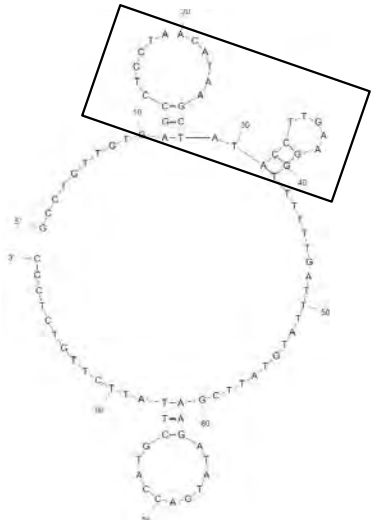

ΔG = -1.09

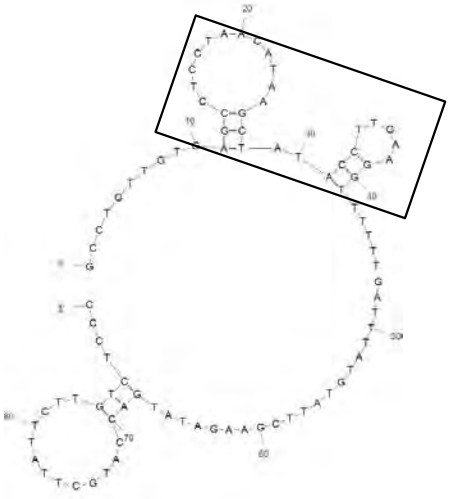

ΔG = -1.33

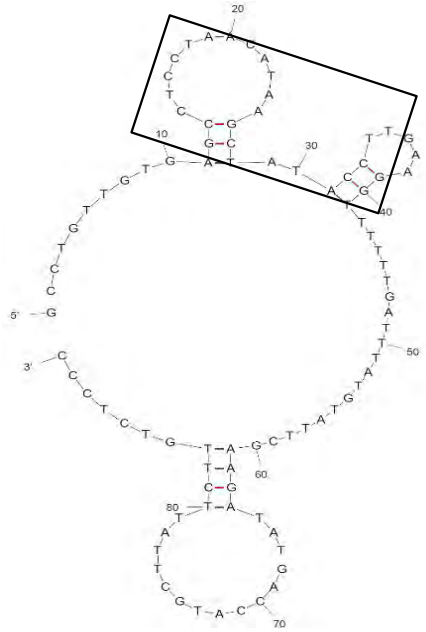

ΔG = -1.55

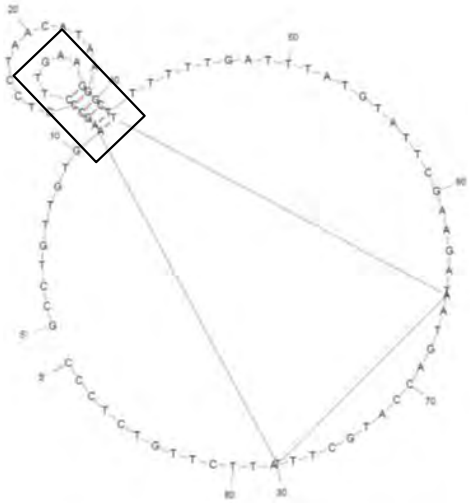

ΔG = -1.84

Aptamer B4

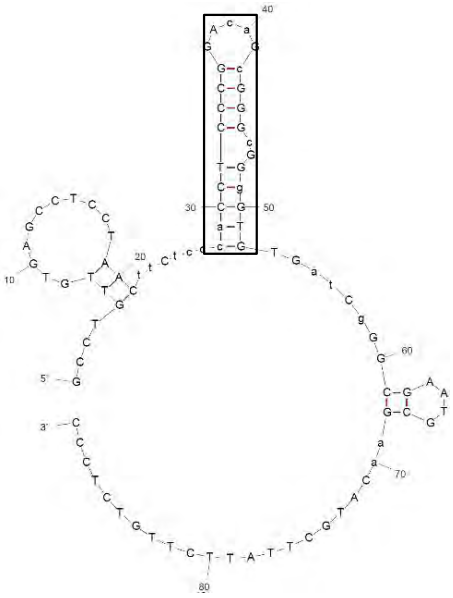

ΔG = -4.91

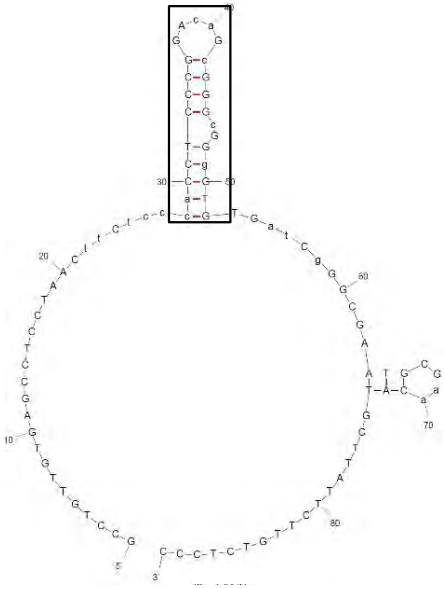

ΔG = -5.24

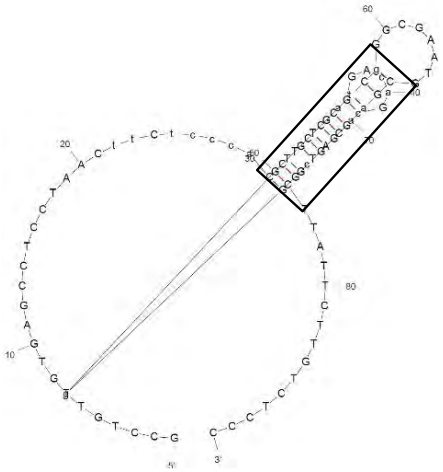

ΔG = -4.79

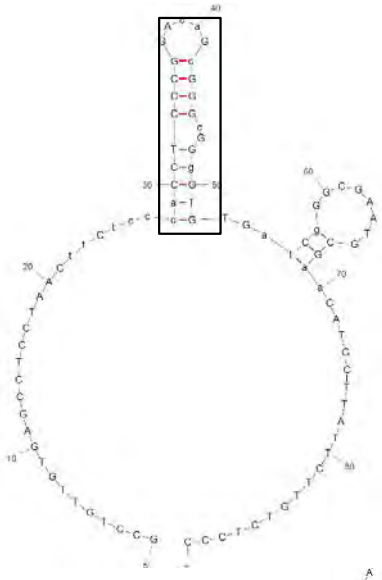

ΔG = -5.72

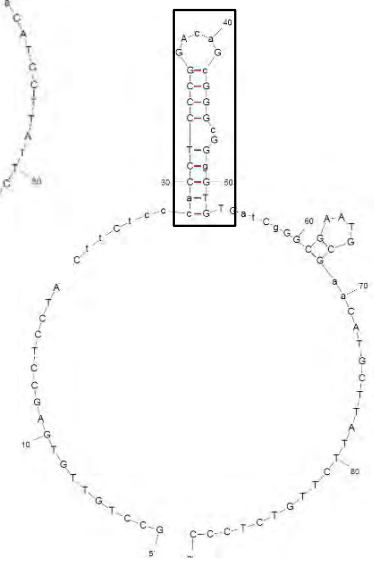

ΔG = -5.72

Aptamer H12

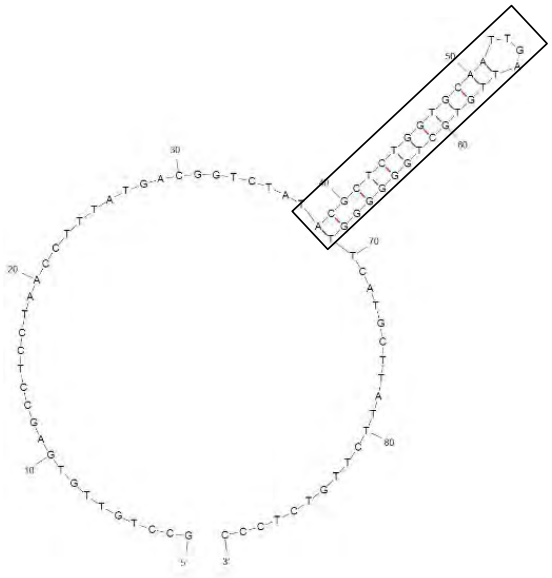

ΔG = -2.13

APPENDIX 4A: Specificity of aptamers using mycobacterial and non-mycobacterial molecules

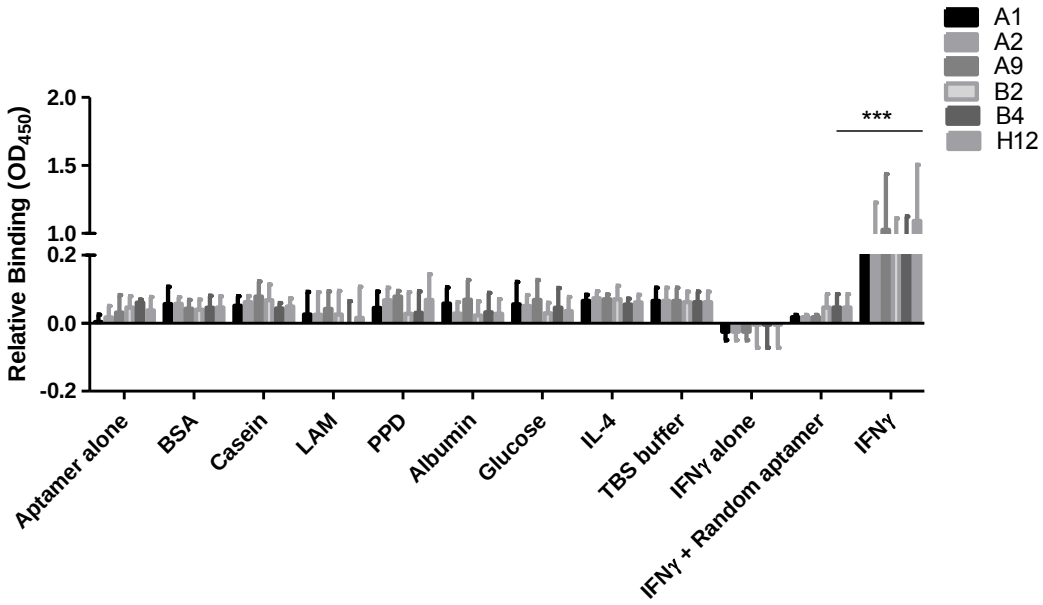

*Each aptamer was t at150 nM aptamer. All the molecules tested were at a final concentration of 10 µg/ml. Blocking buffer (casein) and wash buffer (TBS) used in the assay were tested against the aptamer to rule out any possible binding. Casein, an abundant protein found in milk (hereto used as blocking buffer) was also included as a control to rule out the possibility of the protein blocking all the available binding sites. Bovine serum albumin (BSA) was also included as a negative control. The mycobacterial-related molecules tested were; Lipoarabinomannan (LAM), Interleukin 4 (IL-4), and Purified protein derivative (PPD). Some of the molecules found in abundance in the pleural fluid were also tested: i.e Albumin and Glucose.